2. The string as a transmission line

Within the terminology of systems theory, a special transmission channel that transmits signals from the source to the receiver constitutes a **transmission line**. In the framework of the electric guitar, our thinking in terms of a transmission line will in the first place probably be target the guitar cable. However, while the latter does transmit electrical signals from the guitar to the amplifier in the sense as given above, we do not need the general line theory in order to describe its function. This is because for short lines, a simplification to concentrated line elements is adequate. The guitar cable indeed is a short line – short relative to the *electrical* wavelength that is in excess of 30 km. Transmission line theory is supposed to describe predominantly long lines with dimensions in the order of the wavelength or a length longer than that. In this sense, the **guitar string** does represent a long *mechanical* transmission line. The source of the propagating mechanical wave is the place where the string is plucked. Receiver of the signal transmitted via the string is the bridge that decouples part of the incoming signal energy and feeds it to the guitar body. The remaining part of the signal energy is fed back to the string as reflection. The nut (or the "active" fret) reflects, as well, leading to the manifestation of a **standing wave** on the string.

String vibrations are the basis for all musical signals generated in the pickup; the following section is dedicated to these vibrations. A pickup may also generate interference, but this will be investigated elsewhere (Chapter 5.7). The guitar string is a mechanical system that, strictly speaking, reacts non-linearly in a complicated manner; we will assume it to be linear and time-invariant in order to simplify things. Given such boundary conditions, we can define – as **system quantities –** masses, stiffnesses and resistances, and acting on these we have the **signal quantities** of force, and of vibration velocity = particle velocity. The local distributions of the signal quantities run along the string as a **wave** – the propagation speed being c. On electrical lines, we find very similar relationships: here the system quantities are capacitance, inductance and resistance, and the signal quantities are current and voltage. Using the analogous mathematical description, mechanical and electrical lines will be juxtaposed in the following. The mechanical line is the guitar string; the analogous electrical line is supposed to serve as **model** for illustration it does not actually exist, and it certainly is not the guitar cable!

Translator's remark: *in this chapter, again often the bridge and the nut of the guitar are taken as the points between which the guitar string vibrate i.e. as the string bearings. Of course, all basic considerations apply to the fretted string in the same way – the bearings are then bridge and fret. This is not always explicitly indicated, and therefore the term "nut" should be considered to appropriately include the term "or fret", as well.*

2.1 Transversal waves

On a mechanical transmission line, mechanical waves propagate. These waves may be longitudinal or transversal waves, or a combination hereof. In a pure transversal wave, the differentially small line particles oscillate laterally relative to the direction of propagation, either in a planar movement, or in rotating fashion. In a pure longitudinal wave, the particles oscillate in the direction of propagation; for a guitar string this would be along the string axis, having rather minor significance compared to the transversal wave. In a simple electrical line, an electrical field is generated between two parallel conductors. *Within* the conductors, currents are flowing, and differences in electrical potential (i.e. voltages) result *between* the conductors.

© M. Zollner & Tilmann Zwicker, 2002 & 2020

Electrical line theory distinguishes between various conductor geometries – this will not be required for the fundamental considerations to be discussed here.

It is the local distribution of the signal quantities that propagates along the transmission line with the speed c. Defined as a function of place and time, the **force** F is a signal quantity on the mechanical line: $F(z,t)$. Herein, z is the place coordinate in the direction along the string, and t is the time. A first reason for misunderstandings pops up: it is not the tension force Ψ of the string that is meant here but the wave force F. Tuning the string, a tension force Ψ is exerted onto the string; after conclusion of the tuning process this will (ideally) remain constant. In addition, plucking the string will introduce a lateral **transverse force**; this force is meant with F. On top of the force distribution across place and time we require also a movement quantity to describe the changing geometry. For this we basically look at the distribution of the **lateral velocity** that may be converted into acceleration via differentiation and into displacement via integration. To avoid confusion with the propagation speed c (which is signal-independent constant), this signal speed is termed **(particle) velocity** $v(z,t)$. The signal-carrying **wave quantities** are thus the force $F(z,t)$ and the velocity $v(z,t)$. In the important transversal wave, the direction of the latter is transverse to the string axis, for the longitudinal wave, it is in parallel.

Either wave quantity may not be directly observed. Even as we see *that* a string indeed vibrates, it is impossible to say whether the particle velocity is 1 m/s or 5 m/s. Conversely, the displacement can be estimated – at least if it is sufficiently strong. Easiest to interpret are therefore graphical representations of the **displacement** which is often designated with x or ξ. However, ξ, is dependent on place *and* time: $\xi(z,t)$. This function could be represented in space via a z,t,ξ-coordiate-system, with ξ being the elevation above the z,t-plane. Sections along $t = t_0 = const$ result in a place-function $\xi(z,t_0)$; sections along $z = z_0 = const$ yield a time-function $\xi(z_0,t)$. The **place-function** is a snapshot showing the location-distribution of the displacement at *one* point in time. The **time-function** is a snapshot indicating the course of the displacement of *one* special point on the string. Spacial representations above a z,t-plane do, however, have the big disadvantage that the time t is in fact *not* a space-coordinate. This is not a problem for the general definition of the term "space" but it is not very descriptive for fundamental considerations. A real problem, though, is simplifying $\xi(z,t_0)$ to $\xi(z)$ = position function, and simplifying $\xi(z_0,t)$ to $\xi(t)$ = time-function. Indeed, t_0 and z_0 are both constant quantities, but $\xi(z)$ and $\xi(t)$ remain two distinct, different functions that should not be designated with one and the same letter ξ. We will write $\xi_{ZF}(t) = \xi(z_0,t)$ for the displacement-time-function in order to facilitate that distinction, and $\xi_{OF}(t) = \xi(z,t_0)$ for the displacement-place-function.

For three different wave-shapes, **Fig. 2.1** shows the place-function of the displacement at seven different points in time. In each of the three graphs, a transversal wave runs from right to left. As a contrast to the real string, the wave propagation depicted in Fig. 2.1 is not dispersive i.e. the wave maintains its shape. In the real string, the propagation happens with a frequency-dependent speed (**dispersion**), and the wave changes its shape during the propagation, because higher frequencies propagate with higher speed. For introductory considerations, we may neglect dispersion, but for more exact analyses it will have to be taken into account, with c being not a constant but dependent on frequency.

 © M. Zollner & T. Zwicker, 2002 & 2020

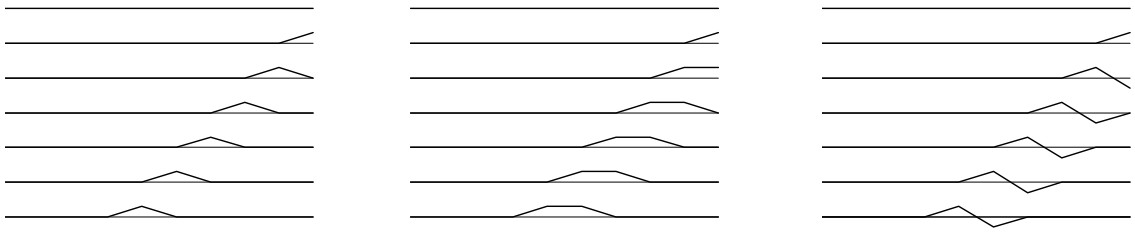

Fig. 2.1: Transversal waves. Each line shows the lateral displacement of the string at one point in time. The wave propagates (in each of the three columns) from right to left; the lower lines show later points in time. At the far right, a short-duration lateral excitation happens, causing a wave running to the left with constant propagation speed. The three graphs depict three different excitation functions.

In the following, $\xi = \xi_{OF}(z)$ is to be interpreted as the analytical representation of a **function**, with **Fig. 2.2** showing the corresponding graphical representation (for a specific example). A function is a rule that unambiguously allocates to each **argument** z a **function value** ξ. Rather than the term "allocate", we often use "map", and thus a function is also a **mapping**: the set of z-points is mapped onto the set of ξ-points.

A **transformation** also is a mapping, because again sets are mapped onto each other. In the following, the term "transformation" is – as a specialization – defined as describing the shifting of the $z\xi$-plane. Each point on this plane is described as a pair of values; the origin e.g. by $z = 0$, $\xi = 0$. Shifting every point on the $z\xi$-plane by the same distance in the same direction results in a special transformation that in this case is termed **shift** or **translation**. Analytical geometry of the plane calls this a *parallel shift of the plane in itself* – the shift belongs to the class of concordant **congruent mappings**.

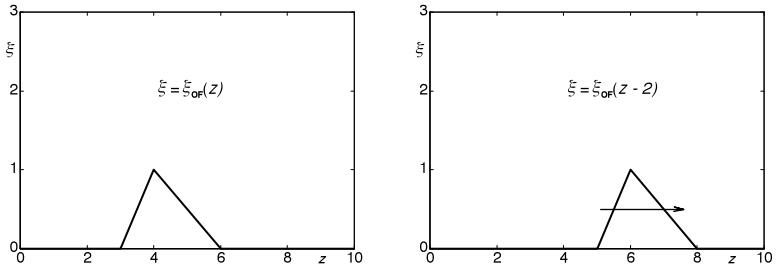

Fig. 2.2: Graphical representation of the function $\xi = \xi_{OF}(z)$. Applying the transformation shifts the function graph in the positive z-direction.
Right: $ct = 2$.

Functions, mappings and transformations are allocation rules. For the following considerations we will use these specializations of the terms: the z-ξ-allocation is termed *function*, while the shift of all z,ξ-points that leads to a shifting of the function graph (the function curve) is designated a *transformation*. The shift of the function graph in the direction of the z-coordinate is of particular importance since this is the axis of the string (i.e. the direction along the string), with elastic waves running along the string in that direction. The place-function of the displacement describes the connection between the place z and the displacement ξ. For the string, each z is tied to a distinct ξ for any special point in time. Analytically described by $\xi = \xi_{OF}(z)$, the function graph is a depiction of the string displacement.

Depending on the changing time t, the function graph changes its position; it shifts along z. Mathematically seen this shift is a time-dependent transformation (specifically: a translation). It is either termed a coordinate transformation or an **argument transformation,** because the transformation rule changes merely the function-argument z.

© M. Zollner & Tilmann Zwicker, 2002 & 2020 Translation by Tilmann Zwicker

All values (ξ) of the function are retained; they are, however, mapped to new z-values via the transformation.

$$\xi = \xi_{OF}(z - ct_0)$$ Time-dependent translation

The transformation changes the argument of the function: z becomes $z - ct_0$. Herein, c is the **propagation speed**[♣] of the wave, and ct_0 is the distance covered during the time t_0. We may interpret $\xi_{OF}(z)$ as place-function at the time $t = 0$, and $\xi_{OF}(z - ct_0)$ as place-function at (a different) time t_0. The function graph defined by $\xi_{OF}(z)$ is shifted in the z-direction by the transformation: if c is positive, the shift is towards the right, and for negative c it is towards the left. Besides the place-function that describes the displacement for a fixed point in time t_0 as a function of place, we may also consider the time-function giving the displacement for a fixed location z_0 as a function of time. If one of the two functions is known, the other can be calculated from it.

Fig. 2.3 exemplarily depicts a triangular place function $\xi_{OF}(z)$. The location (z) is newly defined relative to the specific location $z_0 = 8$ on the string: $z = z_0 - ct$. Basis for this substitution is the consideration that it does not make any difference for the calculation whether the wave runs towards the location z_0 or whether the observer moves towards the wave starting from location z_0. $\xi_{OF}(z_0 - ct)$ becomes the new function $\xi_{ZF}(t)$ that originates from $\xi_{OF}(z)$ via argument-transformation: $\xi_{OF}(z) \Leftrightarrow \xi_{ZF}(t)$. More generally: **the place function becomes the time function via argument transformation, and vice versa**. ξ_{OF} and ξ_{ZF} show a similar behavior but they are not identical.

For a positive c (with the wave running towards the right), one function originates from the other via horizontal stretching, via mirroring relative to the ordinate, and via horizontal shifting. Although other mapping steps would also be definable, these three partial mappings are to be considered. The horizontal stretching (performed in the direction of the abscissa) allocates a new scaling to the abscissa: the place becomes the time, and vice versa ($z = ct$). The mirroring results in a reversal of the direction of the abscissa. Both partial mappings could also be called "stretching with negative coefficient". As a last step, the curve – mirrored and stretched in the direction of the abscissa – is subsequently also shifted in the direction of the abscissa; the place function becomes a time function (or vice versa). For the wave running towards the left (negative c), the mirroring is omitted, i.e. the direction of the abscissa is not inverted. Both graphs in Fig. 2.3 are displacement functions; the functional connection between abscissa and ordinate is, however, different.

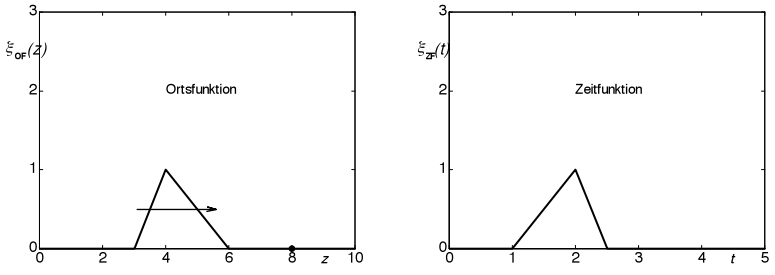

Fig. 2.3: Place und time function. The wave runs towards the right to the point $z_0 = 8$; the displacement of that point is shown in the time function. For the physical units see the text.
"Ortsfunktion" = place function; "Zeitfunktion" = time function

[♣] In literature equations are also found that fundamentally start with a positive c and use a plus- or a minus-sign depending on the propagation direction.

 © M. Zollner & T. Zwicker, 2002 & 2020

In Figs. 2.2 and 2.3, the variables do not possess any physical units – this is not unusual for mathematical representations. We could add **units**, or interpret the location coordinate z in a normalized manner … e.g. normalized to 1 m. That would make $z_0 = 8$ in fact mean $z_0 = 8\,\text{m}$. If, in addition, we assume that the time t is normalized to 1 s, the propagation speed for this example would be $c = z/t = 2\,\text{m/s}$.

In Fig 2.23 it does not make any difference whether the wave (on the left) runs towards the observer located at the fixed point $z_0 = 8$ at a speed of 2 m/s, or whether the observer runs (starting at $z_0 = 8$) towards the motionless (!) wave at a speed of 2 m/s. In both cases the observer sees the same time function. Also (please do remain calm now, dear physicists): waves on guitar strings do not run at light speed. Not even approximately.

The graphs shown so far have represented place- and time-functions of the **displacement** because the latter is easily observed on vibrating strings. From the point of view of systems theory, however, the **(particle) velocity** v is of greater importance because power and impedance result from it (along with the force). The velocity v (at the place z_0) is the partial temporal derivative of the displacement ξ (at the same place):

$$v(z,t) = \frac{\partial}{\partial t}\xi(z,t) \qquad \text{Time function: displacement} \rightarrow \text{velocity}$$

With both v und ξ depending on two variables in the general representation, a partial derivative for t is required. In it, the differentiation is done merely for t with the condition that $z = z_0$ remains constant:

$$v_{\text{ZF}}(t)\Big|_{z=z_0} = \frac{d}{dt}\xi_{\text{ZF}}(t)\Big|_{z=z_0} \qquad \text{Both Functions for the same place } z_0$$

However, place and time are interdependent via the propagation speed: $z = z_0 - ct$. It therefore is possible to reshape the time-differentiation d/dt into a place-differentiation d/dz, and with this to move from the place-function of the displacement $\xi_{\text{OF}}(z)$ directly to the place-function of the velocity $v_{\text{OF}}(z)$ (chain rule of differential calculus):

$$v_{\text{OF}}(z)\Big|_{t=t_0} = -c \cdot \frac{d\xi_{\text{OF}}(z)}{dz}\Big|_{t=t_0} \qquad \text{Place-function: displacement} \rightarrow \text{velocity}$$

In all these equations, the **sign** of the velocity v is oriented relative to the direction of ξ: movement in the direction of ξ yields a positive v. The conversion of the velocity-place-function is done, just as for the displacement, via substitution: $z = z_0 - ct$.

$$v_{\text{OF}}(z) \Rightarrow v_{\text{OF}}(z_0 - ct) \Rightarrow v_{\text{ZF}}(t) \qquad \text{Place-function} \rightarrow \text{time-function}$$

For known place-function and known propagation speed, the time-function is unambiguously defined – and vice versa. For known displacement and known propagation speed, the velocity is unambiguously defined, and vice versa.

© M. Zollner & Tilmann Zwicker, 2002 & 2020

Fig. 2.4 shows the place-function of triangular-shaped displacement waves; the corresponding velocity waves have a square shape. In the figures, z is the abscissa; seven subsequent points in time are shown in the figures. Despite the shape of the displacement-place-function being the same, the velocity-place-function differs in the sign. In the formula used so far, this change of the sign has been covered by c: for waves running towards the right, c has been defined as being positive; for waves running to the left it was negative.

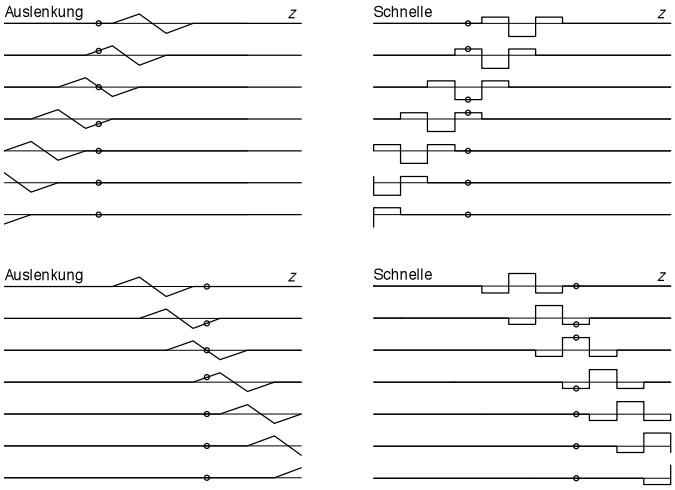

Fig. 2.4a: Place-functions of the wave running towards the left. The marked point is first moved *upwards*: the velocity of this point starts in the positive.
"Auslenkung" = displacement
"Schnelle" = (particle) velocity

Fig. 2.4b: Place-functions of the wave running towards the right. The marked point is first moved *downwards*: the velocity of this point starts in the negative.
"Auslenkung" = displacement
"Schnelle" = (particle) velocity

N.B.: At the left and right border, the wave disappears from the picture frame; there is no reflection.

Displacement ξ and velocity v describe the deformation of the string; the force F may be interpreted as their cause. As was already mentioned, it is not the tensioning force that is meant here, but the transverse force. It is purposeful at this point to look at the electrical transmission line rather than at the mechanical one. At the root of both lines we have the same type of differential equation (it is merely the system parameters that are designated differently). **Considerations of analogy** enable us to extrapolate from the behavior of one line to the behavior of the other [3]. It is particularly obvious to transfer the insights gained from the electrical line theory [5] to the mechanical line using the force-current-analogy. Doing this, the following correspondences result: capacitance ↔ mass, inductance ↔ spring, electrical admittance ↔ mechanical impedance, electrical voltage ↔ (particle) velocity, current ↔ force. For reasons of simplification, we are exclusively looking at loss-free lines with negligible short-term signal damping. Dispersion is not included in the considerations.

As a wave propagates along an electrical line, voltage and current are linked at every position on this line by the **wave impedance** Z_{Wel}: $\underline{U} = Z_{Wel} \cdot \underline{I}$. For loss-free lines, the wave impedance is of purely resistive character (i.e. it is real). There is no contradiction here: the line indeed accepts energy – however, this energy will not be dissipated as heat but will be transmitted. In order to avoid reflections, we usually assume an *infinitely long line*. This is not mandatory, though: as long as the wave is not facing any 'obstacles', we can do calculations using the wave impedance. Applying the *F-I*-analogy to the electrical line yields:

$$\underline{F} = Z_W \cdot \underline{v} \qquad \text{Mechanical line quantities}$$

Distinguishing it from the electrical wave impedance Z_{Wel}, we term the mechanical wave impedance Z_W.

 © M. Zollner & T. Zwicker, 2002 & 2020

With the length-specific mass m', and the length-specific compliance n', the mechanical wave impedance Z_W is calculated as:

$$Z_W = \sqrt{m'/n'} = \sqrt{\tfrac{1}{4}\rho D^2 \pi \cdot \Psi}$$ Mechanical wave impedance

In this formula, Ψ represents the tensioning force of the string, ρ the density, and D the diameter. For a 009-gage string set, 0,68 Ns/m (E2♣) and 0,14 Ns/m (E4) result – see also Chapter A.5.

In the wave propagating without perturbation, this real quantity connects the force F and the velocity v at every location. As example: the E4-string vibrates with an amplitude of 1 mm; its velocity amounts to $2\pi \cdot 330 s^{-1} \cdot 0{,}001 m = 2{,}07$ m/s (330Hz, sine-shape, peak value). Given Z_W = 0,14 Ns/m we obtain for the peak value of the force-wave: F = 0,29 N. Because Z_W is real, force and velocity are in phase at every location. However, this holds only for the wave propagating without perturbation. As soon as reflected waves are superimposed, there are other dependencies. The table below indicates the connections between the wave quantities:

Place-function → time-function: $z = z_0 - ct$. Time-function → place-function: $t = t_0 - z/c$

	Place-function	Time-function
Displacement	$\xi_{OF}(z)$	$\xi_{ZF}(t)$
Velocity	$v_{OF}(z) = -c \cdot \frac{d\xi_{OF}(z)}{dz}$	$v_{ZF}(t) = \frac{d\xi_{ZF}(t)}{dt}$
Force	$F_{OF}(z) = Z_W \cdot v_{OF}(z)$	$F_{ZF}(t) = Z_W \cdot v_{ZF}(t)$

Applying the formulas introduced so far, place- and time-functions can be converted into each other, and relationships between displacement, velocity and force can be set up. We have, however, not paid sufficient attention to the **sign** – its definition is not as trivial as it first may seem. For the displacement, we obtain still relatively simple relationships: the displacements in the ξ-direction are defined positively. For a wave progressing in the +z-direction, a positive displacement therefore implies: seen in the direction of the propagation, the displacement is 'to the left", while for the wave running in the –z-direction, positive displacement means 'to the right", seen in the direction of the propagation.

Evidently, there are two different possibilities for the **definition of the sign**: either referring to the absolute coordinates, or referring to the direction of propagation. If waves propagating in different directions are to be superimposed, **absolute coordinates** are more purposeful; with them, the superposition can be done – independently of the propagation direction – as a simple addition. For **displacement**, this definition is obvious: displacements in the ξ-direction are positive. For the **velocity** and the acceleration this approach is recommended, as well. Positive **acceleration** therefore implies that the string moves in the ξ-direction with increasing velocity. For the **force**, the following holds: a positive force generates a state of pressure in the spring. In an upright-standing coil spring, a *pressure* state can be generated as the upper end is pressed downward, or the lower end upward – both cases have the effect of a positive force.

♣ For wound strings, the calculation needs to consider a density reduced by 10% due to the encased air.

© M. Zollner & Tilmann Zwicker, 2002 & 2020 Translation by Tilmann Zwicker

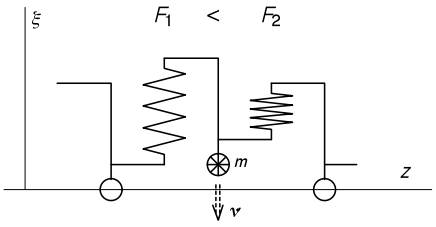

Fig. 2.5: Line-element. The circles are transversely movable masses; the springs model the transverse stiffness.
$F_2 > F_1$ indicates that there is a greater pressure force within the spring on the right. Consequently, a downward-directed acceleration (indicated by the arrow) acts onto the mass. Given the sign convention explained above, this acceleration is negative (negative ξ-direction).

In order to illustrate the transversal forces, the spring-mass-model according to **Fig. 2.5** may serve. The displacement ξ of the points of mass is to be seen directly as distance to the zero-line, and the transversal force F acting within the springs can be taken from the deformation of the springs. The acceleration forces relevant for the masses result as the difference of the two adjacent spring-forces. The force-difference $F = F_2 - F_1$ has the effect of an acceleration directed downwards; the inertia-formula therefore requires a minus sign. Dividing the equation by the differential length dz of the line element, the force becomes the length-specific force, and the mass m becomes the length-specific mass m'.

$$F_2 - F_1 = -\dot{v} \cdot m \quad \Big\} \quad \frac{dF}{dz} = -\dot{v} \cdot \frac{dm}{dz} = -\dot{v} \cdot m' \qquad \text{Law of inertia}$$

The transversal force F acting in a spring depends, via the compliance n, on the change of the length $\Delta\xi$ $F = \Delta\xi/n$. The change of the length is the difference between two adjacent displacements; by relating it to dz, the compliance n becomes the specific compliance n'.

$$F = -\frac{\xi_2 - \xi_1}{n} \quad \Big\} \quad F = -\frac{d\xi}{dz} \cdot \frac{dz}{dn} = -\frac{d\xi/dz}{n'} \qquad \text{Hooke's law}$$

The specific compliance (compliance per length) is the inverse of the tension force Ψ of the string (to be discussed later). A further differentiation of the spring force yields two terms that can be put into an equation:

$$\frac{\partial F}{\partial z} = -m' \cdot \frac{\partial^2 \xi}{\partial t^2}; \qquad \frac{\partial F}{\partial z} = -\Psi \cdot \frac{\partial^2 \xi}{\partial z^2}; \qquad \text{this yields:} \qquad \boxed{\Psi \cdot \frac{\partial^2 \xi}{\partial z^2} = m' \cdot \frac{\partial^2 \xi}{\partial t^2}}$$

The differential equation derived this way is called the **wave equation**. It interconnects the second place-derivative (curvature) with the second time-derivative (acceleration). The general solution consists of the superposition of an arbitrary number of waves that each may run towards the left or towards the right. However, the magnitude of the propagation needs to be equal for all waves because it depends – as a constant – on the transmission line parameters (string parameters). For waves running towards the right, we defined c (arbitrarily) as positive, and for waves running towards the left as negative. The wave impedance $Z_W = F/v$ is also carrying a sign; given the sign-convention used previously here, a positive wave impedance is for the wave running towards the right, and a negative wave impedance is for the wave running towards the left.

$$c^2 = \Psi / m'; \quad c = \pm\sqrt{\Psi / m'} \qquad Z_W^2 = \Psi \cdot m'; \quad Z_W = \pm\sqrt{\Psi \cdot m'}$$

 © M. Zollner & T. Zwicker, 2002 & 2020

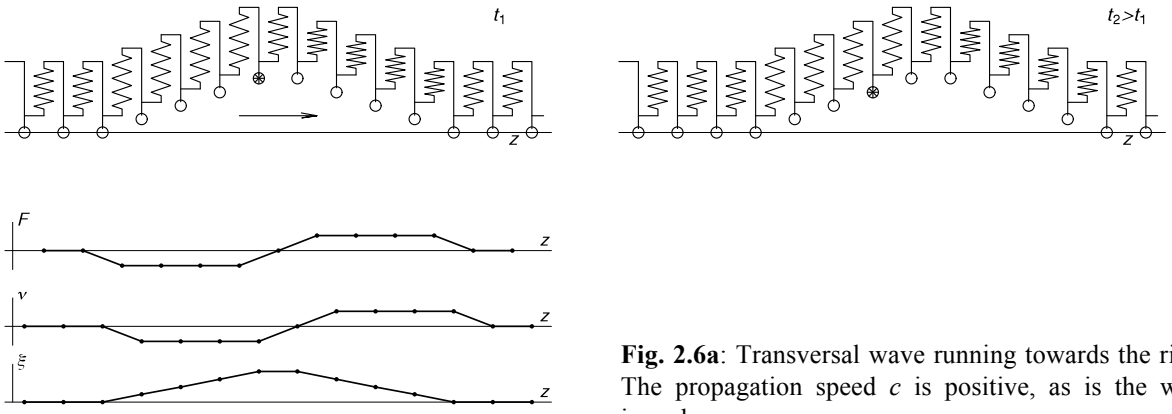

Fig. 2.6a: Transversal wave running towards the right. The propagation speed c is positive, as is the wave impedance.

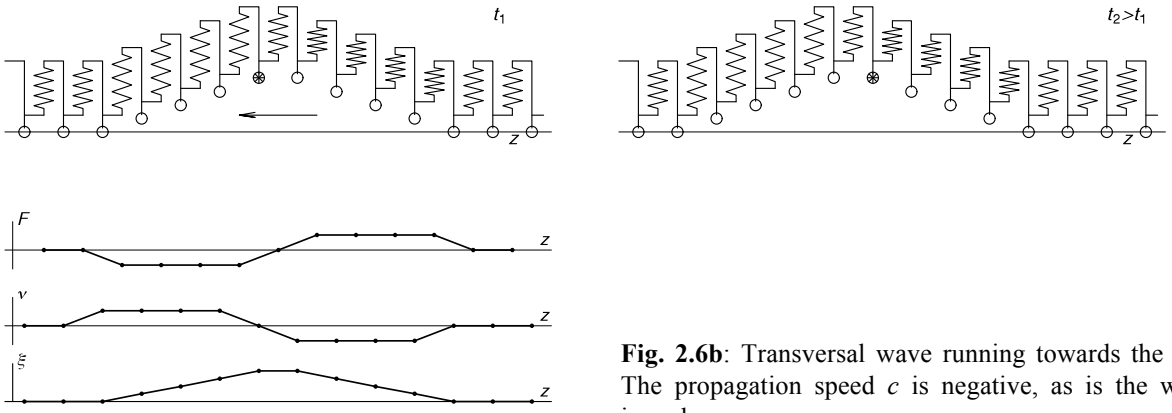

Fig. 2.6b: Transversal wave running towards the left. The propagation speed c is negative, as is the wave impedance.

Fig. 2.6 depicts a progressing wave at the two points in time of t_1 and t_2; the difference in displacement allows for deduction of the momentary velocity. For example, for the wave running towards the right, the mass tagged with * moves downwards, and its velocity therefore is negative. However, the force F shown here is not the inertia force but the force transmitted in the springs. Via the place-function, the displacement F is unambiguously determined; in order to determine v, though, we need to additionally know c.

It is not obligatory to connect the springs as shown in Fig. 2.6. Alternatively, the upper end of the spring could be connected to the mass positioned adjacent, and the lower end could be connected to the mass on the right. However, this connection would require reversal of the sign of the force! As a consequence, the wave running towards the left would have a positive wave impedance, and the wave running to the right a negative one. Both changes do not represent a contradiction: the spring-mass-model is a direct visualization of a mechanical tension state. To start with, the sign in this model may be arbitrarily defined – subsequently, however, all following calculations are committed to this definition. Instead of the spring-mass-model, it would also be possible to define place-discrete shear stresses, but again this would entail freedom in setting the sign.

© M. Zollner & Tilmann Zwicker, 2002 & 2020

The following graph (**Fig. 2.7**) gives an overview for different triangular displacement waves. Seven function graphs – positioned one above the other – indicate seven consecutive points in time; the start is in the uppermost line each. All depictions show the place-functions along the *z*-coordinate. For all examples it is assumed that a transversal wave only moves along the string. As soon as we allow for a superposition of waves running in different directions, a new degree of freedom is introduced for the velocity (Fig. 2.8). The force, however, is always connected unambiguously with the displacement.

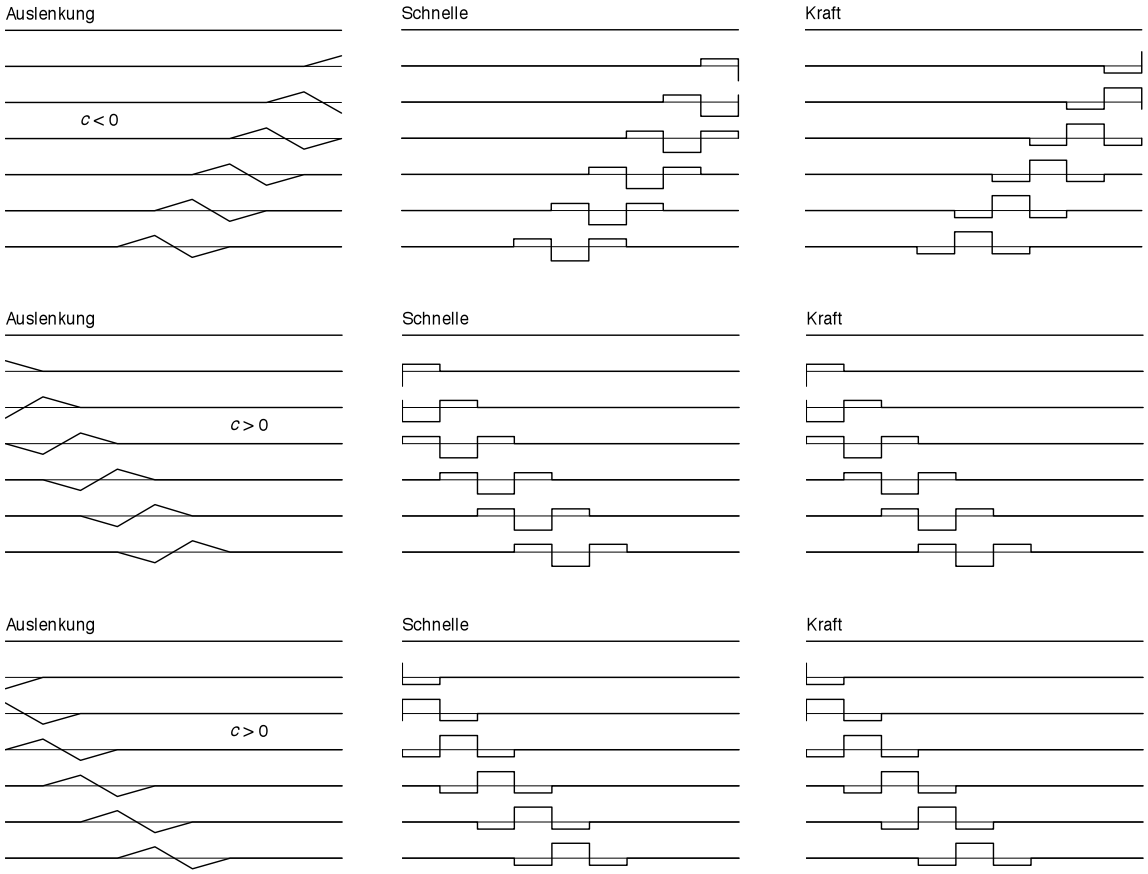

Fig. 2.7: Place-function of the displacement (= "Auslenkung"), the (particle) velocity (= "Schnelle"), and the transverse force (= "Kraft") for three different waves.

In **Fig. 2.8** we see the superposition of two waves running in different directions. At the fifth point in time, the velocity is zero for all points in the string. This special condition cannot be realized with *one single* wave; for $c \neq 0$ the displacement would otherwise have to be always zero for the whole of the string.

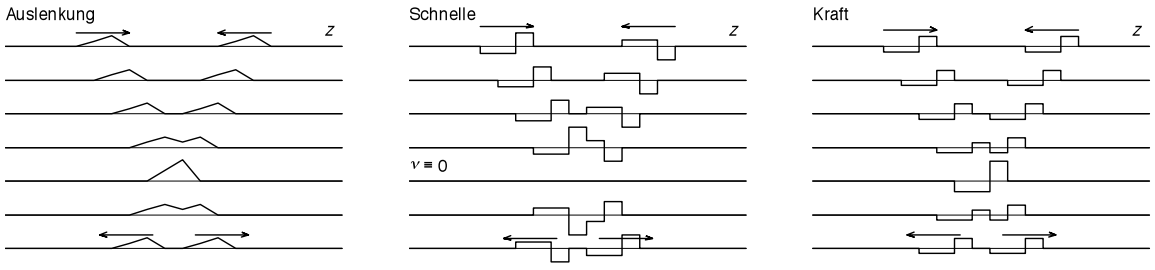

Fig. 2.8: Place-function of the displacement (= "Auslenkung"), the (particle) velocity (= "Schnelle"), and the transverse force (= "Kraft"). The sum of the force cannot be calculated from the sum of the velocity anymore.

 © M. Zollner & T. Zwicker, 2002 & 2020

2.2 Modeling of reflections with mirror waves

As long as the wave impedance of a string remains the same at all locations, there is an unperturbed wave propagation. Conversely, any local change in the wave impedance has the effect of part of the wave reversing its direction and running back to the source (i.e. it is reflected). Particularly strong changes happen at the bearing points of the string: the bearing impedance F/v is very high, while v is almost zero due to the small bearing compliance. In an acoustic guitar, the bridge needs to feature a certain compliance in order to feed part of the energy of the string vibration to the guitar body (and have it radiated as airborne sound from there). For the electric guitar, however, the radiation of sound via the body is not a priority; the **impedance** of the bearing points is very high, and the velocity of the bearing points is approximately zero.

A reflection at a bearing may be described in two ways: either we consider the perturbation of the wave impedance and formulate laws for the reflection, or we ignore the change in the wave impedance and force the bearing condition $v = 0$ via two waves running against each other. Let us apply the latter approach here: the wave propagating in the direction of the bearing is supplemented by a **mirror wave** that runs towards the bearing from the other side. Both waves can run across the bearing in an undisturbed (!) fashion – just as if the bearing points would not exist at all. The parameters of the mirror wave need to be chosen such that at every point in time the bearing condition of $v = 0$ at the bearing persists. The wave and the corresponding mirror wave add up; the sum emulates the reflection process.

Fig. 2.9 shows a triangular displacement wave running to the right towards the bearing indicated by a vertical line. In the right-hand section of the figure, a mirror wave runs towards the first wave; the two displacement waves are point-symmetric (for this bearing that is defined as being un-yielding). Correspondingly, the velocity is shown in the middle graph. Due to the point-symmetric character, displacement and velocity are always zero at the bearing. Via the wave impedance (carrying a sign), we arrive, starting from the velocity, at the axisymmetric force (graph on the right). However, this v-F-transformation only holds for the individual waves but not for their sum. The actual bearing force is double the force that would exist for the individual unperturbed wave running across the bearing. Using the above sign definition we get: **displacement and velocity are reflected with opposite phase, the force is reflected with the same phase**. It does not make any difference in the function graphs whether we interpret the wave running towards the right in Fig. 2.9 as the cause that has as effect a reflection running towards the left, or whether we see it the other way round (i.e. the wave running towards the left is reflected towards the right). Identical graphs result from both cases.

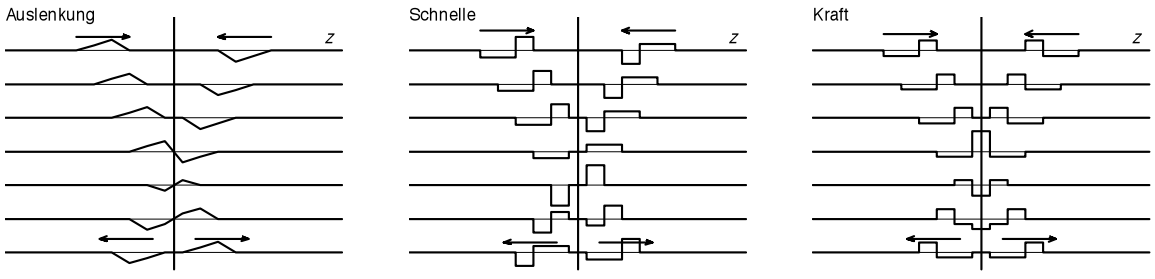

Fig. 2.9: Model of the reflection via a mirror wave running in the opposite direction. The bearing is in the middle of each graph. We see 7 consecutive points in time from top to bottom.
"Auslenkung" = displacement, "Schnelle" = particle velocity, "Kraft" = force.

© M. Zollner & Tilmann Zwicker, 2002 & 2020 Translation by Tilmann Zwicker

2.3 Standing waves

The waves considered so far all featured a direction of propagation: either towards the right i.e. in the direction of increasing *z*-coordinate (positive propagation speed *c*), or towards the left (negative *c*). Such waves are called *propagating waves* or *travelling waves*. They transport **active (wattful) energy**: $E = P \cdot t = F \cdot v \cdot t$. Two superimposed, equal-energy waves running towards each other yield zero energy flux, though. There is reactive energy in the potential spring-energy or in the kinetic mass-energy; however, the mean power value across full periods of the vibration is still zero.

For a transmission line terminated at its end with an infinite bearing impedance *Z*, it is not possible to feed any energy to the bearing. This is because the velocity at the bearing is always zero: $v = F / Z = F / \infty$. Therefore all of the wave energy arriving at the bearing is reflected – with the amplitudes of the waves running to and from being necessarily equal. The superposition resulting from this is designated **standing wave**. This term holds for every waveshape but is particularly descriptive for sinusoidal waves (**Fig. 2.10**). In the propagating wave, the amplitude is constant and the phase changes as a function of time, while in the standing wave, the phase (as a function of place) remains constant but the amplitude changes over time.

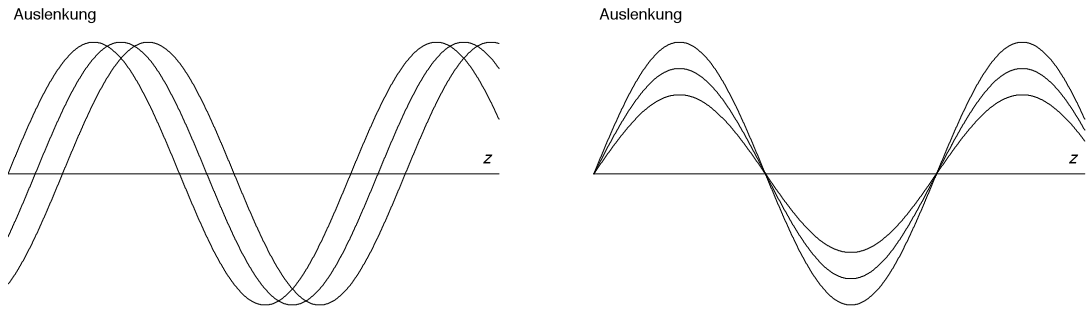

Fig. 2.10: Propagating sinusoidal wave (left); standing wave (right). Along the place-coordinate (*z*) , the displacement is shown at three consecutive points in time. “Auslenkung” = displacement.

Literature often describes waves running on transmission lines as sinusoidal. For guitar strings, however, we find (at least during the plucking process) a **triangular shape**. At the plucking point, the string is deflected by a transverse force, and for a moment there is (approximately) a triangular string deflection. As soon as the contact between pick (or finger) and string breaks off, two triangular waves run from each other in opposite directions. They are reflected at the string bearings and form – as a sum of all reflections – a standing wave. Instead of reflections we could also define **mirror waves** (see the previous chapter) that run in an unimpeded manner across the bearing points (without reflection). In that model, the **boundary conditions** of the triangular excitation shape, and of the idealized bearing condition of $\xi \equiv 0$ need to be respected. Given the simplifying assumption of lossless propagation and reflection, every wave is reflected an infinite number of times. Therefore an infinite number of mirror waves is required that all run along the string with equal magnitude of the propagation speed. All waves running with a positive *c* can be combined (superimposed) into *one* summation wave running to the right; the same way all waves running to the left can be combined. The standing wave thus may be described by two summation waves running in different directions.

 © M. Zollner & T. Zwicker, 2002 & 2020

Since in the present model we assume dispersion-free propagation, the propagation speed c is not dependent on frequency. The distance in time between two reflections (of the same event) occurring in the same direction (!) therefore is $T = 2l/c$ for all spectral components. Herein l corresponds to the length of the string – it needs to be run through twice until the subsequent reflection occurs e.g. at the right-hand bearing. Given knowledge of the place-function of the excitation, the sum of the waves is easily described with this: its place-periodicity is double the length of the string, and the displacement- and velocity-place-functions are point-symmetric relative to the bearing. At the point in time $t = 0$ both summation waves are identical but run away from each other in opposite directions for $t > 0$. The term **summation wave** indicates the sum of all waves travelling *in the same direction*. The summation wave running towards the left needs to be added to the summation wave running towards the right in order to obtain the actual wave on the string. [Animations can be found at: https::/www.gitec-forum-eng.de/knowledge-base-2/collection-of-animations/].

Fig. 2.11 shows a string deflected in triangular fashion between its bearing points. The top row starts on the left with the initial state. To the right, the two summation waves are depicted – the displacement may be thought as both being combined. At the point in time $t = 0$ the two summation waves are identical, and therefore only *one single* curve can be seen. In the right-hand section of the figure we see a later point in time, with the summation waves having already diverged a bit. The superposition of the two summation waves (second row in the figure) gives the actual course of the displacement – which at the bearing points needs to be zero always (unyielding bearing). In the right-hand graph of the lower row of the figure, several subsequent points in time of the wave propagation are depicted.

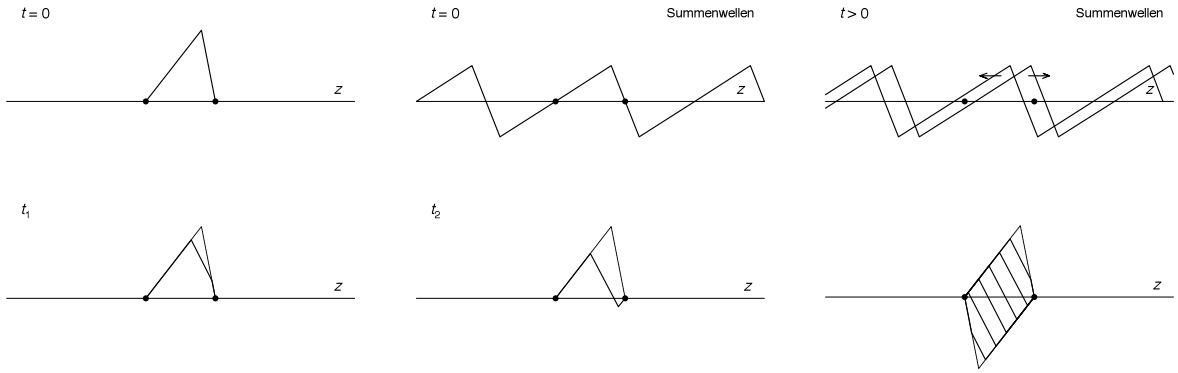

Fig. 2.11: Propagation of a triangular displacement wave. The unyielding string bearings are marked as dots. The wave runs back and forth in a zigzag shape between the dashed end positions.
"Summenwellen" = summation waves.

Books frequently depict string vibrations in a sine-shape – similar to the graphs in Fig. 2.10. These are, however, mono-frequent special cases. The shape of the displacement is – at the moment of excitation – triangular, as shown in Fig. 2.11. The string oscillates back and forth in a zigzag shape; the wave-shape changes over time, though. The damping increases with frequency and blunts the shape, and in addition dispersion occurs (the high frequencies run with a higher propagation speed). These changes in shape are not embraced here; Fig. 2.11 shows a simplification of the basic behavior. The plane of vibration is not considered, either: the vibration of the string is a movement in space, with rotation of the plane of polarization occurring at the bearings. Even with the string plucked e.g. precisely perpendicular to the fretboard, a fretboard-parallel component will emerge over time.

© M. Zollner & Tilmann Zwicker, 2002 & 2020

From the place-function of the displacement shown in Fig. 2.11, the place-functions of the velocity and the force may be deduced – and their time-functions, as well. The velocity is the excitation quantity for the magnetic pickup, and the force is the quantity affecting the bearing (as it is processed e.g. by piezoelectric pickups). It was already shown that the velocity results from the *place*-derivative of the displacement – however this holds only for propagating waves and not for standing waves. In the following equation, the propagation speed c needs to be inserted including its sign: for waves running towards the right this is by definition negative, and thus $-c$ becomes positive.

$$v(z)\big|_{t=t_0} = -c \cdot \frac{d\xi(z)}{dz}\bigg|_{t=t_0}$$ Place-function: displacement → velocity

The standing wave therefore is to be dissected – as shown in Fig. 2.12 – into two summation waves. The place-derivative of each of these waves is then multiplied by $-c$. For triangular excitation, the result is depicted in Fig. 2.12: the triangular **displacement** does not oscillate up and down – rather, a zigzag-wave runs back and forth between the triangular border-positions. The **velocity** has the shape of a rectangular impulse that is reflected in opposite phase at the bearings. The **force**-wave has a rectangular shape, as well, but the reflection happens with the same phase here. All three place-functions are standing waves aggregated from two summation waves each. Between the summation waves, a simple conversion ($\xi \Leftrightarrow v \Leftrightarrow F$) is possible, while for the actual aggregated functions (standing waves) a simple correspondence can only by found between the displacement and the force: $F = -\Psi \cdot \partial\xi / \partial z$.

In order to be able to attribute the place-function of the force unequivocally to the displacement, Fig. 2.13 again shows the spring-mass-model. For two conditions, it very nicely demonstrates the triangular displacement, and the rectangular distribution of the (spring-) force.

With the place-functions known, we can now determine the time-functions. Again this holds: the summation-place-functions can be converted into the summation-time-functions with little effort, while for standing waves this is not directly possible. First we will look at the bearing force that results from two summation waves running towards each other. The starting condition ($v \equiv 0$) forces both summation waves $F(z)$ to have an identical shape at the starting point in time ($t = 0$); the bearing condition ($\xi = 0$) forces an odd (point-symmetric) course of the displacement $\xi(z)$ relative to the bearing, and an even (axisymmetric) course of the force $F(z)$, due to the differentiation. Because both axisymmetric summation waves run towards the bearing with equal-amount propagation speed c, the bearing force amounts – at any given point in time – to twice the force acting on the bearing due to a single summation wave. Therefore, the time-function of the bearing force can be determined from the place-function of the force-summation-wave via a simple argument-transformation ($z = ct$), see Fig. 2.14.

The periodic time-function of the bearing force is linked to a spectrum of discrete lines with the fundamental frequency of $f_0 = 1/T$; $T = 2l/c$ is the time-periodicity here. The spectral envelope is an **si-function** [$\mathrm{si}(x) = \sin(x)/x$]; its zeroes result from the partitioning of the place-related displacement: a string partitioning of 4:1 cancels the 5th harmonic.

Animations at: https::/www.gitec-forum-eng.de/knowledge-base-2/collection-of-animations/

© M. Zollner & T. Zwicker, 2002 & 2020

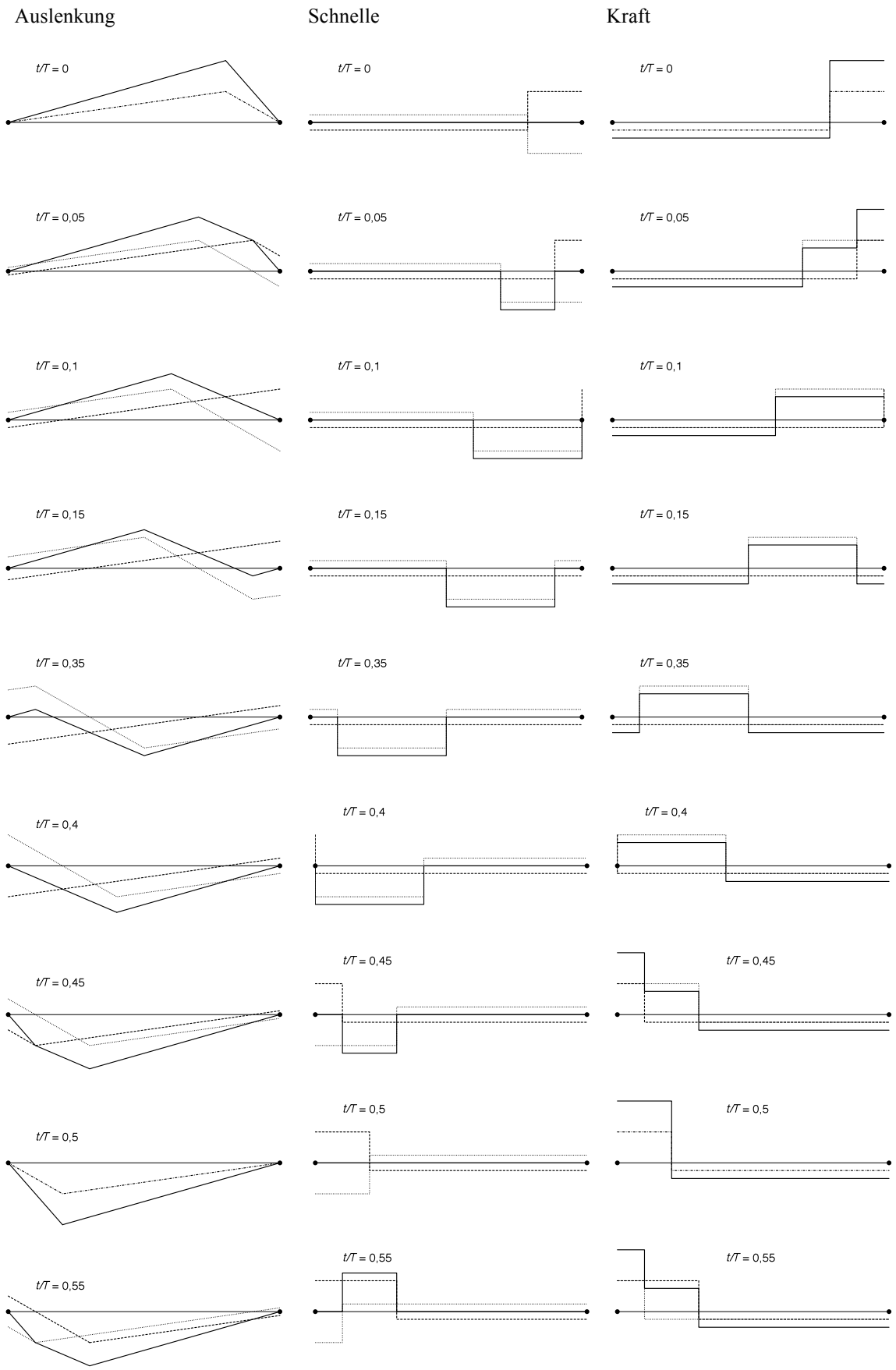

Fig. 2.12: Triangle wave: place-function for 9 different points in time (T = periodicity). The velocity triangle is reflected with opposite phase, the force triangle with the same phase. Direction of propagation: ----→, ←·····. "Auslenkung" = displacement, "Schnelle" = (particle) velocity, "Kraft" = force.

© M. Zollner & Tilmann Zwicker, 2002 & 2020

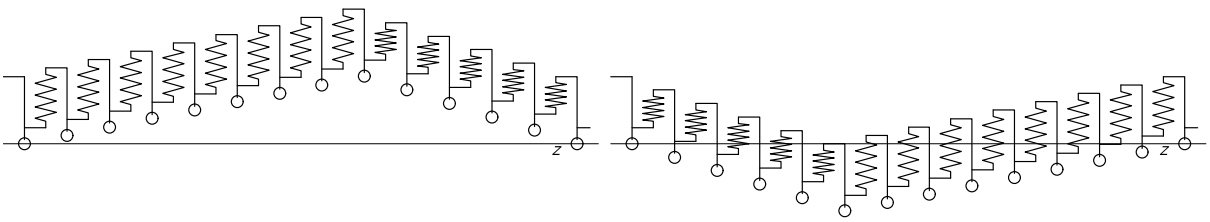

Fig. 2.13: Triangle wave: spring-mass-model (compare to Fig. 2.6). The place-function of the force may be deduced from the deformation of the springs. In the graph on the left, the force left of the salient point is negative, the force to the right is positive (sign convention: compression stress = positive sign). In the right hand graph, the force left of the salient point is positive; to the right it is negative.

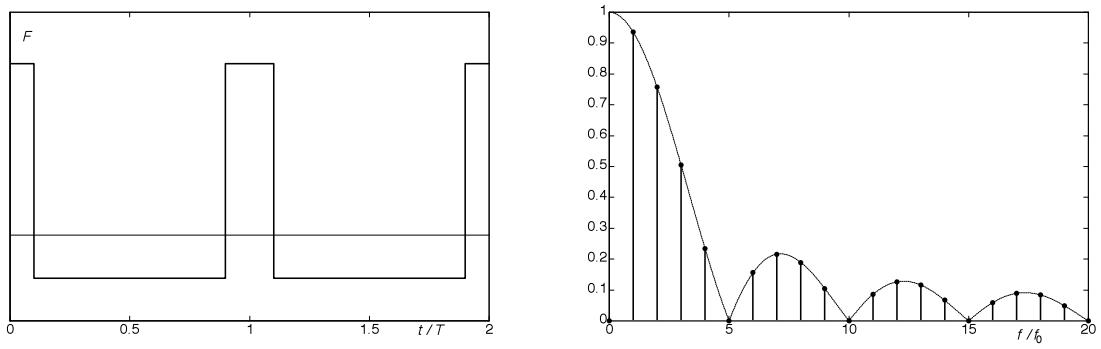

Fig. 2.14: Time-function and magnitude spectrum of the bearing force; triangular displacement similar to Fig. 2.12. The average of the progression of the force over time is zero, and the DC-component in the spectrum thus is zero, as well. Integer multiples of the quintuple of the fundamental frequency are cancelled if the distance between bridge and plucking point is $1/5^{th}$ of the length of the string (graph on the left).

Fig. 2.15 presents the result of a voltage measurement. The E_4-string of an Ovation (EA-86) was plucked using a plectrum, with the built-in piezo pickup serving as sensor. The shape of the voltage is basically rectangular (i.e. a pulse) – the superimposed vibrations are effects of the dispersive wave propagation. We can interpret the piezo pickup in a simplified fashion as a force-voltage converter transforming the wave forces acting in the bridge into a correspondingly proportional electrical voltage. The duty factor of the pulse corresponds to the division-ratio of the plucking point on the string (32:32, 51:13).

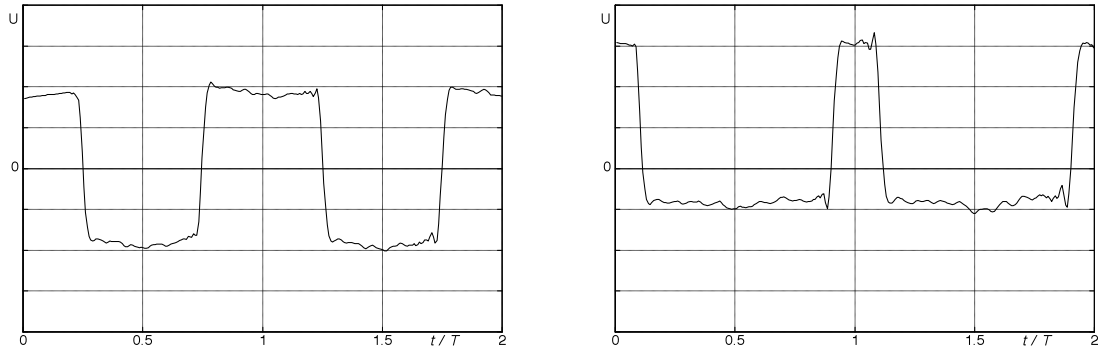

Fig. 2.15: Electrical voltage measured in the piezo pickup built into the bridge. Basically, the shape is rectangular – cause of the vibrations are resonances and dispersive wave propagation. Distance from plucking point to the bridge: 32cm (left), 13cm (right); String length = 64 cm.

 © M. Zollner & T. Zwicker, 2002 & 2020

At the point in time of the plucking action (assumed to be at $t = 0$), the actual **velocity of the string** is zero for all points on the string – the string starts off displaced but at rest. For the two summation waves, opposite signs follow: $v_R(z, t=0) = -v_L(z, t=0)$. Here, the index marks the direction of the propagation: R = running right, L = running left. Moreover, the actual velocity is always zero at the bearings (assumed to be immobile), and therefore the summation waves need to be point-symmetric relative to each other for $t = 0$. Consequently, $v_R(z, t) = -v_L(-z, t)$ is valid for all points in time. From these two conditions it follows that both summation waves are even functions for $t = 0$: $v_R(z, t=0) = v_R(-z, t=0)$, $v_L(z, t=0) = v_L(-z, t=0)$.

For the electric guitar, the string velocity is the input quantity for the **magnetic pickup**. Determining the spectrum is more complicated than for the piezo pickup because velocity sensors cannot be operated at the bridge. Typically, the magnetic pickup is located below the string at 3 – 15 cm away from the bridge, this distance being designated z_{TS} while the corresponding delay time is termed τ_{TS}. To determine the string velocity above the pickup, we start from the triangular string displacement, and require several transformations. The actual displacement is dissected into two summation waves, and the local derivative yields the place-function of the velocity. Then, an argument-transformation ($z = z_0 - ct$) yields (from the place-function) the time-function, with the time-delay τ_{TS} corresponding to a phase-shift in the frequency domain. At the bridge, the actual velocity is the result of two components that always sum up to zero due to the above mentioned symmetries: $v_\Sigma(t) = v(t) - v(t)$. At the position of the pickup, the delay time needs to be considered with different signs: $v_\Sigma(t) = v(t + \tau_{TS}) - v(t - \tau_{TS})$. With the displacement law of the Fourier-transform, this results in:

$$\underline{V}_\Sigma(j\omega) = \underline{V}(j\omega) \cdot e^{j\omega\tau} - \underline{V}(j\omega) \cdot e^{-j\omega\tau} = \underline{V}(j\omega) \cdot 2j \cdot \sin(\omega\tau) \qquad \text{mit } \tau = \tau_{TS} = z_{TS}/c$$

Herein, $\underline{V}_\Sigma(j\omega)$ is the velocity spectrum of the string at the location of the pickup; this spectrum results from the velocity spectrum $\underline{V}(j\omega)$ of a summation wave via multiplication with a sine-function. The summation wave of the velocity features a harmonic spectrum of discrete lines with the zeroes in the si-shaped spectral envelope determined by the plucking location – as it was for the bearing force. This spectrum is to be multiplied with the above-mentioned sine-function, the zeroes of which are determined by the position of the pickup. **Fig. 2.17** shows the velocity spectra for an E_2-string. Depending on the pickup placement and the place of plucking, a characteristic, sound-determining envelope results (shown in red in the figure).

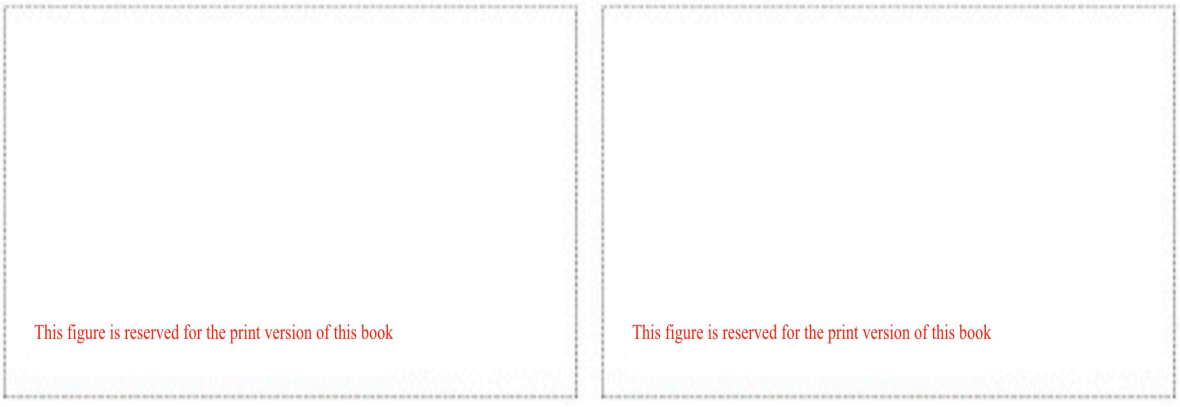

Fig. 2.17: Level-spectrum of the actual string velocity at the place of the pickup. The place of plucking is 11 cm from the bridge; the pickup is located at a distance of 15 cm (left) and 5cm (right) from the bridge. Scale length (length of the string) = 66 cm. f_0 = 82,4 Hz.

© M. Zollner & Tilmann Zwicker, 2002 & 2020

2.4 Transitory processes

Systems theory describes linear, time-invariant (LTI-) systems via their **impulse response**. In fact, the impulse response $h(t)$ is a *system*-quantity; it may however also be seen as a *signal*-quantity found at the output of the system that in turn is excited at its input with a (Dirac-) impulse $\delta(t)$. Using, instead of the Dirac-impulse, its particulate integral over time, the output of the system yields the particulate integral of the impulse response: this is the **step response**. Dirac-impulse and step are idealizations that, in reality, occur merely approximately. As a pre-consideration, let us excite the string with a **force step**: a transverse force acting externally on the string changes its value from 0 to F at the point in time of $t = 0$, with the string at rest (not deflected) for any time $t < 0$. It is unimportant for the model consideration how such a force-step can be realized, but it is important that F remains constant – and in particular that it does not depend on the displacement. The string bearing is immobile at *one* position ($z = 0$), and the other (right-hand) bearing is very far away. At the distance d from the bearing at $z = 0$, the **external force** F acts on the string (**Fig. 2.18**).

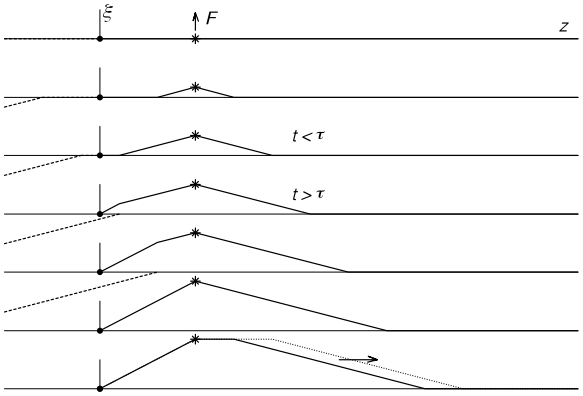

Fig. 2.18: Place-function of the displacement. Shown from top to bottom are 7 subsequent states. The immobile bearing is given by a dot; a constant external force acts at the place marked by a star. For the first 5 graphs, the mirror wave arriving from the left is indicated by the dashed line; for the last two graphs it is not shown. The further course of the wave is represented as a dotted line in the bottom graph.

The wave impedance Z_W is defined via the (mechanical) string data. As long as no reflection has arrived at the excitation point (star), Z_W describes the quotient between force F and velocity v. Since the excitation point is, however, loaded by *two* transmission lines (to the left and to the right), the input impedance is doubled i.e. it is $2Z_W$ (seen from an external point of view). In considerations of analogy with an electrical line, we need take into account that the *F-I*-analogy results in reciprocal impedances: impedance ↔ admittance. Imprinting a constant force at the location of the star will generate a transverse movement with the constant velocity: $v = F/(2Z_W)$. The **reflection** is considered via a mirror wave arriving from the left; it reaches the location of the star after the time $\tau = 2d/c$ (c = propagation speed). For $t > \tau$, the quotient between F and v is not determined by Z_W anymore, because there are now two waves superimposed at the location of the star. The two counteracting velocity-waves interact such that the point of the string marked by a star changes its velocity from v to zero at $t = \tau$. This point remains at a fixed displacement for $t > \tau$. The displacement $\hat{\xi}$ at this location may be calculated:

$$\hat{\xi} = \tau \cdot v = \frac{2d \cdot F}{c \cdot 2Z_W} = \frac{d \cdot F}{\Psi}$$

Maximum displacement at the location of the star, $t \geq \tau$

The parallelogram of forces yields the same value if the tension force of the string Ψ, and the transverse force are F, are formulated orthogonally: $\hat{\xi}/d = F/\Psi$.

 © M. Zollner & T. Zwicker, 2002 & 2020

The point in time of $t = \tau$ separates two different processes: during $t < \tau$ the transient process (an aperiodic movement) takes place. For $t > \tau$, the stationary final state between the bearing (symbolized by the dot) and the point where the force is applied (symbolized by the star) is reached.

In the case that (as is shown in Fig. 2.18) the right hand bearing is very far away, a slope (indicated as dotted line in the figure) runs to the right without perturbation. The section of the string between the (right-hand) bearing and the position given by the star stops moving at the point in time of τ, it then remains at rest. However, if reflections can happen on the right-hand side, as well, a continuously vibrating **standing wave** results. Still, this model does not simulate the plucking process because in the latter the force does not jump from 0 to F but from F to 0. Given LTI-conditions, though, an $F \rightarrow 0$ jump may be seen as the sum of a negative force-step and a force constant at all times:

$$F = F_1 + F_2; \qquad F_1 = \begin{cases} 0 & t < 0 \\ -\hat{F} & t > 0 \end{cases}; \qquad F_2 = \hat{F}\,.$$

The boundary conditions now are: for negative time a constant force $\hat{F}$ acts on a point of the string – the string is displaced but at rest. At the point in time $t = 0$, the force jumps from $\hat{F}$ to 0 with an oscillation starting that is superimposed onto the triangular displacement. The initial situation ($t < 0$) is shown in **Fig. 2.19**. The external force $\hat{F}$ (constant over time) finds its counter-forces in the bearing forces F_L and F_R. While the signs of the string-internal forces and the external forces require some getting-used-to, they are consistent. For positive time $t > 0$, the external force $\hat{F}$ vanishes – from this point in time the two bearing forces thus need to be void of any mean value (**Fig. 2.20**).

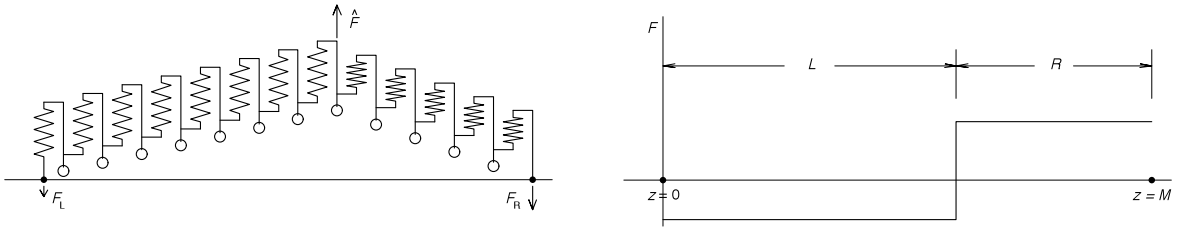

Fig. 2.19: Spring-mass-model for $t < 0$ (left), and corresponding string-internal force-place-function.

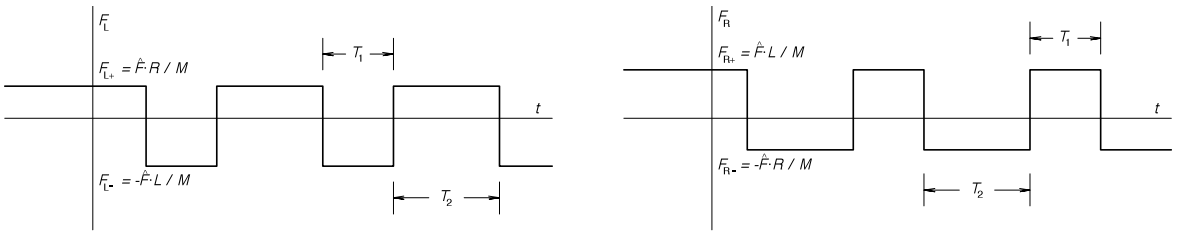

Fig. 2.20: Time-function for the bearing forces; at $t = 0$, the excitation $\hat{F}$ jumps to zero. The signs of the bearing forces are defined comparably among each other: if the string is displaced in the ξ-direction, a counter-force needs to act at both bearings; their direction is indicated with an arrow. The string-length is M – it is divided into a left-hand (L) and a right-hand (R) section. $T_1 = TR/M$, $T_2 = TL/M$, $T = 1/f_G$.

© M. Zollner & Tilmann Zwicker, 2002 & 2020

2.5 Calculation of reflections

In Chapter 2.2, we had introduced a model of mirror-waves in order to describe reflections of waves. In it, the wave under consideration runs across the bearing (and disappears), and at the same time a mirror wave running in the opposite direction emerges from the bearing. As an alternative to these two waves propagating in an unperturbed fashion, it may be expedient to look at only *one single* wave that is reflected at the bearing according to certain criteria. This reflection model gives advantages in particular for the type of modeling of the string that uses delay units.

2.5.1 The reflection factor

Every propagating wave (travelling wave) transports energy: in the electrical transmission line this is the energy of the magnetic and electric field, while in the mechanical line it is kinetic and potential energy. The mean values of the mechanical energy calculate as:

$$E_k = dm \cdot v^2/2\,; \quad E_p = dn \cdot F^2/2 \qquad \xrightarrow{F = v \cdot Z_W} \qquad E_k = E_p$$

The two transported (mean) energies are equal at each place of the transmission line. As the wave arrives at the end of the string, this energy cannot disappear into nothingness; it is either coupled into the bearing (and transported further there, or dissipated) or it is (fully or partially) reflected.

All bearings show complicated **bearing impedances**. The bearing impedance is anisotropic i.e. depends on the plane of vibration, and it is dependent on frequency. The compliance is the inverse of the complex bearing impedance and is defined as a complex **admittance**:

$$\underline{Y} = \underline{v}/\underline{F} = G + jB \quad \text{Admittance} = \text{conductance} + j \cdot \text{susceptance}$$

$$\underline{Z} = \underline{F}/\underline{v} = R + jX \quad \text{Impedance} = \text{resistance} + j \cdot \text{reactance} = 1/\text{admittance}$$

An unyielding, rigid bearing (small admittance, high impedance) can absorb forces but does not allow for movement; the compliant bearing behaves conversely. Strings are anchored in relatively unyielding bearings. For the electric guitar only, the bearings may be totally rigid – in the real world, such an ideal is of course not possible. If the bearings on an acoustic guitar were fully unyielding, they could (due to $v = 0$) not receive any energy from the string, and could not transmit it further to eventually radiate sound.

The bearing impedance (or admittance) connects the two field quantities of force and (particle) velocity; their product is the power P. The requirement for continuity demands $F_{\text{string}} = F_{\text{bearing}}$ and $v_{\text{string}} = v_{\text{bearing}}$. On the string, the quotient F/v is equal to Z_W for the propagating wave, but at the bearing, this quotient may take on any value. At first, this appears to be a contradiction. If a 2-N-force-wave runs through a transmission line of a wave-impedance of 1 Ns/m, the velocity is 2 m/s. As this wave now encounters a bearing of a bearing-impedance of 10 Ns/m, the bearing cannot fully absorb the wave energy. The bearing "extracts" from the arriving wave that part of the energy that matches the bearing impedance in terms of the F- and v-components. The remainder of the energy is "sent back".

 © M. Zollner & T. Zwicker, 2002 & 2020

Therefore, *two* waves (incoming and reflected) running in opposite directions are superimposed at the bearing and at every point of the string. Force and velocity thus result from the sum of two values. The wave running in the opposite direction at the plucking location has to be considered including its reflection – and the subsequently generated reflections, as well. All waves are reflected after having run the length of the string, i.e. more and more waves superimpose. The sum of all superimposed waves results in the **steady-state condition** that may be calculated via the tools offered by network analysis. Calculating the line impedance $Z(z)$ for this steady-state condition at any arbitrary point z will not yield the wave impedance (at least not for the general case).

At this point, the wave "sent back" in the above example is unknown. In order to calculate it, we formulate the force $F(z)$ and the velocity $v(z)$ acting at each point of the line as a sum of two waves♣. The waves $F_h(z)$ and $v_h(z)$ running towards the bearing are given; knowing one of the two is sufficient; the other can be calculated from it. The reflected waves $F_r(z)$ and $v_r(z)$, while also linked via Z_W, are yet unknown. The bearing impedance delivers the missing condition, because at the bearing point (e.g. at $z = 0$) the quotient of $F(z = 0)$ and $v(z = 0)$ is equal to the **bearing impedance** Z_L. As has already been the case a number of times, the **sign** springs a surprise: at the right-hand bearing, $Z_L = F/v$ holds, and at the left-hand bearing, we have $Z_L = -F/v$. This reversal of the sign is easiest seen in Fig. 2.5: a left-hand bearing can be generated by making $F_1 = 0$; the left-hand mass is now removed, and the formula indicated as "law of inertia" carries a minus-sign. Similarly, $F_2 = 0$ yields a plus-sign. The wave impedance includes its peculiarity in terms of the sign, too: for waves running towards the left, Z_W is negative, for those running towards the right, it is positive (Chapter 2.1). Superimposing the waves running back and forth we would have to do the math with two different wave impedances. However, for the following calculations Z_W is **strictly positive** – for the waves running to the left we insert a minus-sign. In the below calculation we consider a wave running ("hither") towards the left onto the left-hand bearing ($z = 0$), and a wave reflected towards the right:

$$F_h = -v_h \cdot Z_W; \qquad F_r = v_r \cdot Z_W; \qquad Z_W = \sqrt{\Psi \cdot m'} > 0$$

$$F_L = F_h + F_r; \qquad v_L = v_h + v_r; \qquad Z_L = -F_L / v_L$$

$$(v_h + v_r) \cdot Z_L = -(F_h + F_r) = -(-v_h + v_r) \cdot Z_W \qquad \Rightarrow \qquad \frac{v_r}{v_h} = \frac{Z_W - Z_L}{Z_W + Z_L}$$

The ratio of the complex amplitudes within the back-and-forth-running wave is the complex **reflection coefficient** r. It is dependent on the wave impedance Z_W and on the bearing impedance Z_L:

$$r_v = \frac{v_r}{v_h} = \frac{Z_W - Z_L}{Z_W + Z_L} \qquad r_F = \frac{F_r}{F_h} = \frac{v_r \cdot Z_W}{-v_h \cdot Z_W} = -r_v \qquad \text{Reflection coefficient}$$

There are three interesting special cases: for $Z_L = Z_W$ (**matching condition**), the reflection coefficient becomes zero: the wave is not reflected and the bearing absorbs the whole of the wave energy without reflection. For $Z_L \to 0$, the reflection coefficient of the velocity becomes +1: the velocity wave is completely reflected with the same phase, and the force wave is completely reflected with opposite phase.

♣ F, v, and Z are complex; we make do without the underscoring here.

© M. Zollner & Tilmann Zwicker, 2002 & 2020

For $Z_L \to \infty$, the reflection coefficient of the velocity becomes –1: the velocity wave is completely reflected with opposite phase, and the force wave is completely reflected with the same phase. This is the case of the unyielding bearing where the velocity of the string is always zero. Of course, a guitar string must not be operated with $r = 0$ – otherwise a "periodic" vibration would never come into being. With $r = \pm 1$, the vibration would never decay – at least within the idealizations underlying here.

In Chapter 1.6, investigations regarding the decay process of the string vibration were introduced. It the vibration of an E_2-string decreases (strictly exponentially) e.g. by 60 dB within 12 s, it decays by 0,06 dB per 12 ms (1 period), corresponding to 0,7%. The reflection coefficient therefore is 0,993 per period. Since the wave on the string is reflected twice per period, this absorption of 0,7% needs to be divided up between bridge and nut (or fret), e.g. 0,3% at the nut/fret and 0,4% at the bridge. Typically, a refection coefficient of close to 1 is found.

Given strictly **real bearing impedance**, the reflection coefficient is real because Z_W is real, as well. For a real r, the phase shift between the original and the reflected wave is either 0° or 180°. In contrast to the reflection at an imaginary bearing impedance, the amplitude of the reflected wave is now smaller than that of the original wave. For a guitar string, the bearing impedance Z_L is large compared to Z_W, yielding the following as an approximation:

$$r_v = \frac{Z_W - Z_L}{Z_W + Z_L} = -\frac{1 - Z_W/Z_L}{1 + Z_W/Z_L} \approx -\left(1 - Z_W/Z_L\right)\cdot\left(1 - Z_W/Z_L\right) \approx -\left(1 - 2Z_W/Z_L\right)$$

A negative-real reflection coefficient indicates that the velocity-reflection happens with the opposite phase. If the real part of the reflection coefficient is not zero, active energy flows into the bearing points (**dissipation**, string damping). It makes no difference for the string whether this energy is radiated from the guitar body, or is converted directly into heat within the bearing – the drained energy is not available anymore as vibration energy.

The other extreme would be a purely imaginary bearing impedance as it is formed by a mass or a spring. Even if the bearing is composed of several masses and springs, *at any one single frequency* there will be either one inert or one stiff bearing impedance. For a **purely imaginary bearing impedance**, numerator and denominator of the reflection coefficient are complex conjugate; the absolute value of r therefore is 1. That is exactly 1! The waves running back and forth are phase-shifted relative to each other, but the absolute value is conserved: the vibration energy does not decrease. However, since the phase of propagating waves changes as a function of the place (wave equation), a phase-shifted reflection may be seen as non-phase-shifted reflection from another place. We can imagine that the wave is reflected without phase shift but at a small distance behind the bridge, with the phase shift resulting from this detour corresponding to the actual reflection. Depending on the sign it may be necessary to shift this imagined reflection place ahead of the bridge. The same holds for the nut (or fret). The effective string length may therefore differ from the geometric one: depending on the bearing impedance, and on the frequency, the length may be longer or shorter. This influences the frequency of the partials:

A springy bearing extends the effective length of the string, and it decreases the vibration frequency; the softer the spring, the lower f is. A mass-loaded bearing shortens the string and decreases the frequency; the lighter the mass the higher f is.

 © M. Zollner & T. Zwicker, 2002 & 2020

The reflection coefficient of the real string has both a real and an imaginary component, with both depending on the frequency. The real part causes the damping of the string, while the imaginary part has a detuning effect. In addition, string-internal mechanisms need to be considered – the present chapter is dedicated to the loss-free transmission line.

EXAMPLE: a tensioned string (L = 64 cm, $\rho = 8 \cdot 10^3$ kg/m^3, S = 0,5 mm^2, Ψ = 100 N) is suspended immovably on one side and springily on the other with s = 10.000 N/m, $s \neq s(f)$.

From this follows: Z_W = 0,633 Ns/m, c = 158,1 m/s, f_G = 123,5 Hz (without influence of the spring). Considering the elastic edge suspension, the fundamental frequency f_G decreases:

$$Z_L = s/j\omega = -j \cdot 12{,}89\,\text{Ns/m} \qquad r = \frac{Z_W - Z_L}{Z_W + Z_L} = -0{,}9952 + 0{,}0979\,j = e^{j \cdot 174{,}4°}$$

The absolute value of the reflection coefficient is 1, the angle is smaller than 180° by 5,6°. Running through a full length of the string, the phase of the wave is changed by 180°; a phase delay of 5,6° corresponds to a path-length of 2 cm. The one-sided elastic suspension effectively lengthens the string by 2 cm, decreasing the fundamental frequency to 119,8 Hz♣. The relative detuning is identical for all harmonics (disregarding the dispersion).◊

2.5.2 A resonator serving as bearing for the string

Any real bearing of a string needs to feature not only components behaving like springs, but also masses – and that makes bearing resonances unavoidable. At the resonance frequencies, the reactances (or conductances) compensate each other. Impedance and admittance are exclusively real. At all other frequencies, impedance and admittance remain complex [3].

As an example, a loss-free spring/mass-system will be investigated in the following. The impedance of its bearing computes to:

$$Z_L = j\omega m + s/j\omega \qquad \omega_r = \sqrt{s/m} \qquad f_r = \omega_r / 2\pi$$

For $\omega = \omega_r$ the impedance of the bearing becomes zero (no force despite movement), while for $\omega < \omega_r$ the bearing acts like a spring (spring-controlled). For $\omega > \omega_r$ it acts inert (mass-controlled). Below resonance, a string coupled to the bearing is in effect elongated. Above resonance, it will in effect be shortened. Even assuming the string to be dispersion-free, the frequencies of the partials are not laid out harmonically anymore: below the resonance frequency of the bearing, the frequency of the partials decreases, and above the resonance frequency of the bearing, it increases. The reflection coefficient for the velocity is:

$$r_v = \frac{Z_W - Z_L}{Z_W + Z_L} = \frac{Z_W - j(\omega m - s/\omega)}{Z_W + j(\omega m - s/\omega)} = -\frac{p^2 m - p Z_W + s}{p^2 m + p Z_W + s} \qquad p = j\omega$$

The frequency dependence of the reflection coefficient $r_v(j\omega)$ leads to a 2nd-order rational function. The even numerator- and denominator-potencies are identical, while the odd ones have an inverted sign. Numerator and denominator thus are complex conjugate relative to each other. This kind of frequency dependence is termed **all-pass function.**

♣ Real bearings are much stiffer; with them the detuning is smaller.

© M. Zollner & Tilmann Zwicker, 2002 & 2020 Translation by Tilmann Zwicker

The magnitude of an all-pass function is 1, and the phase shifts by $n \cdot \pi$ for $0 : f : \infty$, n being the order of the all-pass function. For $f = 0$, $r_v = -1$ holds: the velocity wave is reflected with opposite sign. For $f = f_r$ we obtain $r_v = +1$; for $f \to \infty$ we again get $r_v = -1$.

Therefore, having a resonator terminating the transmission line has the effect of an additional phase shift. Natural vibrations (partials) occur at those frequencies where the phase shift for a full travel-path on the string (2L; back and forth) is an integer multiple of 2π. Assuming dispersion-free wave propagation on a fully clamped-down string, partials at integer multiples of the fundamental frequency result. However, if a bearing acts as a resonator, an additional phase shift is introduced that generates (in our example) an **additional partial**. For resonators of higher order, several additional partials occur.

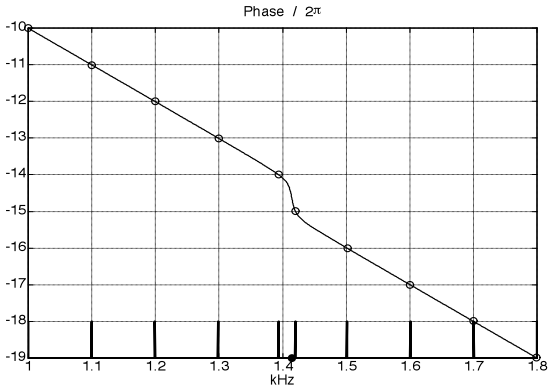

Fig. 2.21: Phase shift along a full travel path along the string. One string bearing is configured as a resonator resonating at 1,415 kHz. An additional natural frequency is the result of the narrow-band additional phase shift.

Fig. 2.21 shows the phase shift occurring for a string vibrating at a fundamental frequency of 100 Hz and a full travel path (double the string length). The phase is negative as it is customary for delays in recent literature. One string bearing is configured as a resonator with a resonance frequency of 1,415 kHz (dot on the abscissa). At the bottom of the graph, the frequencies of the partials are indicated with bars. The partial at 1,4 kHz is substantially detuned downwards by the bearing resonance, and an additional partial is generated at 1,42 kHz. All other de-tunings are too small to be recognizable in the figure.

The spectral derivative $-d\varphi/d\omega$ yields the **group delay** (Chapter 1.3.1). The slope of the phase function is virtually constant with the exception of the range around the bearing resonance. Thus, the group delay is also generally constant – only in the range of the bearing resonance it becomes longer. This leads to a warping in the spectrogram (Fig. 1.8).

2.6 Line losses

Ideal masses and springs store energy but do not dissipate them as heat. These elements are therefore termed “loss-less”. In contrast, any real string also features friction-resistances that irreversibly convert the vibration energy into caloric energy. Line theory considers these energy losses via distributed, differentially small resistances. It is insignificant for the model whether the losses are due to mechanical friction in the string (inner damping), or result from the string *directly* radiating sound energy (i.e. without detour through the guitar body).

 © M. Zollner & T. Zwicker, 2002 & 2020

With a level decreasing by 10 dB within 10s in the decay process, a low E-string looses about 2,8% of its vibration energy per period of the fundamental. The string therefore is included in the groups of weakly damped systems (Q-factor $Q = 2249$) – it may be seen as a transmission line with low losses in good approximation. Considering moreover that the main share of the measured losses is not from the string itself but from the bearings shows that this approximation is justified to a high degree.

For **transmission lines with low losses**, the assumption is that phase- and group-velocity are practically not affected by the damping. It is only the vibration amplitude that decreases slightly as the signal passes through the line. For line lengths in the range of the length of a string, the amplitude damping is so small that it may be disregarded altogether in many cases. However, if the signals are subjected to numerous reflections, and if the objective of the investigations is a decay process lasting several seconds, then the amplitude damping must not be ignored anymore. It is not always necessary, though, to formulate a differentially distributed damping: insofar as merely discrete points on the string are of interest, ladder networks consisting of loss-free delay elements and delay-free damping elements provide a useful model (Chapter 2.8).

Trying to calculate the **internal losses in the string** brings curious issues to light: the loss factors for steel given by different books differ by a factor of 14. Even in one and the same book we may find differences of 600%. That may be because microphysical loss effects depend on manufacturing processes, or because there is not *the one* steel. It is more likely though, that 'internal' losses also include radiation losses. A loss factor of $d = 0{,}0001$ (*Gahlau et al., Geräuschminderung durch Werkstoffe und Systeme, Expert Sindelfingen 1986*) appears plausible; it yields a level decay of 0,22 dB/s for 82,4 Hz – significantly less than that of typical measurement results (0,6 dB/s), and leaving room for further damping mechanisms. The $d = 0{,}0006$ specified only 14 pages on in the same book, however, is too high (1,3 dB/s).

We probably better abandon hope for any consistent terminology – all too entrenched are the habits. Terms like damping factor, damping coefficient, degree of damping, loss factor, etc. may certainly (?) be applied in a consistent manner within one and the same publication, but interindividual differences are the rule. It is therefore not surprising that an author specifies the aperiodic boundary case (called critically damped oscillation elsewhere) with $d = 1$, while another (equally renowned) colleague specifies $d = 2$ for the same case. You can live with such a scenario 💣 – but you gotta be aware (sapienti sat).

The situation is more conducive for the calculation of direct **radiation losses**. Under the heading "air damping", we find in [9] formulas for the radiation of active energy, and evaluations for bass strings. The losses mount with increasing frequency, and decrease as the string-diameter grows. The calculations in [9] relate to the damping of the fundamentals – higher harmonics tend to be radiated less well implying lower string damping♣. For guitar strings, calculations yield radiation-induced time-constants of the amplitude in a range of 20 s (open E_2-string) to 2 s (open E_4-string). We can therefore disregard radiation losses for the low guitar strings, while for the high strings these losses are at the borderline (measurement values are e.g. 1,7 s).

♣ In addition, we can consider that fretboard and guitar body are located in close vicinity of the string and act as reflectors. This compounds the calculation of the radiation impedance.

© M. Zollner & Tilmann Zwicker, 2002 & 2020 Translation by Tilmann Zwicker

As a **bottom line**, we may state: inner damping and radiation losses may be disregarded as long as merely the wave propagation along short sections of the string is discussed. When analyzing vibrations of longer duration, we find – in electric guitars – damping mechanisms having a greater effect towards the higher frequencies (Chapter 7.7), and additional frequency-selective absorptions (e.g. resonances of the bridge). For acoustic guitars, we need to expect substantial absorptions in the low-frequency range, as well, since a non-negligible share of the vibration energy is fed to the bearings (bridge, frets).

2.7 Dispersive bending waves

The simple transmission line theory assumes place-independent wave impedance and frequency-independent propagation speed. However, the transversal waves of the guitar string propagate in a dispersive fashion, i.e. with frequency-dependent speed. The high frequencies run faster than the low ones (Chapter 1.3.1). The reason is the bending stiffness that increases the transverse stiffness, the latter in turn depending on the tensioning force.

Modeling the string as a dispersive transmission line takes much effort and is not always necessary. In most cases, only two or three points on the string are of interest (nut/fret, bridge, and point of plucking). Possibly, the position of the pickup also needs to be added in. It is easy to model the parts of the line between the discrete points via all-passes (Chapter 2.8). However, if precise description of the reflection conditions is required, we need a more detailed model. The simplest solution is found for steady-state (mono-frequent) partials: propagation speed and wave impedance are only weakly dependent on the frequency. For narrow-band considerations they may in fact be assumed to be constant. Transient processes extend across a frequency *range*, though; in such cases we need to apply frequency-dependent quantities.

We had introduced a simple element for modeling the dispersion-free string in Abb. 2.5. As characterizing quantities, force and velocity were sufficient (both quantities being signal-, place- and time-dependent). However, the rigidity of the real string requires that in addition to the (transverse) **force** $\boldsymbol{F}$, a place- and time-dependent **bending moment** $\boldsymbol{M}$ is specified, and also that we introduce an **angular speed** $\boldsymbol{w}$. This gives us a frequency-dependent phase delay (Fig. 1.6). The dispersive line element cannot be described as a quadripole (two-port network); rather, we need to specify a **four-port network** (octapole) [11]. The input quantities of the latter are F_1, M_1, v_1, w_1; its output quantities are F_2, M_2, v_2, w_2. Because the transverse dimensions of the string are small relative to the wavelength, we may disregard shear deformations and rotational inertia moments (Euler-Bernoulli theory for beams). Thus, the length-specific **mass** $\boldsymbol{m'}$, the length-specific **compliance** $\boldsymbol{n'}$, and the **bending stiffness** $\boldsymbol{B}$ remain as the system quantities (inside the four-port network).

The rigid string features *two* **wave impedances** $Z_F = F/v$ and $Z_M = M/w$, and *two* wave powers $P_F = Fv$ and $P_M = Mw$. *Two* bearing impedances each are active at both string bearings (nut/fret, bridge), and in addition the four signal quantities may be intercoupled in each bearing. For example, the edge-force may generate an edge-moment, or a displacement will necessarily lead to torsion. Since all these relationships appear depending both on frequency and direction, simplifications and approximations are indispensable.

 © M. Zollner & T. Zwicker, 2002 & 2020

Waves of lower order (fundamental and low-frequency harmonics) are not influenced much by the rigidity. The effective overall rigidity is practically only determined by the tensioning force Ψ, with the dispersion remaining insignificant (Fig. 1.4). However, for higher-order partials the influence of the rigidity may not be ignored anymore – especially for the low strings. The (overall-) rigidity as it is significant for the higher partials consists of two components: a frequency-*in*dependent portion caused by the tensioning force, and a frequency-dependent portion caused by the rigidity. The differential equation for the bending wave is of 4^{th} order; we therefore require four boundary conditions, and four independent fundamental solutions are possible. As had been the case for the rigidity-free string, a **wave** running forward and a **wave** running backward appear in the longitudinal direction, but in addition, an exponential **fringe field** is superimposed close to the bearings. Fortunately, this fringe field decays already at a short distance, and further away from the bearings we may therefore do the math with only one wave type. Without the fringe field, we obtain a simple coupling between F, v, M, w: knowing one of these four quantities suffices to describe the other three. *One single* wave equation is good enough to describe the string vibration (in one plane); we need a frequency-dependent wave number $k(\omega)$ for it, though.

This simplification is not valid for the description of reflections, though, because the latter indeed occur especially within the fringe zone. In this context, "fringe" refers to the beginning and the end of the string, and not the mantle-surface of the cylinder. Within the fringe zone, we need to formulate – in addition to the wave equation – a fringe field with its own wave number k', designated **fringe-field number**. Although in the fringe field the signal quantities F and v are still linked via Z_F (as M and w are linked via Z_M), F may take on any value independently of M (and the other way round) due to the fringe field. While in the dispersion-free string the reflection coefficient depends only on the ratio of wave impedance / bearing impedance, two wave impedances and two bearing impedances (per bearing each!) define the **reflection coefficients** in the stiff string. Thus, it is (at least theoretically) possible to reflect the *Fv*-wave entirely at the bearing, and to entirely absorb the *Mw*-wave. This does, however, not mean that there is no *Mw*-wave running in the reverse direction: the fringe field will take care of the existence of an *Mw*-wave already at a short distance – the energy necessary for this is "withdrawn" from the *Fv*-wave.

Within the abundance of all the reflection conditions possible in every vibration plane, there are some special cases that may be easily analyzed:

- Open end of the string: the string 'dangles in the air'; its end cannot absorb any transverse force F, nor any moment M. While this seems rather lacking in practical relevance, it may appear at resonance.
- Clamped string: transverse velocity v and angular speed are zero.
- Guided end: angular speed w and transverse force F are zero.
- Supported string: transverse velocity v and moment M are zero.

The real string bearing is not represented in any of the above special cases. This is because the string does normally not end at the bearing but is guided across it. Often the string rests in a small notch that permits for line-shaped contact only. This inhibits any transverse movement but allows for forces, angular movements and moments. If we interpret this bearing as a large blocking-mass, it will reflect *Fv*-waves but not *Mw*-waves! For the extreme case of a string featuring a stiffness that is only determined by the bending stiffness (beam), a barrier-mass reflects 50% of the incident wave energy – the other 50% are coupled as a bending wave into the section of the string beyond the bearing. In the other extreme case ($B = 0$), though, 100% of the energy is reflected.

© M. Zollner & Tilmann Zwicker, 2002 & 2020 Translation by Tilmann Zwicker

In order to assess the significance of the bending stiffness, let's look at the following **model case**: the string is supported by a knife-edge bearing not allowing for any lateral movement. The string also continues indefinitely beyond this first bearing, the other bearing has ideal reflecting characteristics. The percentile energy-portion transmitted beyond the bearing is shown for an A_2-string in **Fig. 2.22**. At low frequencies, the bending stiffness is negligible; the energy is almost completely reflected. However, already from middle frequencies a significant percentile is coupled across the (immobile!) bearing. On the other side of the bearing, we do not see a pure *Mw*-wave; rather, the fringe field again takes care of generating a combination of *Fv*- and *Mw*-waves.

Of course, a real string cannot extend indefinitely; it ends after a few centimeters at the tuner ("machine head"), in the string retainer, in the body, or wherever else there is space to attach it. Fig. 2.22 clearly indicates that it does make a difference where and how the string is fastened, though. The string-part beyond the bearing may indeed tap considerable vibration energy if it has corresponding length, forming a coupled resonator. Still, the power-percentile shown in Fig. 2.22 is not necessarily lost at each and every reflection. The share of energy coupled across the bearing may itself be reflected e.g. at the tailpiece, run back to the bearing, and then is once more coupled across the bearing into the main part of the string. Also, the real string does not have a line-shaped contact to the bearing: via a contact area (groove), not just a pure transverse force may be received but a moment as well. Some bridge/nut-combinations are deliberately (?) designed with larger contact surface, or directly as clamping-devices. For the latter, a further model-case will be discussed at the end of the chapter.

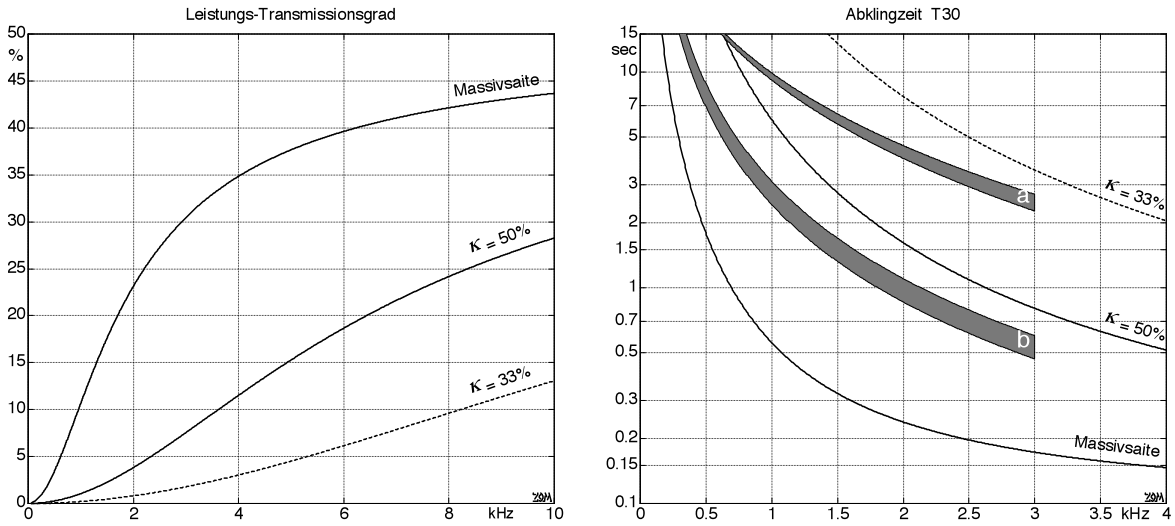

Fig. 2.22: Degree of power transmission ("Leistungs-Transmissionsgrad") for an A_2-string (40 mil); one end is clamped, the other borne on a knife-edge. On the right, the decay time ("Abklingzeit") of the partials purely due to the transmissions is given for a level-decrease of 30 dB via with three calculated lines (decay time T30, Chapter 7.6.3). The ratio of core diameter to outer diameter is κ = 50% (——), or 33% (-----), or 100% for the solid string ("Massivsaite").
The grey areas show results of measurements (A_2, 40 mil, κ = 50%) taken on the stone table. For **a**, the string was clamped at both ends, for **b** one end was clamped and the other supported: remaining string length is 30 m, weakly damped.
Case a fits well to the "orientation line" presented in Chapter 7 (Fig. 7.66); in addition to the bearing, string-internal damping mechanisms are at work, as well.
Case b should be compared to the 50%-line above it. This (calculated) line considers only the absorption occurring at the support-type bearing. In contrast, the measurements (grey area) also include string-internal damping mechanisms, and the absorption at the other bearing (clamp).
In an E_2-string, the losses due to the transmission are even larger.

 © M. Zollner & T. Zwicker, 2002 & 2020

To calculate the conditions for vibration and reflection, the string is divided into small **cylindric sections** of the length *dz*. At rest, the circular separation planes (cross-sections) are perpendicular to the *z*-axis. As the string is excited, the cross-sectional surfaces remain flat but are not in parallel anymore due to the bending moments: they form an angle of curvature. The laws of motion, inertia, and strength result in a partial differential equation for the rigid string (for detail see the supplement):

$$\Psi \cdot \frac{\partial^2 \xi}{\partial z^2} - B \cdot \frac{\partial^4 \xi}{\partial z^4} = m' \cdot \frac{\partial^2 \xi}{\partial t^2}$$ Differential equation for the string

The differential equation (DEQ) is a *partial* one because it includes the derivatives for both place *z* and time *t*; it is *linear* because the variables of transverse displacement ξ, place *z*, and time *t* are present in the first power only; it includes *constant coefficients* because the system quantities of tension force Ψ, bending stiffness *B*, and length-specific mass *m′* are not dependent on *z* and *t* (idealized); and it is homogenous because it does not comprise an external excitation.

B and *m′* are determined from the material data and the geometry of the string; the tension force Ψ results from the required fundamental frequency f_G. Any function $\xi(z,t)$ that will satisfy the DEQ is a **solution** for it. According to DANIEL BERNOULLI, the solution for sinusoidal movement is formulated as a product including a purely time-dependent and a purely place-dependent factor:

$$\xi(z,t) = \hat{\xi} \cdot e^{j(\omega t + \varphi)} \cdot e^{-jkz} = \underline{\xi} \cdot e^{-jkz}$$ Solution approach

The first factor $\underline{\xi}$ includes the angular frequency ω and the initial phase φ; a partial differentiation regarding the time *t* becomes a multiplication with $j\omega$. The second factor holds the wave number *k*; a partial differentiation regarding the place *z* becomes a multiplication with $-jk$. Introducing the corresponding derivatives into the DEQ yields:

$$-k^2 \Psi \underline{\xi} - k^4 B \underline{\xi} = -\omega^2 m' \underline{\xi}$$ Characteristic equation

The characteristic equation may be cancelled by $\underline{\xi}$ (the case $\xi \equiv 0$ being trivial). This yields a conditional equation for *k* that includes only a dependency on the system quantities. Because this equation is of 4th order, there are four independent solutions for which four independent boundary conditions need to be specified. In terms of the solution approach, two *k*-values are real, and the exponent therefore is imaginary (*-jkz*). This describes a **sinusoidal wave** running to the left or to the right, respectively. The other two values for *k* are imaginary, and the exponent thus is real – describing an exponentially increasing/decaying **fringe field** originating from the string bearing. Only the decaying fringe field is of practical importance. The general equation of motion is a superposition of the two wave equations and the equation of the decaying fringe field:

$$\xi(z,t) = \underline{\xi}_1 \cdot e^{+jkz} + \underline{\xi}_2 \cdot e^{-jkz} + \underline{\xi}_3 \cdot e^{-k'z}$$ general solution

The time-dependency is found in the three independent complex amplitudes $\underline{\xi}_i$, the frequency is identical for all three components.

© M. Zollner & Tilmann Zwicker, 2002 & 2020

In the following, we will consider a string ($z \geq 0$); the (left-hand) bearing is located at $z = 0$. The expressions

$$\xi_A(z,t) = \underline{\xi} \cdot e^{jkz}, \qquad \underline{\xi} = \hat{\xi}_A \cdot e^{j(\omega t + \varphi)}; \qquad \text{Excitation}$$

describe a sinusoidal wave running left towards the bearing (ξ = displacement). A part of its energy is reflected at $z = 0$, the remainder is transmitted:

$$\xi_R(z,t) = \zeta \cdot \underline{\xi} \cdot e^{-jkz}, \qquad \xi_T(z,t) = \psi \cdot \underline{\xi} \cdot e^{jkz}; \qquad \text{Reflection, transmission}$$

In the general case, reflection coefficient ζ and transmission coefficients ψ are complex. On the considered section of the string ($z \geq 0$), three displacements are superimposed:

$$\xi(z,t) = \underline{\xi} \cdot \left(e^{jkz} + \zeta \cdot e^{-jkz} + \gamma \cdot e^{-k'z} \right) \qquad z \geq 0$$

γ represents the complex fringe-field coefficient. Beyond the bearing (i.e. in the range of the transmission) two displacements are superimposed:

$$\xi(z,t) = \underline{\xi} \cdot \left(\psi \cdot e^{jkz} + \delta \cdot e^{k'z} \right) \qquad z \leq 0$$

Here, too, a fringe field with a different wave number k' and fringe-field coefficient δ is generated (in addition to the transmitted share). Fringe fields and waves are functions of the place (z) and the time (t). The dependency on time is described by $\underline{\xi}$ with ω as circular frequency; the place-dependency is described via the **fringe-field numbers** k and k'. For the propagating waves, $k = 2\pi / \lambda$ is reciprocal to the wavelength λ. The fundamental frequency f_G is the lowest eigenfrequency (natural frequency) of a string; λ_G corresponds to double the length of the string – in the E_2-string this is about 1,3 m for 82,4 Hz. Partials in the range around 10 kHz therefore have a wavelength around 1 cm ($\lambda_n = \lambda_G / n$). This still much exceeds the string diameter – we thus may do the math using approximations. For the high strings, these conditions are met to an even higher degree.

From the fringe-field number k', a limit distance $z_g = 1/k'$ may be estimated; it indicates at which distance the fringe field has decayed to 1/e. Since the characteristics are those of a flexural wave, the calculations require somewhat more effort (in particular for the wound strings). **Fig. 2.23** shows typical values of z_g.

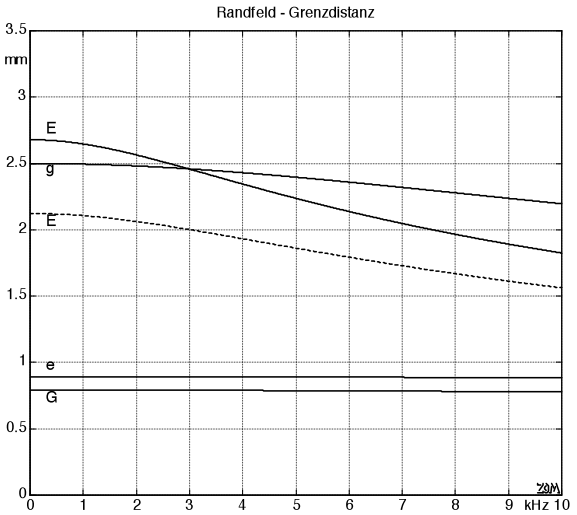

Fig. 2.23: Limit value z_g of the fringe field (in mm)
E_2-string: 53 mil, $\kappa = 0.4$
E_2-string: 42 mil, $\kappa = 0.4$ ----
G_3-string: 24 mil, $\kappa = 0.5$
g_3-string 20 mil, plain
e_4-string: 12 mil, plain

"Randfeld – Grenzdistanz" = limit value z_g of the fringe field

 © M. Zollner & T. Zwicker, 2002 & 2020

Running towards the bearing, the excitation wave is specified by its amplitude $\hat{\xi}_A$ and its frequency ω. For *this same* wave, F, M and w are defined via the system quantities B, m' and Ψ, and so are the wave impedances Z_F and Z_M, as well as the velocity v with $v = \partial\xi/\partial t$. The bearing (at $z = 0$) is – to begin with – defined by its two **bearing impedances** $Z_{FL} = F(0)/v(0)$ and $Z_{ML} = M(0)/w(0)$. Considering the string to be a linear system, there is the superposition of three oscillations in the range of $z \geq 0$: the given excitation wave ($\hat{\xi}_A$), the reflected wave (ζ), and the fringe field (γ). At first, ζ and γ are two unknown quantities; however, they may be calculated via the two bearing impedances.

The system quantities of the string are tension force Ψ, length-specific mass $m' = \rho S$, and bending stiffness $B = ES^2/4\pi$. Herein defined are ρ = density, S = cross-sectional surface, and E = Young's modulus. For wound strings, it is predominantly the core that defines the bending stiffness; the densities of core and winding may differ [appendix]. From these quantities, the w**ave number *k*** and the fringe **field number *k'*** may be calculated:

$$k = \sqrt{\frac{\Psi}{2B}\left(\sqrt{1 + 4B\omega^2 m'/\Psi^2} - 1\right)} \qquad k' = \sqrt{\frac{\Psi}{2B}\left(\sqrt{1 + 4B\omega^2 m'/\Psi^2} + 1\right)}$$

Both k and k' are system quantities, as well, i.e. they are signal independent. The rigid, tensioned string can be transformed into two borderline cases by varying B and Ψ: for $B = 0$ we obtain the dispersion-free string (fully flexible), and for e $\Psi = 0$ we get the cantilever (without any tensioning force). The wave numbers are calculated as:

$$k \to \omega\sqrt{\frac{m'}{\Psi}} = \frac{\omega}{c} \qquad k' \to \infty \qquad B \to 0 \qquad \text{String without bending stiffness}$$

$$k \to \sqrt{\frac{\omega}{B}\sqrt{Bm'}} = \frac{\omega}{c(\omega)} \qquad k' \to k \qquad \Psi \to 0 \qquad \text{Beam without tensioning force}$$

The phase velocity c is frequency-dependent for $B \neq 0$, and for $B \to 0$ it is constant. The wave-reflection coefficient ζ is calculated as:

$$\zeta = \frac{\left(Bk^2 + \Psi + \omega Z_{FL}/k\right)\left(\omega Z_{ML}/Bk + jk'/k\right) + \left(Bk'^2 - \Psi + j\omega Z_{FL}/k'\right)\left(1 + \omega Z_{ML}/Bk\right)}{\left(Bk^2 + \Psi - \omega Z_{FL}/k\right)\left(\omega Z_{ML}/Bk + jk'/k\right) - \left(Bk'^2 - \Psi + j\omega Z_{FL}/k'\right)\left(1 - \omega Z_{ML}/Bk\right)}$$

The formulas now do start be become rather lengthy – but they still do not fully describe the bearing. In fact, the simplification based on two bearing impedances Z_{FL} and Z_{ML} (as it is sometimes found in literature) is not always sufficient. In the general case, a coupling between the transversal quantities F or v, and the bending quantities M or w, respectively, may occur; the bearing impedance in that case receives the form of a matrix, and moreover an additional coupling term. Using this, a formal description is still explicitly possible, but the practical use of the formulas is increasingly limited because the individual bearing quantities cannot be measured with sufficient accuracy anymore. The vast diversity of bearing parameters forces to simplify – and it calls for the question how well these simplifications fit in the individual case.

© M. Zollner & Tilmann Zwicker, 2002 & 2020

The string vibration may be approximated in different ways:

a) The simplest approximation describes the string without its bending stiffness. The partials are positioned harmonically, and the propagation velocity is frequency-independent. To describe the bearing and the reflection, a single bearing impedance Z_{FL} is sufficient – it may be determined e.g. with an impedance head. For the fundamental f_G and the lowest partials, this approximation is adequate in many cases, but already in the middle frequency range we recognize clear deviations between calculation and measurement (Figs. 1.5, 1.7).

b) The calculation of the partials with consideration of the bending stiffness represents an easily obtainable improvement. On average, the actual spreading of the partials is quite well met. Considering moreover also the dilatational waves (Fig. 1.17) yields a useful approximation for the level spectrum.

c) In order to calculate the decay processes, the bearing impedances need to be known. For very light strings, we may disregard the bending stiffness, but for heavier strings knowledge of the bearing impedance Z_{FL} is required besides knowledge of the bearing impedance Z_{ML}.

d) The supposed "fully comprehensive" description of the bearing quickly degenerates into a confusingly extended system of equations: in two orthogonal vibration planes, we need to define three bearing impedances each – not to forget additional coupling impedances between the two planes. In addition, the impedance of the longitudinal wave should be borne in mind, again including mode coupling to the two orthogonal transversal waves. Presumably, a torsion wave on the string may be ignored – but this assumption is still under scrutiny: for the bowed string, the torsion wave is significant. Since all bearing- and coupling impedances depend (in some cases strongly) on the frequency, a confusing multitude of parameters results.

The next **example** shows that the bending stiffness of the string can make for problems even at low frequencies although the tensioning stiffness should in fact be predominant in this frequency range. For the calculation, we assume an idealized support bearing that is immobile in the transverse direction. The transversal velocity therefore is zero at this bearing. However, for bending processes that are coupled to the angular speed, this bearing is supposed to feature a moment of inertia (**blocking mass**). Due to the (material- and geometry-dependent) bending stiffness of the string, and due to the inertia of the bearing, a resonance may arise that (depending on the circumstances) may absorb a significant part of the vibration energy, or may couple this energy into the section of the string beyond the bearing (**total transition**). For a very small or a very large blocking mass, the resonance frequency will appear at very high or very low frequencies – it will then not cause any disturbance. However, given a corresponding dimensioning, resonances can appear in the middle frequency range, as well. Such resonances are not generally undesired – possibly, the luthier seeks to obtain a somewhat stronger absorption exactly in that frequency range. However, to use this in a targeted manner, the (frequency-dependent) moment of inertia at the bearing would have to be known – this poses problems for the instrumentation.

The following calculation circumvents the instrumentation issue and defines idealized bearing parameters; the approach does not orient itself on a special realization. In the discussion of the cone-parameters following later, we will again look into this subject matter, and we shall dive some more into the details.

 © M. Zollner & T. Zwicker, 2002 & 2020

As EXAMPLE, we look at a wound E-string of a diameter of 46 mil. It rests on a bearing such that its lateral movement is zero; Z_{FL} thus becomes infinite. The reflection coefficient:

$$\zeta = \frac{\left(Bk^2 + \Psi + \omega Z_{FL}/k\right)\left(\omega Z_{ML}/Bk + j\,k'/k\right) + \left(Bk'^2 - \Psi + j\omega Z_{FL}/k'\right)\left(1 + \omega Z_{ML}/Bk\right)}{\left(Bk^2 + \Psi - \omega Z_{FL}/k\right)\left(\omega Z_{ML}/Bk + j\,k'/k\right) - \left(Bk'^2 - \Psi + j\omega Z_{FL}/k'\right)\left(1 - \omega Z_{ML}/Bk\right)}$$

therefore is simplified. It reads:

$$\zeta = \frac{\left(1 - j\,k'/k\right)\omega Z_{ML}/Bk \;+\; 1 + (k'/k)^2}{\left(1 + j\,k'/k\right)\omega Z_{ML}/Bk \;-\; 1 - (k'/k)^2}$$ Reflection coefficient

The bending impedance Z_{ML} of the bearing is negative because the excitation wave runs towards the left:

$$Z_{ML} = -(j\omega\Theta + W)$$ Θ = moment of inertia of the bearing, W = bearing resistance

Using this, the complex reflection coefficient can be calculated:

$$\zeta = -\frac{Bk - \omega(j\omega\Theta + W)/(1 + j\,k'/k)}{Bk + \omega(j\omega\Theta + W)/(1 - j\,k'/k)}$$

Together, the bending stiffness B and the moment of inertia Θ form a resonance that can be located e.g. in the range of the middle frequencies (**Fig. 2.24**). With a suitable choice of W, total absorption is possible within a narrow frequency range. Such extreme cases may not be expected in typical string bearings, but it is still clearly evident that the bending stiffness can have effects at middle and low frequencies, too. ◊

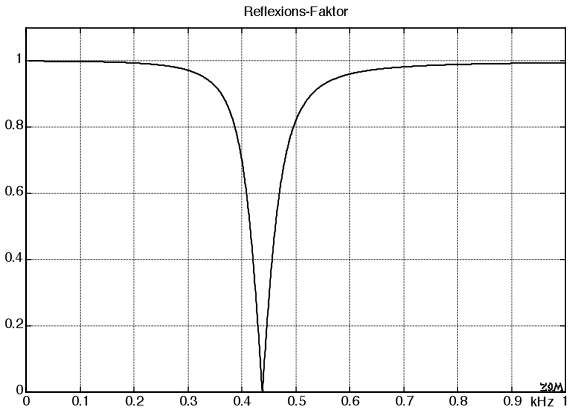

Fig. 2.24: Magnitude of the reflection coefficient of an E_2-Saite, 46 mil, core/outer diameter 50% ($\kappa = 0.5$).
The bearing is unyielding in the transversal direction, but has a moment of inertia Θ towards bending stress. $\Theta = 4{,}2{*}10^{-8}$ kgm^2 corresponds to the rotation moment of inertia of a steel ball of a diameter of 10 mm.
$W = 1{,}07{*}10^{-5}$ Nsm.
"Reflektions-Faktor" = reflection coefficient

Finally, let us look again at the calculation of the transmission coefficient ψ. Given known excitation and known bearing impedance, ψ can be calculated; conversely, an unknown bearing impedance (preferable Z_{ML}) may be calculated if ψ is known. For the bearing that is immobile in the transverse direction, and given a fully flexible string, the transmission is zero – the vibration energy is entirely reflected. Strings that are not ideally flexible can, however, transmit part of their vibration energy across such a bearing (Fig 2.22).

© M. Zollner & Tilmann Zwicker, 2002 & 2020

The calculation of the **transmitted part** assumes that a flexural wave with the transversal velocity $\underline{v}$ propagates in the main section of the string. The transverse velocity $v(z = 0)$ at the bearing is supposed to be zero by definition (ideal knife-edge bearing). We see the angular speed $w(z = 0)$ as the coupling quantity; it is identical on both sides of the bearing. The following equation describes v as it occurs in the main section of the string:

$$v(z,t) = \underline{v} \cdot \left(e^{jkz} + \zeta \cdot e^{-jkz} + \gamma \cdot e^{-k'z} \right) \qquad z \geq 0$$

From this, the place-derivative ($w = \partial v / \partial z$) yields the angular speed:

$$w(0) = jk\underline{v} \cdot \left(1 - \zeta + j\gamma\, k'/k\right)$$ Angular speed at the bearing

For the knife-edge bearing ($Z_{FL} = 0$), the reflection coefficient ζ contained herein results from:

$$\zeta = \frac{\left(1 - j\,k'/k\right)\omega Z_{ML}/Bk \; + \; 1 + (k'/k)^2}{\left(1 + j\,k'/k\right)\omega Z_{ML}/Bk \; - \; 1 - (k'/k)^2}$$ Reflection coefficient

The ideal knife-edge bearing does not have any bending impedance Z_{ML}. However, the flexural wave arriving at the bearing still does meet a bending impedance: the one of the string extending beyond the bearing ($z < 0$). This impedance is:

$$Z_{ML} = \frac{-Bk}{\omega} \cdot \frac{1 + (k'/k)^2}{1 + j\,k'/k}$$ Input impedance of the remaining section of the string

The bearing impedance Z_{ML} is negative, because the excitation wave runs *towards the left* to the bearing ($z > 0$). Using Z_{ML}, the (complex) reflection coefficient is simplified:

$$\zeta = \frac{-1}{1 - j\,k'/k}$$ Reflection coefficient of the knife-edge bearing (z>0)

With this result, the fringe-field coefficient γ is also defined for the knife-edge bearing:

$$\gamma = \frac{-1}{1 + j\,k/k'}$$ Fringe-field coefficient of the knife-edge bearing (z>0)

Using the above, we can now calculate the angular speed present at the bearing: $w(0) = j\,k\,\underline{v}$. However, the progressive wave does not simply travel across the bearing being unimpressed: directly at the far side of the bearing we have $w(-0)$ consisting of the ψ-part of the progressive wave, and the δ-part of the fringe field. The fringe field has decayed at a small distance ($z < 0$), though, and only the ψ-part of the (transmitted) wave running away from the bearing remains.

Given $w(0)$, the remaining section of the string is now excited in the range $z < 0$ (transmitted part); the wave running away and the fringe field superimpose here:

$$v(z,t) = \underline{v} \cdot \left(\psi \cdot e^{jkz} + \delta \cdot e^{k'z} \right) \qquad z \leq 0$$

At $z = -0$, the transversal velocity needs to be zero, too (knife-edge bearing), thus $\delta = -\psi$ holds.

 © M. Zollner & T. Zwicker, 2002 & 2020

The absolute scaling is calculated using the angular speed $w(0)$ of the bearing:

$$w(0) = j k\underline{v} = j k\underline{v}\left(\psi - j\delta\, k'/k\right) \qquad \Big\} \qquad \psi = \frac{1}{1 + j\, k'/k}$$

ψ represents the complex **transmission coefficient** – it states which part of the excitation wave runs across the bearing. Given a cantilever without any tensile strain ($\Psi = 0$), $k'/k = 1$ holds. The transmitted amplitude portion amounts to 70%, and the transmitted energy portion is 50%. The other 50% of the energy are reflected. In a guitar string, the tension force Ψ dominates, and thus the reflected portion is larger (Fig. 2.22).

We may not entirely ignore the **coupling across the bridge**, though, as shown by the following experiment. For a semi-solid guitar (Gibson ES-335 TD with trapeze tailpiece), the strings of which continue for 10 cm beyond the bridge to the tailpiece, the E_2-string was set in motion by tapping it between the bridge and the tailpiece, and then immediately damped again. By this, the section of the string between bridge and nut was set in motion, as well, and sustained audibly. However, tapping the string directly above the bridge there is practically no excitation – the transverse impedance of the bridge is indeed very high.

The coupling across the bridge is also pointed to by this experiment: the decay time (sustain) of the ES-335 TD was established for the E_2-string, using third-octave bandwidth. Subsequently, the palm of the hand was placed on the section of the string between bridge and tailpiece, damping it. Again, sustain was measured (for the section of the string between bridge and nut), and it indeed was shorter across the whole frequency range.

Neither experiment provides absolute proof: the sting is supported at the nut, as well, and excitation or damping could have been present here, too. Therefore we carried out a supplementary experiment on the **vibration test rig**: a solid steel wire of 0.7 mm diameter and 13,3 m length was stretched between two bearings each with the shape of mono-pitched roof. A **laser beam** samples the transversal velocity of this "string" at 4 mm ahead of one of the bearings. Beyond the bearing the string continues for 65 mm to where it is fastened (i.e. this is the remaining section of the string). Between the bearing and the measuring point of the laser, the string is hit with a small drop hammer providing an impulse-shaped excitation. The transverse displacement over time is shown in **Fig. 2.25**: once with un-damped remaining section of the string, and next to that with damped remaining section of the string. The bending-coupling is not pronounced very much but it is still clearly visible.

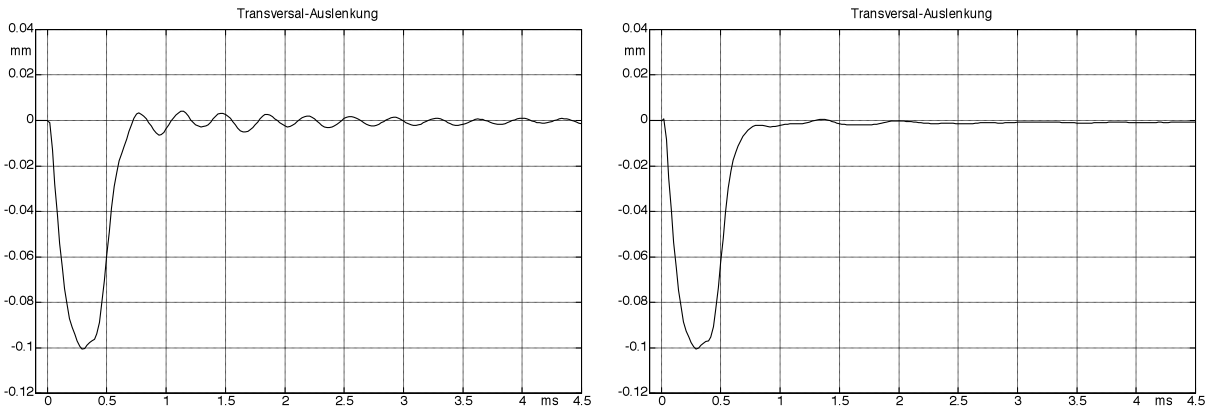

Fig. 2.25: Transverse displacement ("Transversal-Auslenkung") without (left) and with (right) damping of the remaining section of the string (Chapter 1.4).

© M. Zollner & Tilmann Zwicker, 2002 & 2020 Translation by Tilmann Zwicker

2.8 The generalized transmission-line model

The guitar is part of a signal-processing system generating sound from the movement of a plectrum (pick). With the input quantities of plectrum-force and plectrum-velocity, and the output quantities of bearing force and bearing velocity (in an acoustic guitar), or pickup voltage and pickup current (in the electric guitar), respectively, the string is a subsystem of the guitar. In Chapter 1.5 we had defined the plucking process as imprinting a force step with the effect that a special square wave runs back and forth on the string. This (more of less) periodic repetition of the excitation signal may be very nicely described with signal-flow diagrams, as they are also used in the context of digital FIR-/IIR-filters. It is not a problem that the signals in digital filters are usually time-discrete and discrete-valued, while the signals on the string are time- and value-continuous. In the simple transmission-line model, only the delay times occurring between the string bearings are emulated via delay lines. Conversely, plucking point and pickup position may be arbitrarily chosen.

2.8.1 Ideal string, bridge pickup

The following signal flow diagrams **SFD** (block diagrams) represent the signal processing via arithmetical operations. The basic operations are delay, summation, subtraction, and multiplication with a constant. The graphs do not give any indication of the source- and load-impedances and must not be confused with a circuit diagram.

A transverse force jumping to zero at the time $t = 0$ is defined as the excitation signal for the string. This force step runs in both directions from the plucking point; its phase velocity is c. The delay time necessary to reach bridge or nut, respectively, depends on c and the distance that needs to be covered. At the end of the string, each force step is reflected – here, we need to distinguish between $r_{bridge} = R$ and $r_{nut} = r$. Thereafter, both force steps circle in a recursive loop with an overall delay time of $T = 2L/c$. **Fig. 2.26** shows the corresponding SFD:

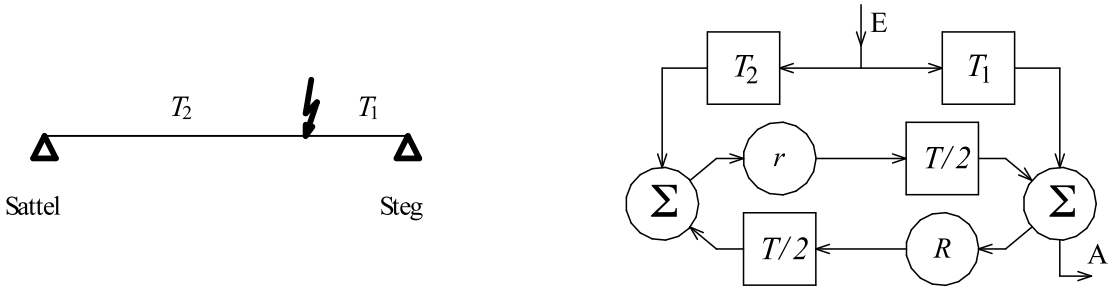

Fig. 2.26: Signal flow diagram (SFD) for non-dispersive string vibration. T_1 and T_2 are delay times from the plucking point to the bridge ("Steg") and the nut ("Sattel"), respectively; R is the reflection coefficient at the bridge, r is the reflection coefficient at the nut, $T/2$ is the delay time between bridge and nut, or nut and bridge, respectively. E = input, A = output (bridge).

The SFD shown in Fig. 2.26 differs from the ideal string in one significant aspect: the impulse created by the plucking runs back and forth on one and the same string, while in the SFD, the paths in the two directions manifest themselves in two separate, serially connected signal branches. Still, the signal processing is identical, and in both cases one cycle includes *two* reflections.

 © M. Zollner & T. Zwicker, 2002 & 2020

By repositioning of single delays, the SFD can be reshaped to result in a ladder network of three systems (**Fig. 2.27**):

- A basic delay T_1, modeling the delay time from point of plucking to the bridge.
- A recursive system with the delay time T, modeling the string vibration maintained via the reflections (IIR- and AR-filter respectively)
- Am interference filter with a delay difference of $2T_2$, modeling the shaping of the sound color via the point of plucking (FIR- and MA-Filter, respectively). For any one reflection at the nut /(or fret), $r \approx -1$ holds.

This representation has the main advantage that the "plucking"-filter (FIR-filter) and the section of the generator (IIR-filter) are considered independently from each other in separate stages. Assuming un-damped, loss-free vibrations ($R \cdot r = 1$), the IIR-filter (operating just shy of self-oscillation) generates – after impulse excitation – a periodic signal. Obligatorily, there is a matching harmonic line spectrum with the frequency distance of the lines equal to the fundamental frequency of the string.

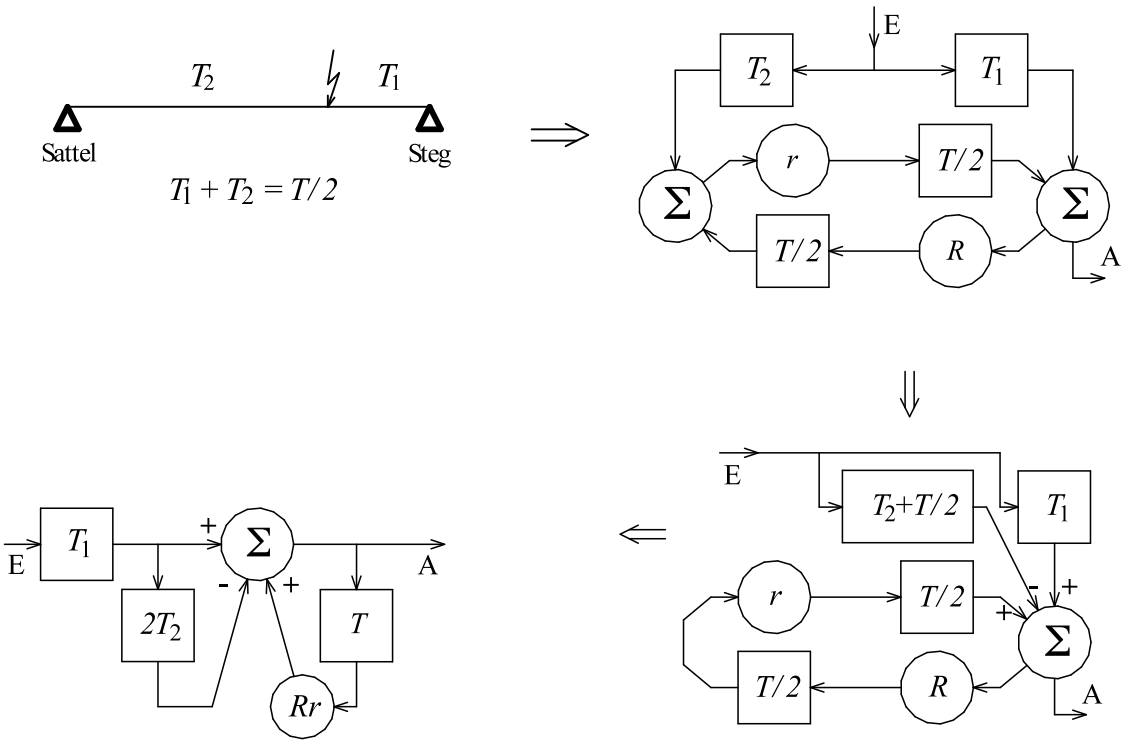

Fig. 2.27: Rearranged signal flow diagram (only a single signal path string → bridge). The sequence of the FIR-filter ($2T_2$) and the IIR-filter (T) is permutable (commutative mapping in the linear system). "Sattel" = nut, "Steg" = bridge.

Rearranging the FIR-delay time is done with $T_1 + T_2 = T/2$, resulting in:

$$(T_2 + T/2) - T_1 = T_2 + T/2 - (T/2 - T_2) = 2T_2$$

Using simple methods known from signal processing [e.g. 5], we can now derive from the SFD shown in Fig. 2.27 the behavior regarding frequency. If we take, as excitation signal, a short impulse (idealized a Dirac) periodically repeated in the IIR-filter, a spectrum with equidistant lines of constant height results. This spectrum is filtered as it runs through the subsequent systems, i.e. it is modified.

© M. Zollner & Tilmann Zwicker, 2002 & 2020

A pure signal delay by a constant delay time (e.g. T_1) only changes the phase spectrum but not the magnitude spectrum. We will ignore this basic delay since it is immaterial for the following considerations whether or not the output signal arrives a few milliseconds later. However, the delay time in the FIR-filter must not be ignored since here two signals are superimposed that are delayed with respect to each other – with the resulting frequency-selective amplifications and cancellations (comb-filter). The sequence of FIR/IIR, or IIR/FIR, respectively, must not be interchanged.

The filter effect of the **comb-filter** is extensively described in literature; we will only cover it in short here. The temporal input signal of a delay line arrives at the output after a delay (generally: T_x), the spectrum of the input signal is to be multiplied with the transfer function to yield the spectrum of the output signal. The transfer function $\underline{H}$ of a (pure) delay line with the delay T_x is:

$$\underline{H}(j\omega) = e^{-j\omega T_x}; \qquad \omega = 2\pi f \qquad \text{Transfer function of a delay line}$$

In a comb-filter, delayed signal and un-delayed signal are added or subtracted, respectively; this yields the transfer function of the comb-filter:

$$\underline{H}_{FIR} = 1 - \exp(-j\omega T_x); \qquad \left|\underline{H}_{FIR}\right| = 2 \cdot \left|\sin(\omega T_x / 2)\right| \qquad \text{FIR-filter}$$

The designation **FIR-filter** (Finite Impulse Response) is due the impulse response being of finite duration. The magnitude of the frequency response is the magnitude of a sine-function with zeroes at 0 Hz and integer multiples of the reciprocal of the delay time T_x. This calculation is formally correct but inconvenient for illustrations, as **Fig. 2.28** shows. Similar problems are known from time-discrete signals if the sampling theorem is not adhered to: too low a sampling rate results in (usually undesirable) reverse convolution. In the present special case, however, the ambiguity due to the sampling is helping. Via the identity

$$\left|\sin(m\pi - \varphi)\right| \equiv \left|\sin(\varphi)\right| \text{ only for } m = \text{integer}$$

and a few intermediate steps, the FIR-transfer function may be converted into:

$$\left|\underline{H}_{FIR}\right| = \left|\sin\left(\pi \cdot \frac{f}{f_G} \cdot \frac{d}{M}\right)\right| \qquad \text{FIR-filter, reformulated}$$

Herein, d represents the distance between the plucking point and the bridge, and M is the length of the open string (scale). For the fretted string, the scale needs to be applied here, as well, because it is included in the formula for the propagation speed of the wave. If the open string is plucked precisely in the middle, the long-term spectrum holds only odd harmonics – the zeroes of the sine-function are located at the even harmonics. The closer the plucking point is to the bridge, the wider the minima of the envelope are spaced. The conversion only holds in the steady-state part (discrete line-spectrum) but not for the transitory process. This is a basic condition for every transfer function, though: it always holds for the steady state only. Furthermore, we need to consider that the delays in the above model are frequency-independent – dispersion is not (yet) emulated. Spread-out spectra require, instead of simple delay lines, **all-passes** that approximate the string dispersion in the frequency response of their delay (Chapter 2.8.4).

 © M. Zollner & T. Zwicker, 2002 & 2020

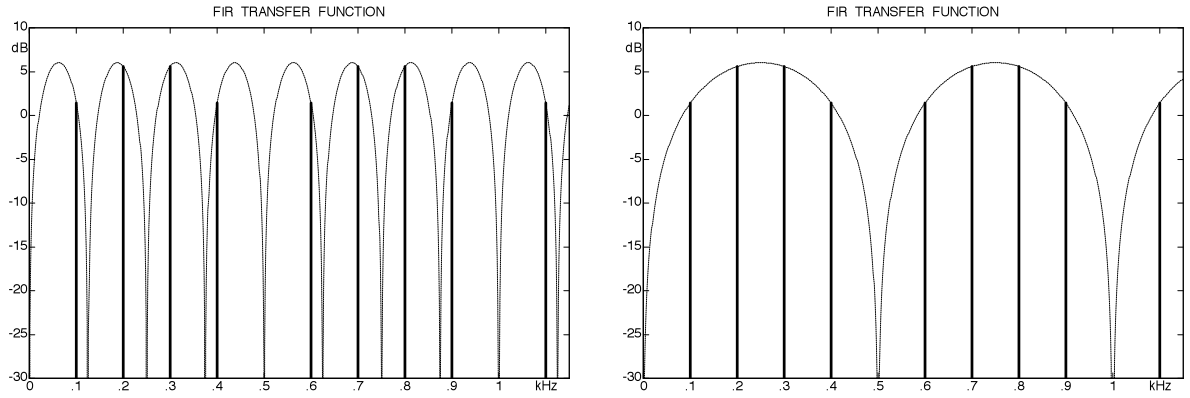

Fig. 2.28: FIR-filter frequency response (magnitude, ---) and filtered line spectrum for $d = M/5$. The lines shown are identical in both graphs; the graph on the right shows the transformed FIR-transfer-function.

In **Fig. 2.29** we see the measurements for a plucked E_2-string. The distance between plucking location and bridge amounted to d = 4,7 cm and 1,5 cm, respectively. From the results, the first minimum of the comb-filter calculates as 1,1 kHz and 3,5 kHz, respectively. In the low frequency region, the comb-filter structure is clearly visible in the spectral envelope – it is however perturbed by strain-wave resonances (Chapter 1.4, marked via dots). In anticipation of Chapter 2.8.4, Fig. 2.29 already includes the dispersive spreading of the spectral envelope. In addition, further selective damping mechanisms have an effect, especially in the high frequency domain. The associated causes will be elaborated on in Chapter 7.

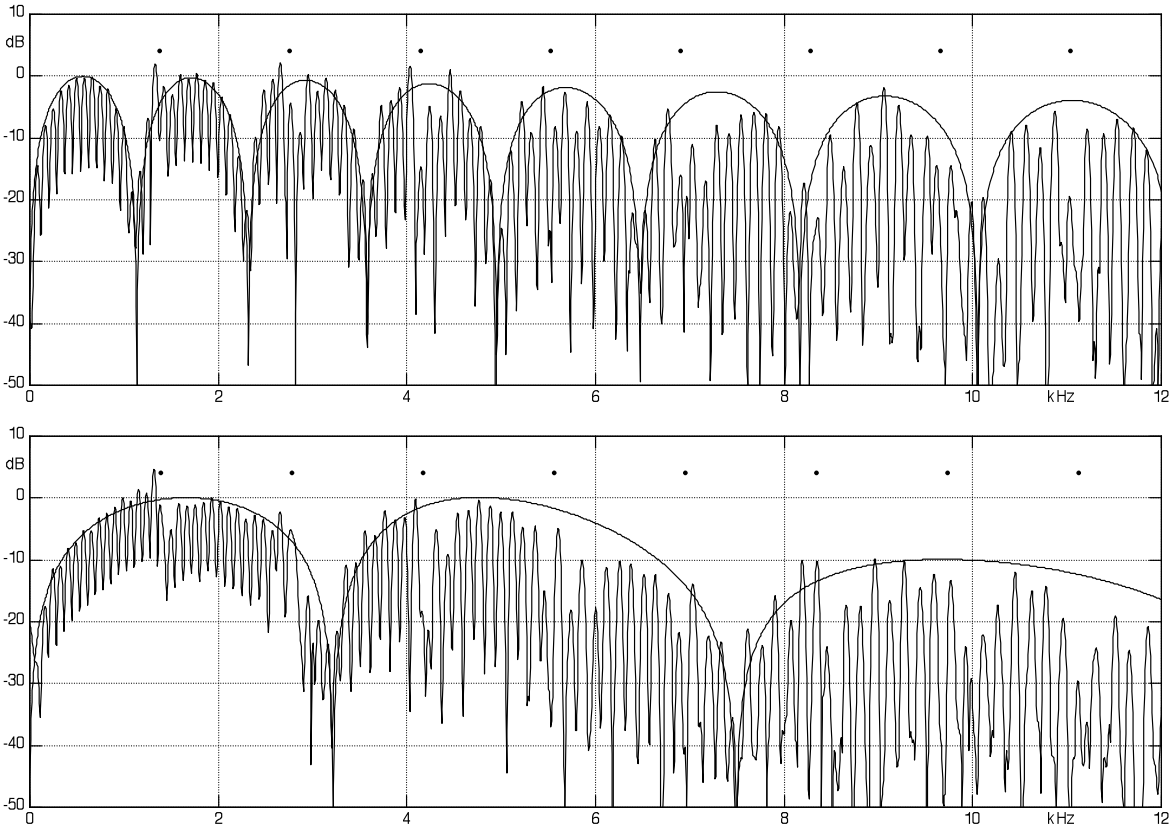

Fig. 2.29: Measured spectra; E_2-string (impulse excitation), d = 4,7 cm (top) and d = 1,5 cm (bottom). The shown envelope was spread out (dispersion) and slightly attenuated towards the high frequencies. The two measurements were taken with two different E_2-strings (OVATION Viper EA-68).

© M. Zollner & Tilmann Zwicker, 2002 & 2020

While the FIR-filter determines the spectral envelope, the recursive filter defines the frequency of the individual spectral lines. The impulse response of a recursive filter is of infinite length, which is why the term **IIR-filter** (Infinite Impulse Response) is common for this filter type. With both reflection coefficients being equal to 1, a short excitation impulse would circulate in the loop indefinitely without attenuation; such a filter is called borderline stable. Real strings have reflection coefficients of <1; the impulse-shaped excitation therefore decays over time. For a run through the full loop, both reflection coefficients act in multiplicative manner ($R \cdot r$).

Given $R \cdot r = 0{,}9$, for example, the height of the impulse decreases e.g. from 1 to 0,9 for a single loop, to 0,81 for a double look, and to $0{,}9^n$ for an n-fold loop. The amplitudes of the impulses following each other with a distance in time of T represent a geometric progression; for $R \cdot r < 1$, the term used is **exponential decay**. Chapter 1.6 had already included quantitative statements regarding the decay process; for the guitar string, the loop coefficients are very close to 1 (e.g. 0,993). In the FIR-filter only a single reflection occurs, and therefore $r = -1$ may be used with very good approximation. However, in the IIR-filter, the loop is run through an infinite number of times, and consequently this approximation is not allowable.

Chapter 2.5 had shown that the reflection coefficient is not constant but frequency-dependent. The reason are resonances in the bridge and the nut (or fret) formed from a combination of springs and masses. These springs and masses are not necessarily all found within the bridge (or the nut or fret) but may be located e.g. in the neck of the guitar and act on the nut [8]. When integrating a frequency-dependent reflection coefficient into the SFD (Fig. 2.17), we need to pay attention to the fact that the system shown as circle ($R \cdot r$) becomes a filter that way: $R \cdot r(j\omega)$ is the frequency dependent transfer function of this **reflection filter**. The decay time-constant for each partial results from the loop-delay-time T (frequency dependent if the dispersion is considered), and from $R \cdot r(j\omega)$. The SFD (Fig. 2.27) does not consider the reason for the damping: it is the *overall* damping that is modeled via $R \cdot r(j\omega)$. If required, several individual filters may be connected in series, for example to be able to model the internal string damping in a separate subsystem.

Ahead of the input designated with E in Fig. 2.27 we need to position the **plectrum filter** that shapes the real excitation force from the ideal step (or from an impulse). The **piezo-filter**, or – for acoustic guitars – the body- and radiation-filter follows the output A. The structure-borne sound path is not modeled herein. If we think of the nut merely as a vibration absorber, this is not necessary, either: the damping caused by the nut is considered in $R \cdot r$, after all. However, part of the vibration energy flowing into the nut might be radiated, or fed back to the string via the bridge – something that necessarily would have to work in reverse, as well. The dilatational waves discussed in Chapter 1.4 use a similar bypass (albeit directly via the string).

Additional recursive loops enable a simple emulation of such parallel paths. It should be emphasized again, though, that this does not automatically make for a correct representation of the energy flows. In the SFD, a summation point adds two signals (e.g. two forces), but it does not model the impedances – these would a have to be considered separately depending on the circumstances.

 © M. Zollner & T. Zwicker, 2002 & 2020

2.8.2 String with single-coil pickup

The SFD presented in Fig. 2.26 is now extended by the output of a magnetic pickup, assuming that the pickup will not influence the vibration of the string. This assumption is not fundamentally justified, because the attraction force of the permanent magnet does change the string vibration, and moreover the law of energy conservation demands that the string delivers the electrical energy generated. While the latter effect may be neglected when high-impedance pickups are deployed, strong magnets are indeed known for their interference when adjusted too close to the strings (Chapter 4.11). However, on order to explain the transfer characteristic in principle, the attraction does not need to be modeled.

Fig. 2.30 depicts the simplified model for the ideal string and a single–coil pickup. T_1 and T_2 designate the delay from the plucking point to the bridge and the nut, respectively. τ_1 and τ_2, respectively, is the delay from the location of the pickup to the bridge and the nut. Multiple rearranging of the drawing yields a ladder network consisting of four different filters:

- A basic delay from plucking point to pickup
- An FIR-filter with the long delay $2T_2$ (or $2\tau_2$, respectively)
- A recursive IIR-filter to model the string vibration
- An FIR-filter with the short delay $2\tau_1$ (or $2T_1$, respectively)

The sequence of these four subsystems may be changed arbitrarily. The pitch depends on the IIR-filter, and the sound color depends on the FIR-filters with their interference effect retraceable to the delay times T_1 and τ_1. There are three cases for the position of the pickup and the plucking point: $T_1 < \tau_1$, $T_1 > \tau_1$, and $T_1 = \tau_1$. It is immaterial whether pickup or plucking point is located closer to the bridge. For example, the pickup may be mounted 10 cm off the bridge, and the string is plucked 4 cm from the bridge, or the pickup may be mounted 4 cm from the bridge and the plucking may happen 10 cm from the bridge – in a *linear model*, the result will be the same (Fig. 2.35). What is not modeled: the string hitting and bouncing off the frets.

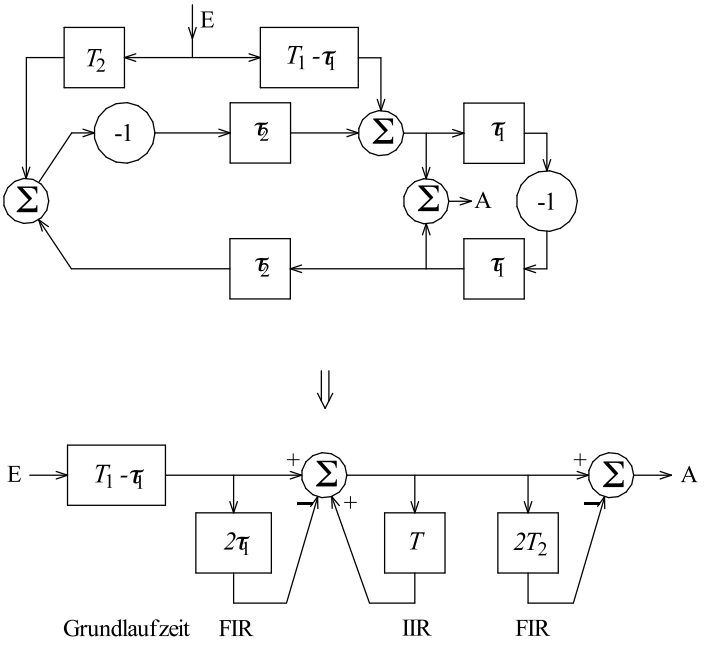

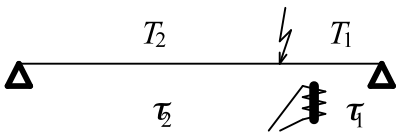

Fig. 2.30a: Ideal string with single-coil magnetic pickup, $T_1 \geq \tau_1$.
Reflections at bridge and nut are taken to be loss-free ($R = r = -1$).
"Grundlaufzeit" = basic delay time

© M. Zollner & Tilmann Zwicker, 2002 & 2020

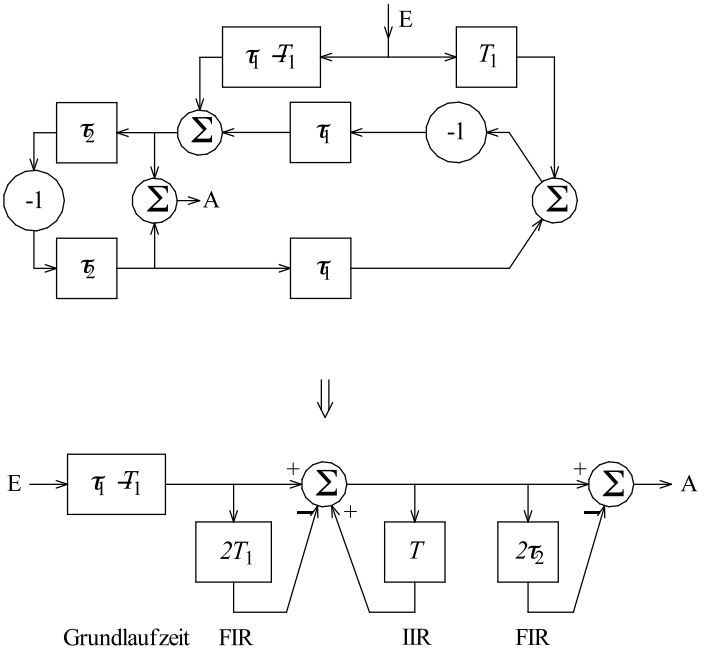

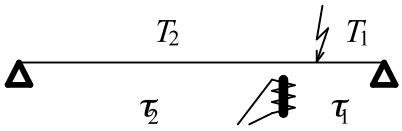

Fig. 2.30b: Ideal string with single-coil magnetic pickup, $T_1 \leq \tau_1$.
Reflections at bridge and nut are taken to be loss-free ($R = r = -1$).
"Grundlaufzeit" = basic delay time

The **step response** associated with the step excitation is indicated in **Fig. 2.31**. Like Fig. 2.30, Fig. 2.31 shows that when changing from $T_1 < \tau_1$ to $T_1 > \tau_1$, merely the delay times T_1 and τ_1 need to be interchanged. The periodicity of this dispersion-free filter is $T = 2(T_1 + T_2) = 2(\tau_1 + \tau_2)$. Two square impulses are located within that period, centered around the point in time t_0, and $T - t_0$, respectively. For $T_1 < \tau_1$ we get $t_0 = \tau_1$, while $t_0 = T_1$ results for $T_1 > \tau_1$. The impulse width amounts to $\Delta t = | T_1 - \tau_1 |$.

The impulse width corresponds to the delay time of the transversal wave running from plucking point to pickup. If this distance is e.g. 4 cm, the impulse width calculates as 4·T/2·64 = T/32. Herein, the scale is assumed to be 64 cm. If the string is plucked exactly over the pickup, the two square impulses are perfectly contiguous.

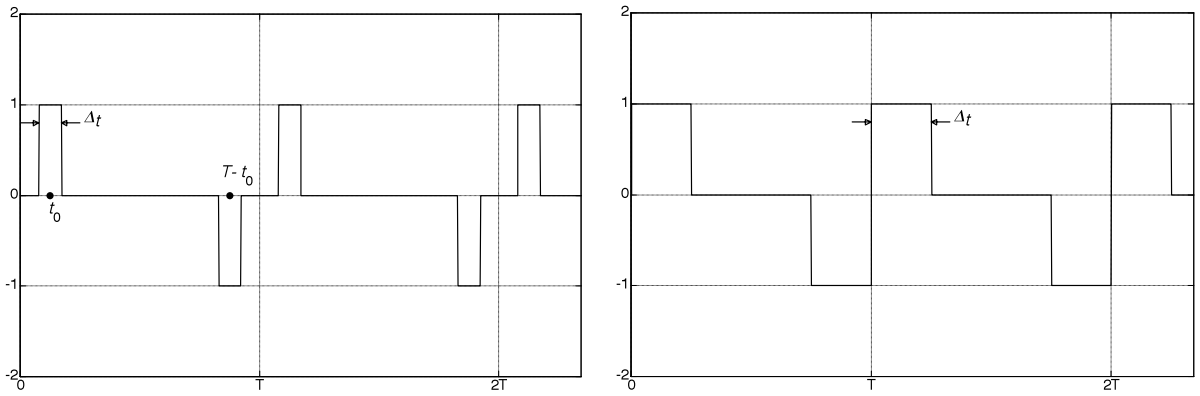

Fig. 2.31: Step response of the filter from Fig. 2.30. Left: $T_1 \neq \tau_1$; right $T_1 = \tau_1$. Input quantity for the filter is a force step at the plucking point. Output quantity is the string velocity over the magnet of the pickup – the source voltage of the pickup is proportional to this velocity. The terminal voltage results from low-pass filtering of the source voltage (Chapter 5.9). In particular for the low strings, the frequency-dependent propagation velocity (dispersion, Chapter 2.8.4) takes care of reshaping the rectangular waveform. In order to model this effect, the delays in Fig. 2.30 need to be realized as all-passes (Fig. 2.39).

 © M. Zollner & T. Zwicker, 2002 & 2020

The calculation of the **overall transfer function** of the 4 serially connected individual filters requires a multiplication of the individual transfer functions, resulting in somewhat more complicated frequency responses (**Fig. 2.32**).

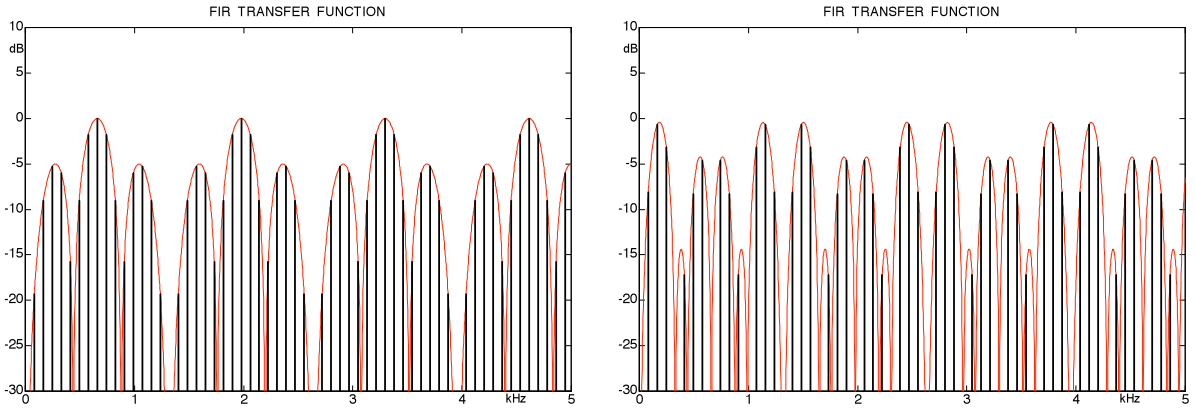

Fig. 2.32a: Transfer frequency response, E_2-string plucked 12 cm away from the bridge. Scale = 64 cm. Left: bridge-pickup (4 cm distance from the bridge); right: neck-pickup (16 cm distance from the bridge).

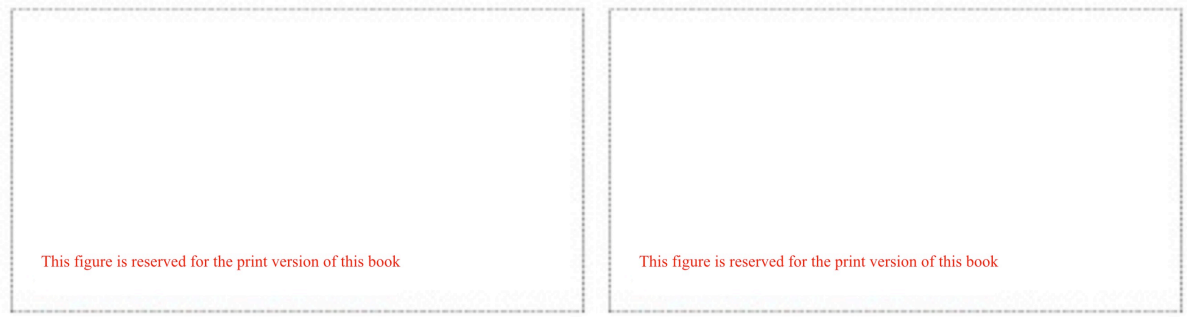

Fig. 2.32b: Transfer frequency response, string plucked 12 cm away from the bridge; bridge pickup (5cm distance from the bridge, scale = 64 cm). Left: E_2-string, right: A-string.

It should be noted as particularly important that the two FIR-filters act **string-specifically** and do not have a global filter effect (as the magnetic pickup discussed in Chapter 5 would show it). The winding of the pickup coil is permeated by field-alterations of all 6 strings, and thus the resonance peak of the pickup will affect all 6 strings in the same way. The cancellations of the FIR-filter, however, are based on the propagation speeds of the waves, and these are string specific. As already elaborated, these propagation speeds do not depend on the (fretted) pitch, but on the pitch of the open string. The latter determines the propagation speed c_P, after all. It is therefore not possible to generate the FIR-characteristic electronically with an effects device … not with your regular pickups, anyway.

Fig. 2.33 shops the FIR frequency responses of a **Stratocaster** dependent on the pickup position. The effect of the second FIR-filter (plucking location) was not included in the calculations. To ensure a clear representation, the minima are only shown to a depth of 18 dB; according to the theory, the graph should extend to $-\infty$ dB in the minima.

© M. Zollner & Tilmann Zwicker, 2002 & 2020

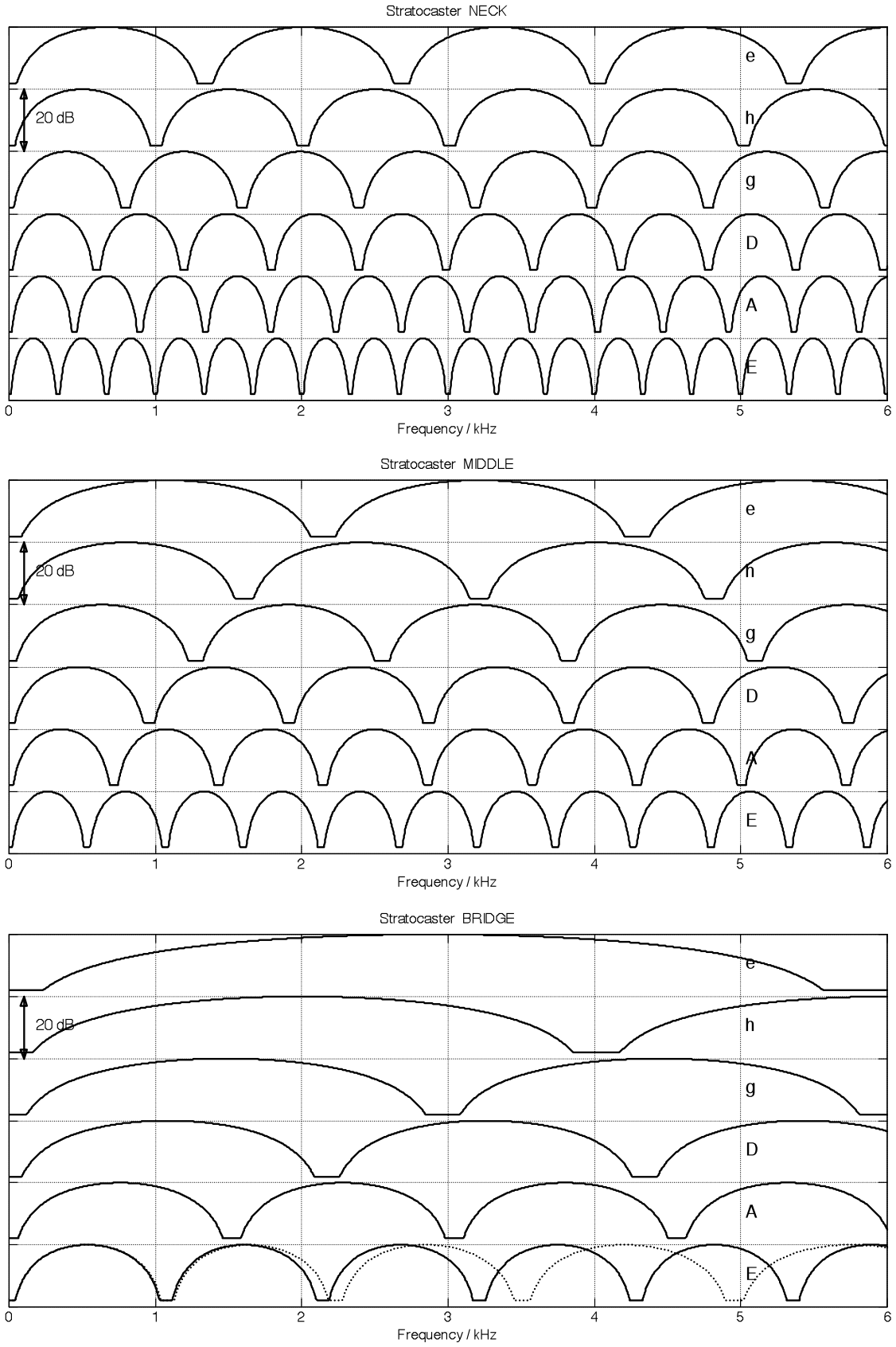

Fig. 2.33: Calculated FIR frequency responses for the Stratocaster; without dispersion. The dynamic is limited to 18 dB. In the lowermost graph, the effect of dispersive propagation is shown as a dotted line (compare to Chapter 1.8.4).

 © M. Zollner & T. Zwicker, 2002 & 2020

In **Fig. 2.34**, we see a comparison between measurement and calculation. A Stratocaster is connected to an instrumentation amplifier (input impedance: 100 kΩ) via a cable of a capacitance of 200 pF. The E_2-string is plucked directly at the bridge with a plectrum, and the signal of the bridge-pickup was evaluated.

The comparative calculation of the line spectrum includes both FIR-filters, the IIR-filter, and the equivalent circuit diagram of the pickup (Chapter 5.9.3). In addition, a small treble-attenuation was included to emulate the window of the magnetic field (Chapter 5.4.4). There is a clear correspondence. The measured spectrum nicely depicts the spreading of the frequency of the partials; it was emulated for the calculation using a simple model. The simulation easily reproduces the comb-filter structure, as well – at high frequencies, however, differences between measurement and calculation become evident. For a further improvement, e.g. the reflection coefficients would have to be adapted.

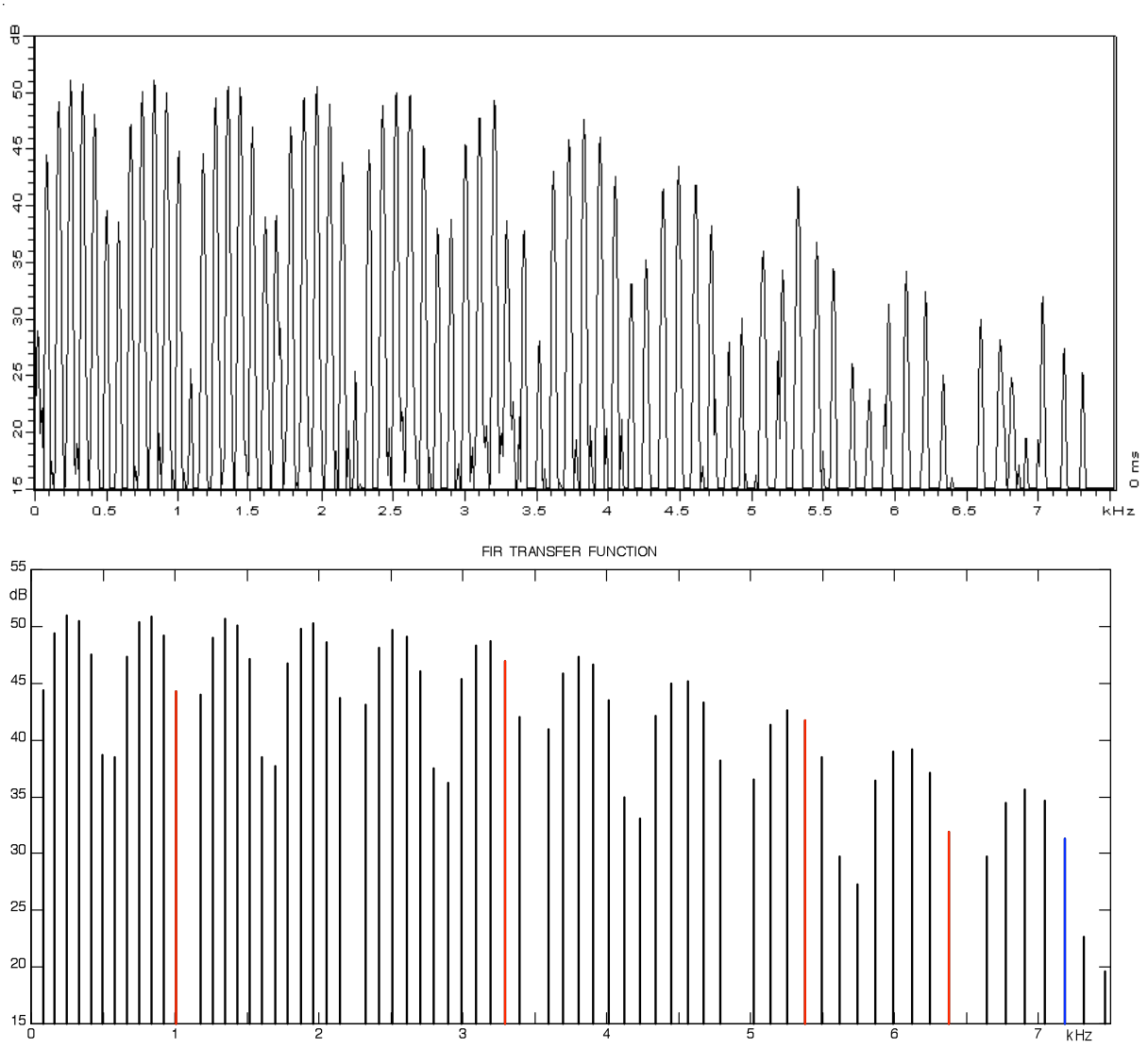

Fig. 2.34: Spectrum of an E_2-string plucked directly at the bridge (Stratocaster, middle pickup).
Top: measurement (with DFT-leakage). Bottom: calculation (with dispersion, compare to Chapter 2.8.4).
The inharmonic spreading is considerable; the 70th "harmonic" is at 7,37 kHz rather than at 5,84 kHz.

© M. Zollner & Tilmann Zwicker, 2002 & 2020

It was already noted with respect to Fig. 2.30 that the plucking point on the string and the location of the pickup result in an FIR-filter each (with different delay times). Two serially connected filters represent two *commutatively* connected mappings the sequence of which may be interchanged. It therefore should not make any difference whether the string is plucked at point A with the pickup being located at point B, or the string is plucked at point B with the pickup located at point A.

To check this hypothesis, the E_2-string of a Stratocaster was plucked over the neck-pickup while the signal from the bridge-pickup was recorded. Subsequently, the E_2-string was plucked over the bridge-pickup and the signal of the neck-pickup was recorded. **Fig. 2.35** shows the DFT-spectra of both signals. The agreement is uncanny – especially considering that the reproducibility of the plucking process is not particularly good.

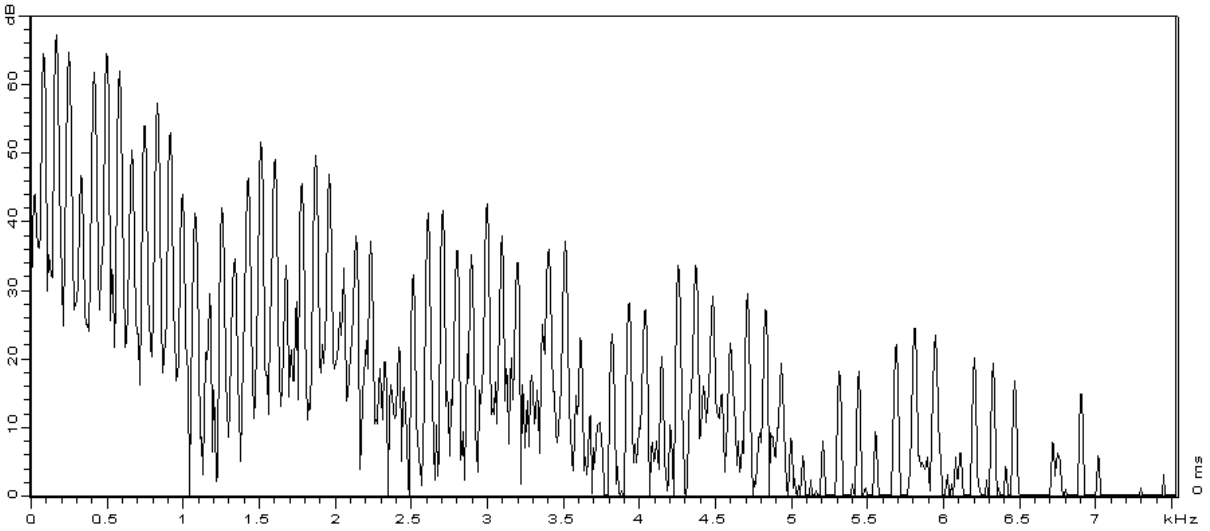

Measured signal of the bridge-pickup; string plucked over the neck-pickup.

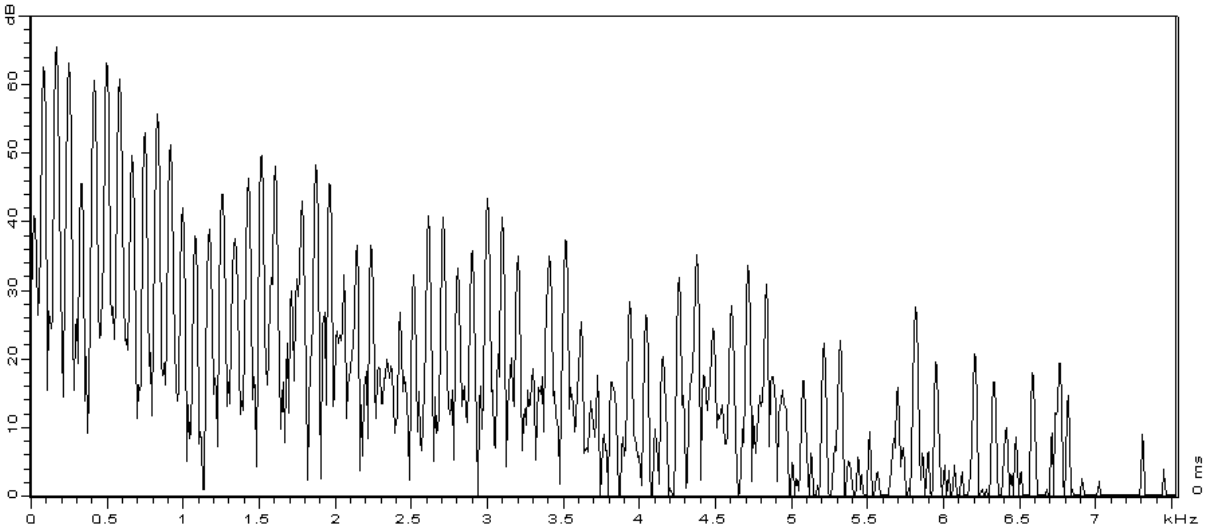

Measured signal of the neck-pickup; string plucked over the bridge-pickup.

Fig. 2.35: Spectrum of the E_2-string of a Stratocaster; pickup and plucking position interchanged.

 © M. Zollner & T. Zwicker, 2002 & 2020

2.8.3 String with humbucking pickup

In the hum-cancelling humbucking pickup, two coils are connected in opposite phase. In order for the electrical output signals to interact constructively, the magnetic permanent flux is reversed in one of the coils. Many pickups (e.g. Gibson) generate the permanent field using a bar magnet located under the coils; the field is conducted through the coils using so-called pole-pieces. Other designs (e.g. Fender) use 6 individual magnets in each coil; in one of the coils, the north-pole is directed upwards, in the other it is the south-pole. The two coils are usually connected serially in opposite phase; opposite-phase parallel connection is less common.

The humbucker samples a wave running along the string at two adjacent areas. The distance between the two pole-pieces is 18 mm for the Gibson Humbucker – there are, however, also very narrow humbuckers that fit into the housing of a regular single-coil pickup.

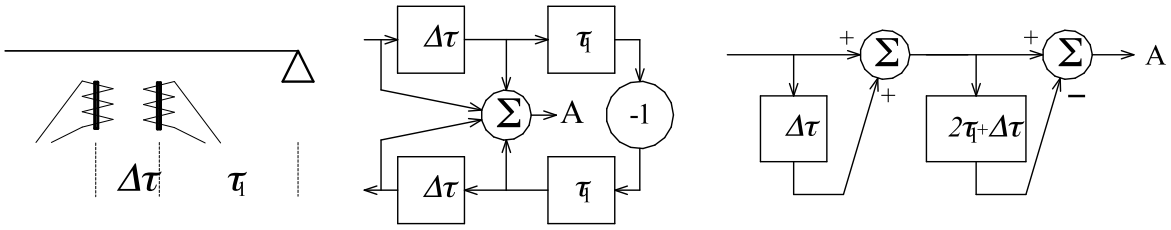

$$\underline{H}(j\omega) = 1 + e^{-j\omega\Delta\tau} - e^{-j\omega(\Delta\tau+2\tau_1)} - e^{-j2\omega(\Delta\tau+\tau_1)} = \left(1 + e^{-j\omega\Delta\tau}\right) \cdot \left(1 - e^{-j\omega(2\tau_1+\Delta\tau)}\right)$$

Fig. 2.36: Signal flow diagram for a humbucking pickup with two equivalent coils.

In **Fig. 2.36**, τ_1 represents the (single) delay time between the coil located closer to the bridge and the bridge, while $\Delta\tau$ is the delay between the two coils. Using suitable conversion, we arrive at a simple ladder-network of two FIR-filters. The first filter models – with same-phase superposition – the delay time $\Delta\tau$ between the coils; the other filter emulates – using opposite-phase superposition – double the delay time between the middle of the humbucker and the bridge. The humbucker positioned at a location x differs from a single-coil pickup located at the same position only in the $\Delta\tau$-filter. The modeling as ladder network offers the considerable advantage that the overall transfer function can be represented as the product of the individual transfer functions. Given a humbucker with a distance between pole-pieces of 18 mm, we get an additional **signal cancellation** for the E_2-string in the range around 3 kHz; for the higher strings, the humbucker-minimum is located at correspondingly higher frequencies. The exact frequency of the minimum depends not only on the pole-piece distance, but also on the dispersion (Chapter 1.3)

As is shown in **Fig. 2.37**, the differences between single-coil pickup and humbucker are string-specific: for the E_4-string, only small variations in the treble range will be recognizable, while for the E_2-string, the humbucker will absorb the 3-kHz-range that is important to obtain a brilliant sound. Reducing the distance of the two humbucker coils to 13 mm (as it was done e.g. in the **Mini-Humbucker** fitted to the Les Paul Deluxe) will shift all interference-minima toward higher frequencies. A particularly small distance of the coils (7 – 9 mm) is realized in the single-coil format; still, a treble loss remains for the low strings.

© M. Zollner & Tilmann Zwicker, 2002 & 2020

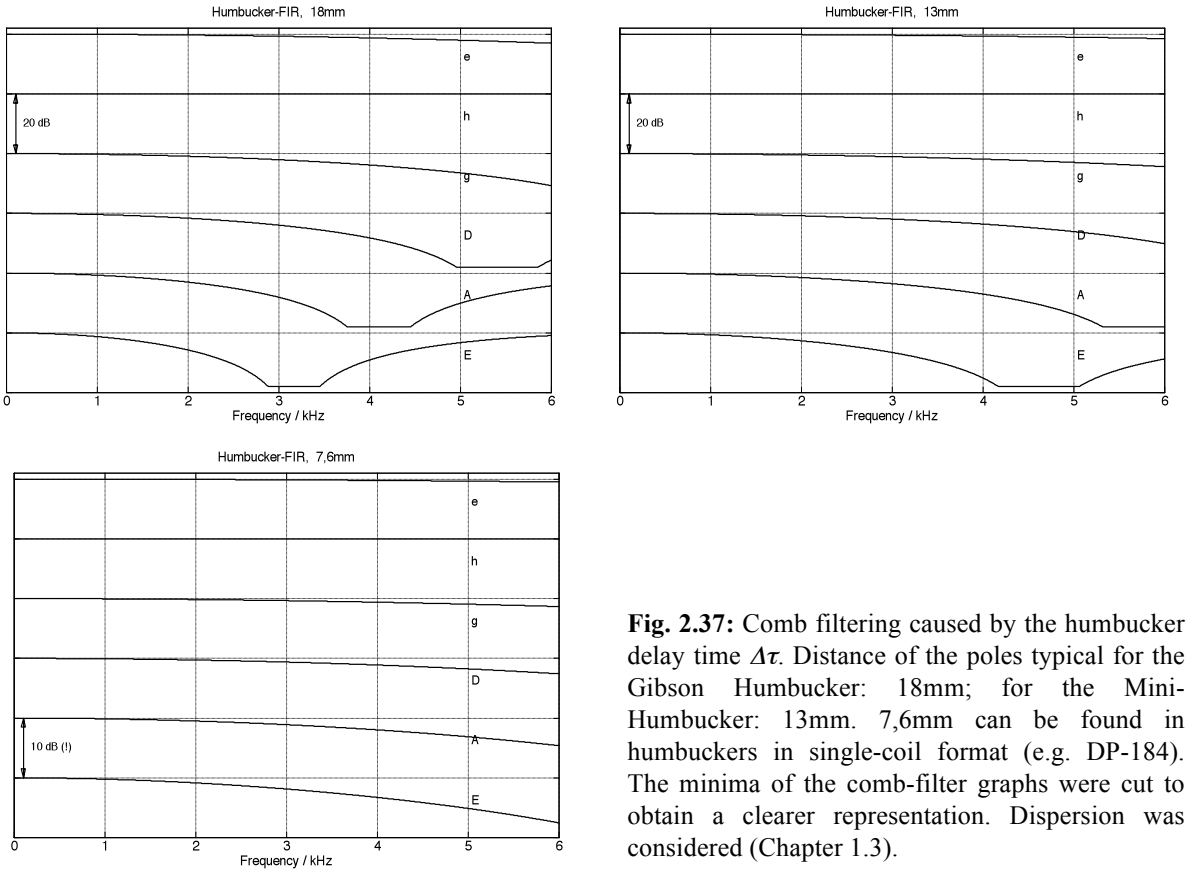

Fig. 2.37: Comb filtering caused by the humbucker delay time $\Delta\tau$. Distance of the poles typical for the Gibson Humbucker: 18mm; for the Mini-Humbucker: 13mm. 7,6mm can be found in humbuckers in single-coil format (e.g. DP-184). The minima of the comb-filter graphs were cut to obtain a clearer representation. Dispersion was considered (Chapter 1.3).

If the two humbucker coils do not feature the same sensitivity in both coils, we get differences in particular in the range of the humbucker-minimum (**Fig. 2.38**). Such **imbalances** have their roots in different numbers of the turns of the coils (deliberately produced for the *Burstbucker*) and/or in the field guides: the pole pieces in the shape of slugs have a different magnetic resistance compared to the threaded pole-screws. For differing coils, the SFD may not be separated into two FIR-filters, and thus Fig. 2.38 shows the frequency responses of the overall signal flow diagram.

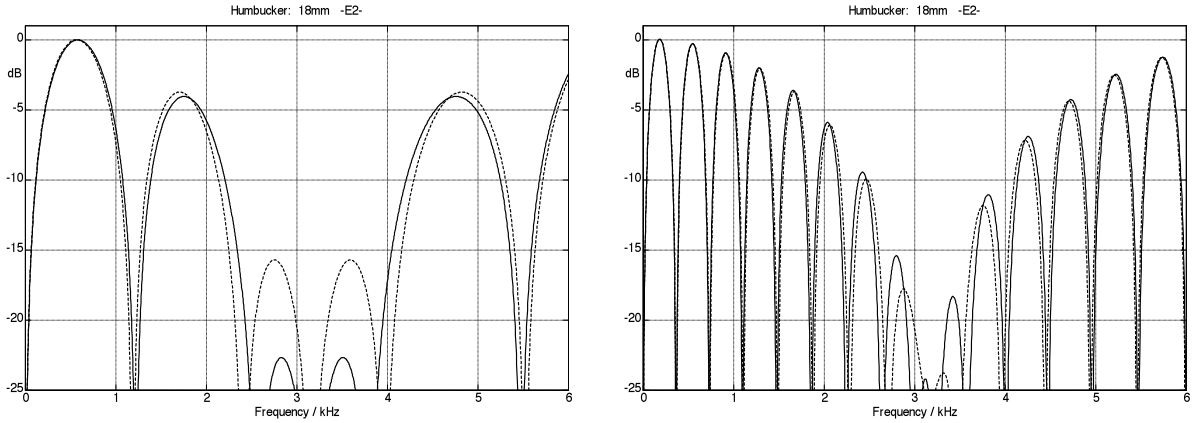

Fig. 2.38: Magnitude frequency responses for unmatched humbucker coils. Left: bridge humbucker (distance to bridge 45 mm); right: neck humbucker (distance to bridge 147 mm). The sensitivity of the coil with threaded pole pieces (screws) is better by 1 dB compared to the "slug"-coil (——), or smaller by 1 dB (---). Dispersion was considered (Chapter 1.3).

 © M. Zollner & T. Zwicker, 2002 & 2020

For a Gibson ES-335 TD (E_2-string), **Fig. 2.39** considers the transfer function of the equivalent circuit established in Fig. 2.36. In **Fig. 2.40**, the RLC-transfer-function (Chapter 5-9) is added in. Via **Fig. 2.41**, we can compare a measurement. For all graphs, dispersive wave propagation was included.

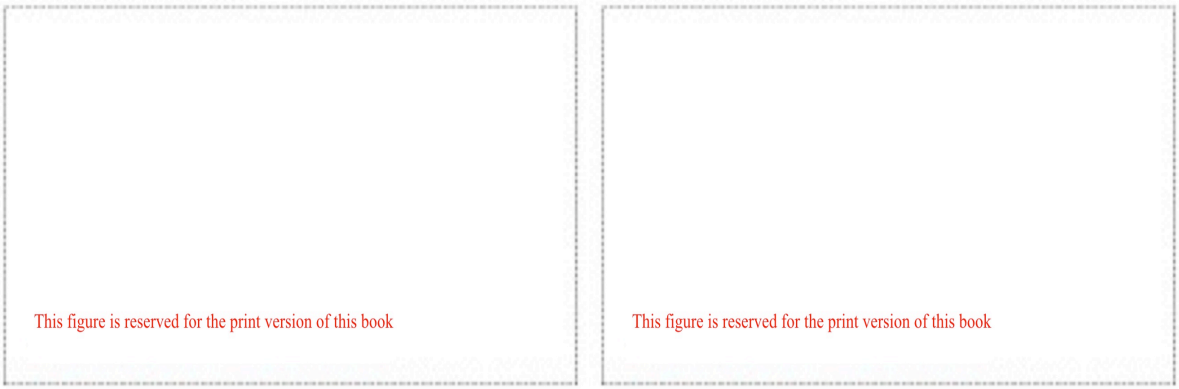

Fig. 2.39: Gibson ES335, E_2-string, model without RLC-filter. Left: bridge pickup. Right: neck pickup.

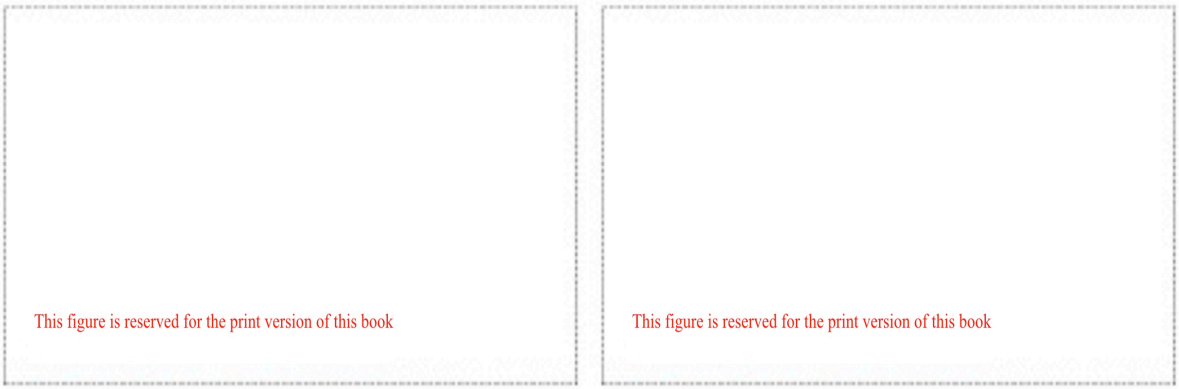

Fig. 2.40: ES335, E_2-string, model with RLC-filter and 707-pF-cable. Left: bridge pickup. Right: neck pickup.

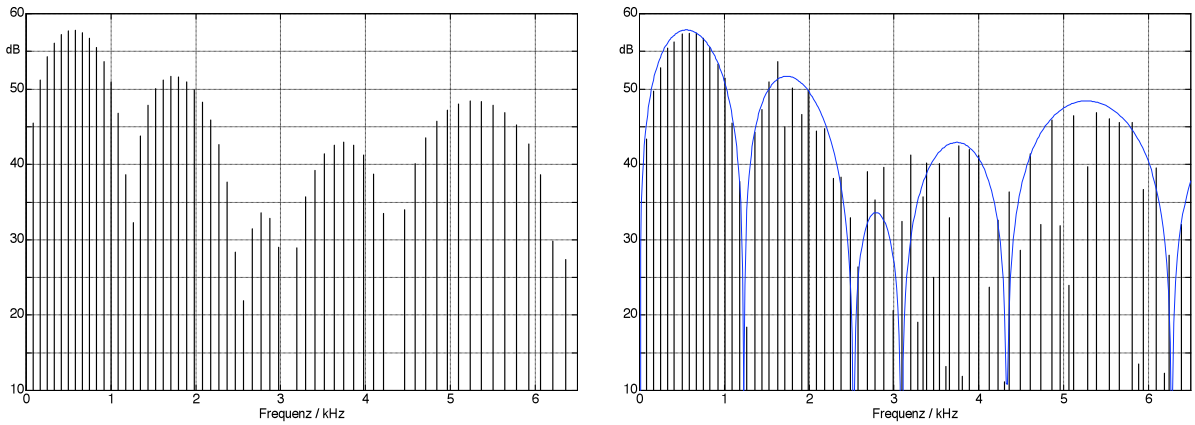

Fig. 2.41: ES335, E_2-string plucked directly at the bridge; bridge pickup. Left: model calculation; right: measurement. The differences do not refute the basic model assumptions; rather, they indicate how important the modeling of both strain-wave and bearing impedances is – this was not included here.

© M. Zollner & Tilmann Zwicker, 2002 & 2020

2.8.4 Dispersive line elements

In Chapter 1.2, we had discussed that the propagation speed of the transversal waves is frequency dependent (**dispersion**), leading to a "spreading out" of the frequencies of the partials. This effect may be modeled in the SFD using frequency-dependent delay times. If we first assume the string to be loss-free, the magnitude spectrum will not change during the wave propagation. The phase spectrum does change – but not with a linear-phase characteristic like it would in a delay line. Rather, it assumes the characteristic of an **all-pass function** due to the frequency-dependent delay time. From the spreading of the partials, we can deduce the all-pass transfer-function (Chapter 1.3.1), and from this the all-pass impulse response (Chapter 1.3.2) via inverse Fourier transform. The simulations shown in Chapter 1 were calculated using such an SFD.

All-pass: linear system with a frequency-independent magnitude transmission coefficient and frequency-dependent phase shift.
Minimal-phase system: linear all-pass-free system.
Linear-phase system: linear system with frequency-proportional phase shift.
System order: number of the independent storage elements in the system.

For a wound E_2-string (b = 1/8000), **Fig. 2.42** shows the phase shift φ as it appears in a transversal wave running the distance of 8,65 mm (Chapter 1.3.1). Cascading 74 of the digital filters indicated in the figure yields a good approximation of the overall phase-shift of an E_2-string of 64 cm length (single travel path). The relatively high number of filters is due to the chosen sample frequency: a 2nd-order all-pass can turn shift the phase by no more than 2π.

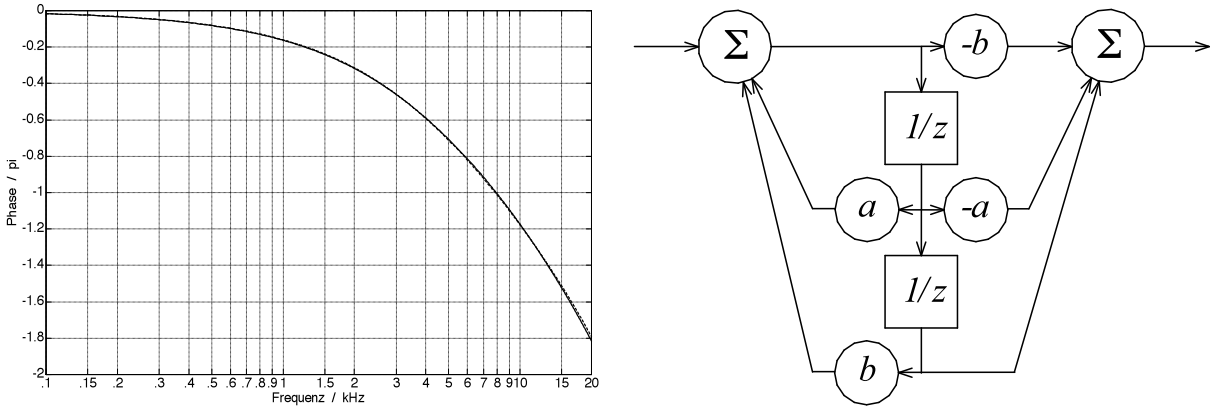

Fig. 2.42: Block-diagram and frequency response of the phase of a 2nd-oder canonic digital all-pass filter. Sample frequency: f_a = 48 kHz, a = 0,5378, b = -0,03668. The frequency response of the filter phase is indicated as a dashed line; the differences to the phase of the string (——) are insignificant. "Frequenz" = frequency.

Given f_a = sample frequency, the transfer function of the digital all-pass is:

$$\underline{H}(z) = \frac{1 - az - bz^2}{z^2 - az - b}; \qquad |\underline{H}(z)| = 1; \qquad z = \exp(j\omega / f_a)$$

If the sample frequency is changed, the parameters a and b need to be adapted, as well.

 © M. Zollner & T. Zwicker, 2002 & 2020

The phase delay of the all-pass filter shown in Fig. 2.42 features the same tendency as it is found in dispersive waves on strings: high frequencies get to the output of the filter faster than low ones. Given a step excitation, we will therefore see a reaction in the high frequency range first; the low frequency components follow with a delay (**Fig. 2.43**).

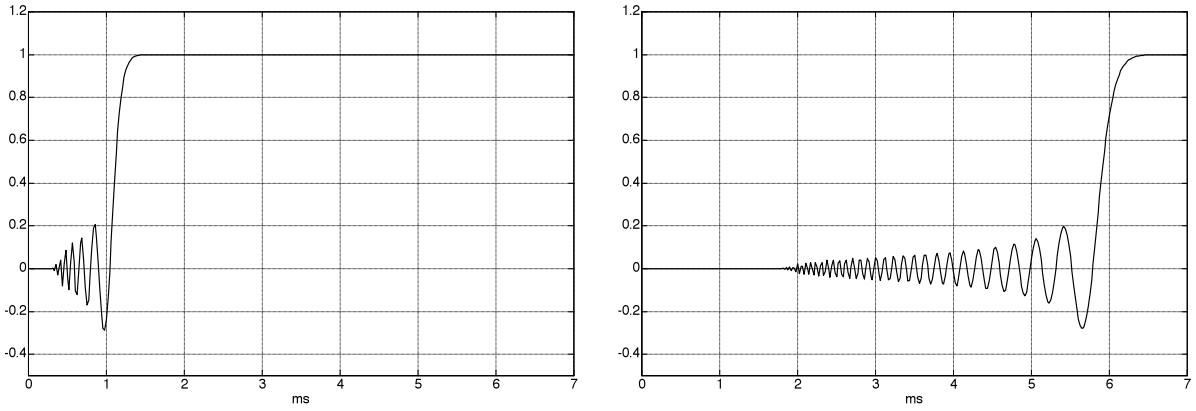

Fig. 2.43: Step response of a cascade of 14 (left) and 74 (right) all-pass filters. Data as in Fig. 2.42. In addition to the all-passes, a slight treble attenuation was included (*one* 1st-order low-pass at 10 kHz).

On the one hand, **dispersion** has the effect of a progressive spreading of the frequency of the partials. For the perceived sound, it is more important, though, that the FIR-filters depicted in Figs. 2.30 and 2.36 are subject to the same mechanism, as well: their interference effect happens progressively spread out towards higher frequencies. Given a dispersion-free E_2-string, the bridge pickup of a Stratocaster would feature an interference cancellation at $3 \cdot f_G \cdot 65\text{cm} / 5\text{cm} = 3214\,\text{Hz}$. However, your commercially available string is not free of dispersion, and therefore the interference cancellation mentioned above will happen somewhere in the range of 3330 – 3520 Hz, depending on the specific design of the string. In case the loudspeaker contributes narrow-band resonances in that same frequency range, a change of the make of strings may indeed bring audible differences. In this context, it should not be left unmentioned, though, that moving the guitar loudspeaker may well lead to changes in the sound: the room represents an FIR-filter, as well – due to the various occurring sound paths.

© M. Zollner & Tilmann Zwicker, 2002 & 2020

2.9 Magnetic pickup with excitation by dilatational waves

Does an axial shift in the string induce an electrical voltage in the magnetic pickup? The distance between string and pole-piece of the pickup does remain constant, after all – which is why we would not expect any voltage. Measurements do not support this hypothesis, though. Apparently, the distance between string and pole-piece is not the only criterion for the generation of a voltage: due to hysteresis and associated memory processes, a dilatational wave running along the string may indeed induce a voltage in the pickup, as well. The following model considerations discuss the basic context:

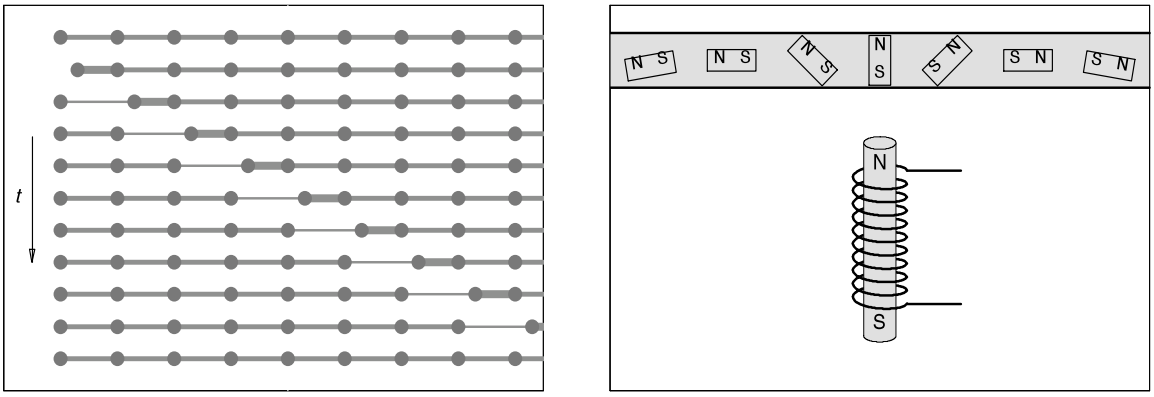

Fig. 2.44: Dilatational wave (left), string with elementary magnets and pickup coil (right). Both figures show considerably simplified, discretisizing models.

In the left-hand section of **Fig. 2.44**, we see a model of a string depicted at 11 different times; the bold points are masses, and in between them there are springs♣. On the top left, a compression impulse is generated that propagates along the string with progressing time (dilatational waves are generally free of dispersion). A pickup mounted beneath the string generates a permanent magnetization within the string – this is shown in the right-hand graph with a few elementary magnets. The dilatational-wave impulse sequentially shifts each of the elementary magnets: first a little to the right, then back to the original position. This shift varies the magnetic flux axially penetrating the coil. Looking at the right-hand graph seen in Fig. 2.44: for the elementary magnets shown towards the left, the variation of the location (resulting from the impulse) causes an increase in the magnetic flux penetrating the coil, and a decrease for the elementary magnets shown on the right.

The efficiency of the voltage induction caused by this effect depends on many factors: the magnet, the turns-number of the coil, or the material of the string. Of particular importance for the above model consideration are two parameters: the distance between the elementary magnets and the coil, and the angle between the axis of the elementary magnets and that of the coil. The compression impulse running along the string from left to right generates – in the coil – first an increase in the flux, and then a decrease. These variations in the flux induce an electrical voltage in the coil (law of induction: the voltage induced per turn of coil-winding corresponds to the temporal derivative of the magnetic flux penetrating this turn).

♣ The shown change in diameter is strongly exaggerated.

© M. Zollner & T. Zwicker, 2002 & 2020

For a half-wave-shaped displacement impulse, **Fig. 2.45** presents the time functions of the flux change $\Delta\Phi$, and the corresponding temporal derivative. The graphs – put together from simple functions – are meant to merely familiarize us with the shape in principle; an exact calculation would require considerable effort. Given a geometric distance of the ranges of maximum sensitivity of about 1 – 2 cm (the typical dimensions of pickups), we obtain the distance in time of the extrema of about $\Delta t = 2 - 4$ μs (with a propagation speed of dilatational waves of about 5 km/s).

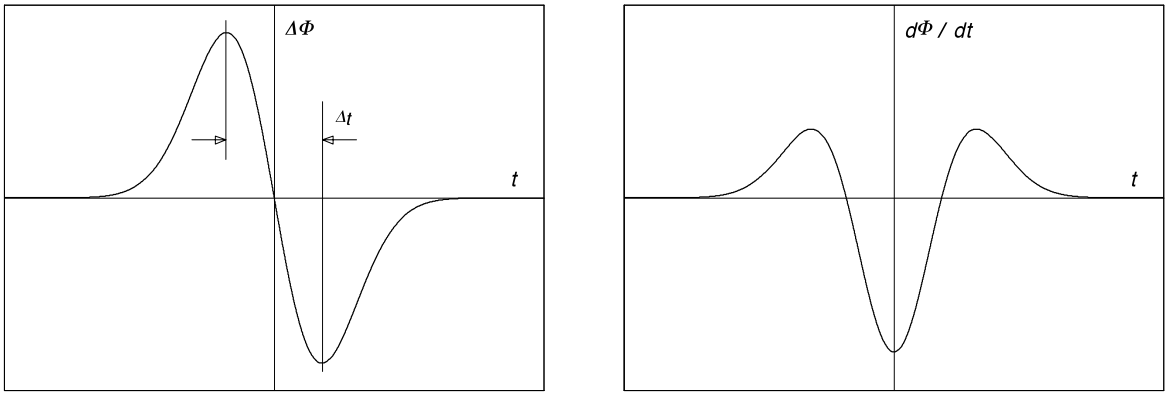

Fig. 2.45: Variation of flux (left) and its temporal derivative, caused by a compression impulse.

The signal shown in the right-hand part of Fig. 2.45 may be interpreted as impulse response $h_{U\xi}$. The first index (U) points to the pickup voltage U being seen as the output value that results from the differentiation of the magnetic flux. The second index ξ relates to the source signal: a *displacement* impulse. From the impulse response $h(t)$ of an LTI-system [6, 7], and using the help of a Fourier-transformation, we arrive at the transfer function $\underline{H}(j\omega)$ of this system♣. Herein, input and output signals remain the same; they are merely represented in different "domains": the impulse response connects (via the convolution) the input- and the output-**time-function**, and the transfer function connects (as a multiplication) the input- and the output-**spectrum**. The Fourier transform of the impulse response $h_{U\xi}$ is therefore the transfer function $\underline{H}_{U\xi}$. Model-considerations for equivalent circuits have, however, shown that $\underline{H}_{Uv}$ represents the more easily interpretable transfer function (Chapter 5.9.3), rather than $\underline{H}_{U\xi}$. Instead of the displacement impulse, a (*particle*-) *velocity* impulse is applied as trigger of the dilatational wave (the corresponding displacement function is the step). Instead of exciting a dilatational wave within the string with an excitation impulse, the temporal integral (the displacement step = velocity impulse) of the dilatational wave is impressed optionally. This additional integration is taken into consideration in Fig. 2.45 by requiring that the induced voltage shown in the right part of the figure is subject to an integration (commutativity of LTI-systems). Since the right-hand part of the figure was derived from the left-hand part via differentiation, we can use the left-hand graph to establish the time-course of h_{Uv} – merely the units are different. The following summary results:

A dilatational wave resulting from a displacement impulse induces the pickup voltage shown in the right-hand graph of Fig. 2.45. A dilatational wave resulting from velocity impulse induces the voltage shown in the left-hand graph of Fig. 2.45.

♣ The additional low-pass filtering occurring in pickup and cable is ignored here to begin with.

© M. Zollner & Tilmann Zwicker, 2002 & 2020 Translation by Tilmann Zwicker

The Fourier-transform of h_{Uv} (i.e. the transfer function $|\underline{H}_{Uv}|$) is depicted in **Fig. 2.46**. We can see a frequency-proportional rise in the frequency range particularly relevant for the magnet pickup (< 10 kHz) – corresponding to the magnitude frequency-response of a differentiator. It becomes clear that the exact shape of the h_{Uv}-curve is of minor importance: any (odd numbered) origin-symmetric impulse response will exhibit the characteristic of a differentiator in the low-frequency range. Due to the high propagation speed of the dilatational waves, the maximum of the transfer characteristic is located at such high frequencies that its specific range does not need to be determined.

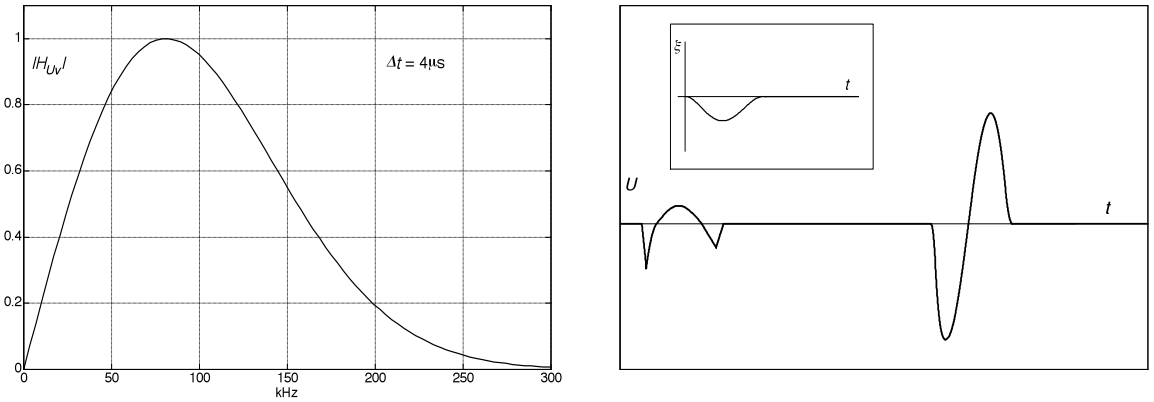

Fig. 2.46: Magnitude of the transfer function of (particle) velocity → voltage, without LC low-pass (left). Voltage induced in the pickup: string-excitation by a drop hammer, w/out dispersion, w/out LC low-pass (right).

Excitation of the string via a **drop hammer** generates two subsequent impulses in the pickup winding: first, we get the impulse induced by the dilatational wave, and then the impulse induced by the (slower) flexural wave. If at first the dispersion (that occurs only for the flexural wave) is disregarded, a voltage shaped similarly to the one shown in Fig. 2.46 would be expected. A displacement impulse shaped similar to a sinusoidal half-wave (small figure) runs along the string both as a (simplified) dispersion-free, slow transversal wave, and as fast dilatational wave. The first temporal derivative of this impulse corresponds to the voltage induced by the transversal wave; the second derivative corresponds to the voltage generated by the dilatational wave. However, the **dispersive propagation** of the flexural wave leads to a considerable reshaping of the impulse. Therefore, the shape of the voltage shown in Fig. 2.46 on the right will not occur during measurements in reality. Rather, all-pass-induced impulse deformations appear (Chapter 1.3.2, Chapter 2.8.4). In order to be able to compare the above theoretical model-calculations with measurements, the transversal-wave impulse (that looks similar to a full sine oscillation) needs to be first sent through an **all-pass filter**.

The measurements used for comparisons in the following were done using a 30 m long string of 0,7 mm diameter mounted below a Jazzmaster pickup. Due to its very low winding capacitance, and given suitable electrical loading, this pickup allows for broadband measurements up to about 20 kHz. While not exactly typical for use in electric guitars, the corresponding circuitry is highly qualified for measurements. At 3 mm from its mounting point (clamp), the string was excited by a short displacement impulse, leading to the propagation of a dilatational and a flexural wave along the string. At a distance of 68 cm from the clamp, the transversal velocity was sampled both with a laser vibrometer and with the Jazzmaster pickup, and the resulting signal was digitally stored.

 © M. Zollner & T. Zwicker, 2002 & 2020

In **Fig. 2.47**, we see on the left the transversal velocity measured by the laser vibrometer. The dilatational-wave impulse reaches the measuring point 0,13 ms after the drop hammer has struck the string – this instant represents the origin of the time-scale. The laser vibrometer practically ignores the dilatational-wave impulse; the pickup, however, shows an impulse that resembles a twice-differentiated sinusoidal half-wave impulse (Fig. 2.46). After about 1 ms, the high-frequency components of the flexural wave reach the measuring point, and the low-frequency components follow after about 6 ms (dispersive propagation); these waves are received by both sensors in a similar way.

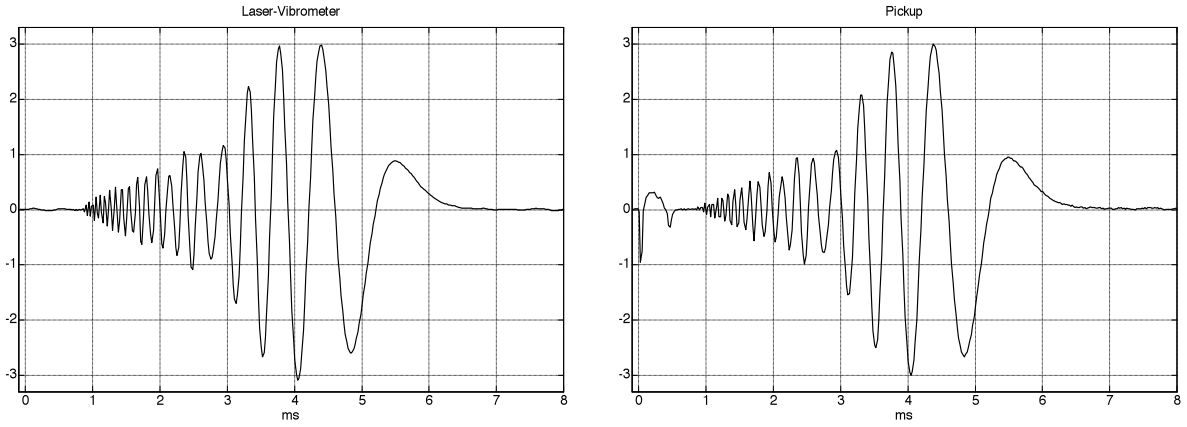

Fig. 2.47: Time function measured after impulse excitation of the string; laser (left), pickup (right).

From the point of view of **systems theory**, the tensioned string represents – with good approximation – an LTI-system that maps input quantities onto output quantities. A separation according to the two wave types yields two sub-systems: a dispersion-free delay line (dilatational wave), and a dispersive delay line (flexural wave). **De-convoluting** the output quantity of the system measured at the pickup gives the input quantity of the system. The effect of this de-convolution is shown in **Fig. 2.48**: of the pickup voltage indicated on the right in Fig. 2.47, the time-snippet between 1 ms and 7 ms was de-convoluted with the impulse response of the all-pass (Chapter 1.3.2). The result was drawn into the right-hand half of the left-hand section of Fig. 2.48; for comparison, the original dilatational-wave impulse is presented on the left. The part of the figure on the right shows the twice-integrated functions corresponding to the displacement. While the curves juxtaposed in the figure are not identical, they still are very similar – this could not be expected given the original functions that are, after all, of an entirely different character.

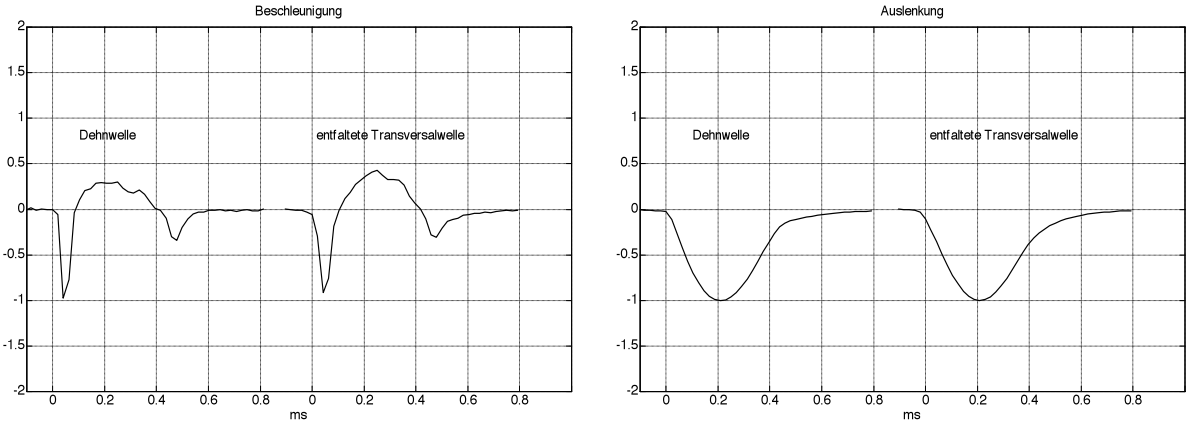

Fig. 2.48: Comparison between measured dilatational-wave impulse and de-convoluted flexural-wave impulse. "Beschleunigung" = acceleration; "Auslenkung" = displacement; "Dehnwelle" = dilatational wave; "entfaltete Transversalwelle" = de-convoluted transversal wave.

© M. Zollner & Tilmann Zwicker, 2002 & 2020 Translation by Tilmann Zwicker

The pronounced similarity of the shape of the curves presented in Fig. 2.48 leads to the following conclusion: **dilatational wave and flexural wave have approximately the same time-function at the moment of their formation**. This hypothesis may be further corroborated via mapping the dilatational-wave impulse onto the flexural-wave impulse. For this, the section from 0 ms to 1 ms of the impulse shown in Fig. 2.47 on the right is integrated and convoluted with the impulse response of the all-pass: the signal depicted on **Fig. 2.49** on the right results. This latter signal corresponds with good approximation to the signal of the flexural wave (on the right in Fig. 2.47; repeated in Fig. 2.49 on the left). An example for which measurement and calculation correspond even better still is given in **Fig. 2.50**.

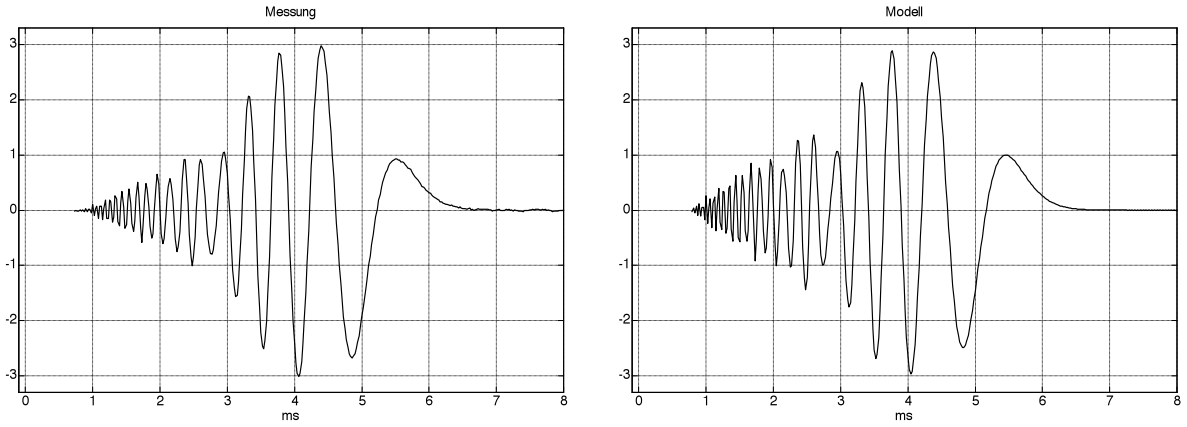

Fig. 2.49: Pickup voltages: flexural wave (left); impulse derived from the dilatational wave (right).

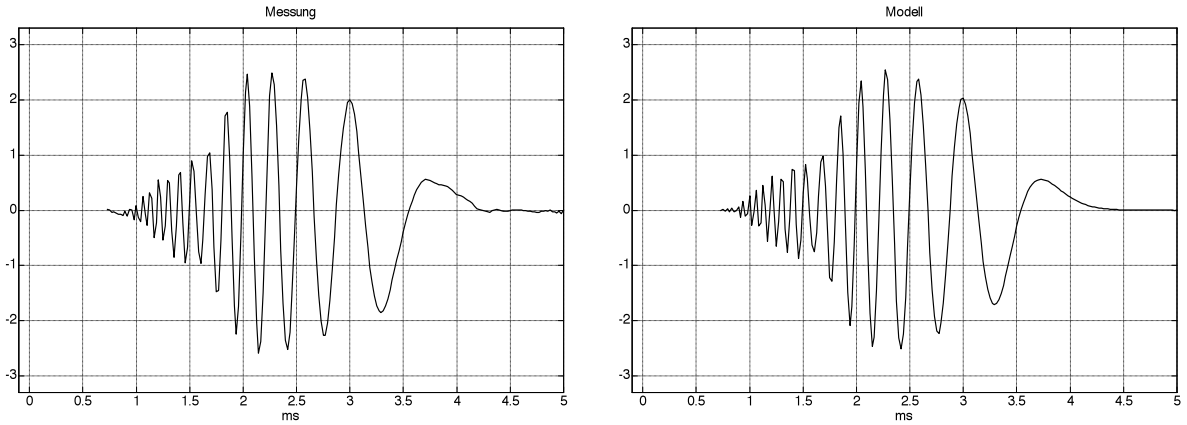

Fig. 2.50: As in Fig. 2.49, but established at a different pickup-position (55 cm instead of 68 cm).
"Messung" = measurement, "Modell" = model.

There is no absolute scaling of the ordinate in the above figures – for that a transfer coefficient for the individual pickup would be required. To get an impression of the wave-parameters, the following table lists typical (rounded-off!) values. The relationship of the two wave energies depends on the respective string bearing.

	Flexural wave	Dilatational wave
Maximum displacement	30 μm	5,7 μm
Maximum (particle) velocity	0,4 m/s	0,07 m/s
Maximum force	0,2 N	1,2 N
Wave impedance	0,5 Ns/m	17 Ns/m
Maximum power	88 mW	88 mW
Impulse-energy	8,0 μWs	8,5 μWs

 © M. Zollner & T. Zwicker, 2002 & 2020